SPECKLE SUPPRESSION IN HANDHELD LASER PROJECTION DISPLAYS

SPECKLE SUPPRESSION IN HANDHELD LASER PROJECTION DISPLAYS

By

Mahmoud Mohamed Talaat

BSc., MSc.

A Thesis Submitted to the School of Graduate Studies in Partial Fulfillment of the Requirements for the Degree

Doctor of Philosophy

Doctor of Philosophy (2019) (Engineering Physics)	McMaster University Hamilton, Ontario
TITLE:	Speckle suppression in handheld laser projection displays
AUTHOR:	Mahmoud Mohamed Talaat BSc., MSc. (Electrical engineering) Military Technical College, Cairo, Egypt.
SUPERVISORS:	Professor Chang-Qing Xu
NUMBER OF PAGES:	XIX, 129

Lay Abstract

Projection display technology today has garnered a large amount of interest due to its vast market. The display technology has evolved alongside the development of various light sources for their light engines. For example, the technology started with the use of a conventional lamp, progressed to light-emitting diodes, and recently has arrived at laser sources. Laser-based projection displays have caught the attention of those seeking to develop display technologies due to many advantages for projection, thanks to the intrinsic properties of the laser. Laser projectors have significant benefits that include high brightness, wide colour gamut, long lifetime and high electrical to optical efficiency. There have been multiple types of laser-projector created to satisfy the requirements of the intended applications. A large scale and high-power laser projector will be used in applications requiring a big screen, large audiences, and wide-open spaces found in a cinema or theatre. A mini projector on the other hand will typically be used for home cinema, while micro-/pico-projectors are intended for personal use. Although laser projectors up until now have been useful, they are expensive and have safety concerns. Moreover, laser projectors encounter a technical problem due to the high coherence of the laser source. This issue is known as “speckle” noise. Speckle noise results in a reduction of the quality of images generated with laser-based projectors. Many types of research have been conducted to reduce the laser speckle noise to be lower than human eye perception limits. As a result, most of these speckle reduction

techniques are applied to large scale projectors, and a few of them have been successfully applied for smaller projectors, such as micro-/pico- projectors.

Abstract

Micro-/pico-projectors are exciting technology as they represent a core enabling technology for the future growth of portable devices. They are currently involved in many fields such as automotive, defence & aerospace, healthcare, and media/entertainment. Solving the issue of speckle noise in such small projectors has been a challenge until now, as most of the effective techniques for speckle suppression are not suitable for such small sizes.

The purpose of this dissertation is exploring and applying practical solutions for reducing the laser speckle noise for a handheld laser projector (micro-/pico-projectors).

The first method is to introduce a laser source with low-level speckle noise. The source is designed based on end pumping of two cascaded laser crystals in the same cavity. The first crystal is $Nd:YVO_4$ and the second is $Nd:GdVO_4$ crystal. The output power ratio is adjusted mechanically to be 1:1. The output optical to optical efficiency is close to 50%. The output power at 1:1 power ratio has the lowest speckle noise level. The laser source is compact. Such a laser source is promising for micro-/pico-projectors.

The second method is to reduce the laser speckle noise by a simple, low cost and compact optical method. Our novel method is to vibrate a lens with a small

focal length in just one dimension (1D) in front of an optical diffuser. The method reduced the speckle noise by 81.25% and 75.6% for laser diode (LD) and diode-pumped solid-state (DPSS) laser sources, respectively.

Finally, an optimisation was performed as follows: First, two laser sources are blended under specific conditions. Second, by adding another vibrating lens with a direction of vibration orthogonal to that of the first lens. Afterwards, the two optimisations are tested with a real pico-projector engine setup. The speckle contrast ratio was < 5%.

Acknowledgements

My PhD was an extraordinary chapter in my life! I spent many hours thinking, crying, laughing, cooking, studying, working, and praying. I am grateful to God for the good health that was necessary to complete this dissertation.

Firstly, I would like to express my sincere gratitude to my advisor Prof. Chang-Qing Xu for the continuous support of my PhD study and related research, for his patience, motivation, and immense knowledge. He was like my second father in Canada; his guidance is helped me not only in the time of research but in my individual life. I cannot forget his words and advice in every meeting. I could not have imagined having a better advisor and mentor for my PhD study. I know that I am lucky to have him as my supervisor.

Two, special thanks to Prof. Adrian Howard Kitai and Prof. Qiang-yang Xu; they gave me many remarkable academic suggestions on my research as my supervisory committee members during my study.

Dr Qianli Ma, I cannot find words to thank you. You proved to me that the man could have a true brother not belong to his blood. Really, I appreciate what you did for me; you have an impact on every success I did during my PhD study. I am lucky for the second time to have a brother like you.

Thanks to every member of my group, especially Bin Zhang, Liam Flannigan, and Tyler Kashak. All of them helped me and introduced great scientific support to me.

Thanks to all the professors in the Department of Engineering Physics for their valuable suggestions on my research work. I would like to express my sincere gratitude to all Engineering Physics members and McMaster staff that has helped me generously during the past three years. Without their help, this work does not exist. I would like to thank my local supervisor Dr Mostafa Elshershaby for his support from my home country Egypt. Special thanks to my friend Farooq Kamil.

Eventually, I would like to thank my father and my mother for their lifelong encouragement and support. Also, all respect for my wife, Manar, she was my guard angel. She suffered with me a lot without complain to let me focus on my work. I would like to thank her for giving me the most precious motivation recently, our baby, Malek. I hope from God to make him a good servant for humankind.

Table of contents

List of Figures

List of Tables

Declaration of Academic Achievement

This dissertation was prepared according to the guidelines of the School of Graduate Studies at McMaster University for theses which contains a group of already published papers (Chapter 2 and 3) or submitted papers to be published (Chapter 4). The work on the thesis was done only by Mahmoud Mohamed, where the technical guidance and advice was presented from the academic supervisor Prof. Chang-Qing Xu. Dr. Qianli Ma has provided some editorial comments to the papers presented in Chapters 2, 3 and 4. Bin Zhang has provided some editorial comments to the paper presented in Chapters 2. Josh Kneller, Liam Flannigan, and Tyler Kashak revised the academic writing in chapters 2, 3, and 4, respectively. Information from any external sources used in the work inside the thesis has been cited where suitable. The main contribution of the author in each chapter (paper) and the explanations for their insertion in this thesis are designated below:

Chapter#2: Mohamed M, Zhang B, Ma Q, Kneller J, Xu C. Q. **Efficient Dual-Wavelengths Continuous Mode Lasers by End-Pumping of Series Nd**: **YVO_4 and Nd**: **$GdVO_4$ Crystals and Speckle Reduction Study.** In Photonics 2019 Jun (Vol. 6, No. 2, p. 53). Multidisciplinary Digital Publishing Institute.

The idea of that paper originated from Mahmoud Mohamed, who also prepared the experimental setup, main framework, and testing. Mahmoud Mohamed drafted the paper manuscript. The manuscript was then reviewed and edited by Bin Zhang, Qianli Ma, Josh Kneller, and Chang-Qing Xu. This work

should be included in this dissertation as it introduces an efficient, stable, low speckle noise, compact size useful alternative laser source. Such a laser source is essential for the new compact handheld projectors and medical applications.

Chapter#3: Mohamed M, Qianli MA, Flannigan L, Xu C. Q. **Laser speckle reduction utilized by lens vibration for laser projection applications.** Engineering Research Express. 2019 Sep 10.

The idea of that paper originated from Mahmoud Mohamed, who also prepared the experimental setup, main framework, and testing. Mahmoud Mohamed drafted the paper manuscript. The manuscript was then reviewed and edited by Qianli Ma, Liam Flannigan, and Chang-Qing Xu. This work should be included in this dissertation as it introduces a new method to reduce the laser speckle. Such a compact, simple, and low-cost method is essential for the new compact handheld projectors and medical applications.

Chapter#4: Mohamed M, Qianli MA, Tyler K, Xu C. Q. **Speckle reduction by employing two green lasers and two-dimensional vibration of lenses.** Engineering Research Express. 2019.

The idea of that paper originated from Mahmoud Mohamed, who also prepared the experimental setup, main framework, and testing. Mahmoud Mohamed drafted the paper manuscript. The manuscript was then reviewed and edited by Qianli Ma, Tyler Kashak, and Chang-Qing Xu. This work should be

included in this dissertation as it introduces an optimisation for the new method to reduce the laser speckle more efficiently and improve the color quality for handheld projectors. Such optimization is essential for reducing the speckle noise to be lower than human eye perception limit for such unwanted phenomenon to improve the quality of the projected image handheld projectors.

Chapter 1

INTRODUCTION

1.1 LASER PROJECTION TECHNOLOGY

Display technology plays a vital role in our modern life. It can be used in many applications for different purposes which include cinemas, small meeting rooms, or rear projection TVs. The first use of a laser as a light source in projection systems appeared a few years after the demonstration of the first laser in 1960 [1]. Lasers introduced significant advantages to the physical characteristics of the projected images based on the intrinsic properties of the laser light.

There are three main pillars for any display system: a projection device, a screen, and the observer. The specifications of the projection devices must satisfy the requirements for practical applications. For example, cinemas, have ample space, large audiences, and screen dimension is large. As a result, the projectors must provide enough illumination, better color, and better image quality. In other words, the power of the illumination light must be increased, which causes the size of the projector light engine to be significantly increased. In other applications, such as handheld device projectors, the projectors are characterized by their small sizes for personal use. Generally, any optical engine of any projector device contains an illumination source, optics, and display image devices.

ILLUMINATION SOURCE

The illumination performance of any projector is dependent mainly on the nature of its light source. There are three types of light sources used in projection systems: lamps, light-emitting diodes (LEDs), and lasers. Any potential light source must contain the three essential colors (red, green, and blue colors, i.e. RGB colors) to form the colored images.

Lamp as an illumination source

Currently, most projectors on the market are based on arc lamps. Such lamps can cover a wide power range from 50-900 W [2] with a reasonable life lime > 1,000 hours [3].

There are two types of arc lamps that are used for projection purposes: Xenon lamps and Metal-halide lamps. First the Xenon lamp, which is a glass tube filled with high pressure noble Xenon gas [4]. Such lamps do not suffer from a long warm-up time, have good colourimetry [5], and high brightness. As a result, it is commonly used in large-screen cinema projectors [6], [7]. However, because it has a broad spectrum, it is necessary to use filters to extract the three prime colours; red, green, and blue, which causes the lumen-efficiency to be very low [8].

Second, in Metal-halide lamps, a mixture of mercury and halide salt metal is used [9]. As an advantage, the illumination spectrum characteristics can be adjusted easily [9]. However, the use of metals inside the lamp leads to a long warm-up time to reach maximum brightness and proper colour. Moreover, the

metals inside the lamp can interact with the material of the electrodes and transform them into different compounds. This causes the colour to drift in the projected images over the lifetime of the lamp [2].

LEDs as an illumination source

The development of LED technology has been very interesting. Nowadays, LEDs are covering all colours needed for projection. LEDs have many attractive attributes such as compactness, a fast switching response, and no warm up time [10]. Moreover, LEDs have excellent colourimetry and long lifetime [11].

LEDs can provide white light – which contains all three RGB colours – with two approaches. The first method is to utilize a combination of three LEDs where each one emits a single colour from the three RGB colours.

The second method relies on turning the blue colour in to the desired colour with a Fluorescent (or Phosphorescent) material. For example, a blue LED can be combined with a yellow phosphor, but the produced white colourimetry is poor. Thus, such a technique can be useful for applications that need low power consumption, such as cell phones [2]. A mixture of blue LEDs with green or red phosphors is a much better solution for achieving better colourimetry. However, the efficiency is much lower than in yellow phosphors. Additionally, LEDs have a long lifetime, but the output light decreases slowly with time [12]. LEDs have a very impressive lifetime; it is typically around 20,000 hours until the output light has diminished by 50% from its original value [13].

Even though LEDs can claim many advantages, they have large étendue. This is because the emitted light from LEDs has a broad emission angle. Thereby preventing any output light from escaping a light engine containing LEDs is a real challenge.

Moreover, the LEDs have limited brightness, so they are not suitable for high lumen projection [14], but they are considered to be a probable source for handheld projectors where brightness can be less important than overall compactness [15], [16].

Lasers as an illumination source

From the previous sections, it is clear that the performance and the lifetime of conventional lamps are limited [17]. It is also clear that the performance and lifetime of LEDs are significantly better than lamps. However, LEDs have power limitations which makes them unsuitable for high brightness projection systems.

Lasers can provide much higher power levels with very low étendue. This makes lasers a proper candidate for building very high brightness projectors -the brightness of lasers is greater than that of LEDs by 5×10^6times [18]- with smaller displays [19]. Lasers need a projection lens with a smaller diameter (40% lower than in lamp projector [20]). This will reduce the cost of using a high aperture F-number projection lens, as smaller lenses can be used thanks to the small divergence angle of the laser beam [2]. The laser has a lifetime of 50,000 hours [21] which is greater than the lifetime of a lamp or LED by a significant margin. The ability to

design any desired wavelength provides a wide colour gamut for the displayed image [22]. The laser source adds an advantage to projection systems in general as it is suitable for all types of projection applications. For example, it has sufficient power to meet the requirements of the large projectors used in cinema and home theatre, while being compact enough to be used in handheld projectors such as mini-/pico- projectors for personal use. **Figure 1-1** shows some types of laser projectors.

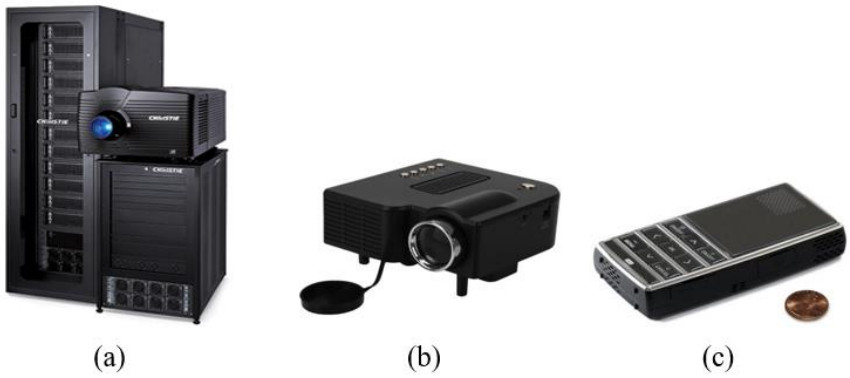

Figure 1-1: Some types of laser projectors; (a) cinema projector [23], (b) mini-projector [24], and (c) pico-projector [25].

However, the cost of manufacturing commercial laser sources is still high compared to that of the conventional lamps. Additionally, direct exposure to the laser beam can be very harmful to the human eye, so it is a requirement not to let any stray light leak outside the light engine of the projector.

Besides the cost and safety concerns, there is also a technical issue with implementing laser light sources called speckle noise. Speckle noise serves to decrease the quality of the projected image. The origin of laser speckle is a result when a coherent laser light scatters and interferes randomly with itself after reflecting from a rough surface such as a projection screen [26].

Figure 1-2 shows a projected image with and without speckle noise. As shown in **Figure 1-2b**, the output image suffers from a granular appearance of dark and bright patches. As a result, the image quality will be reduced significantly. Hence, the reduction of the laser speckle must be considered in all types of laser projection systems.

Figure 1-2: projected image (a) without speckle noise, and (b) with speckle noise.

OPTICAL COMPONENTS

Generally, the optics inside the light engine play an essential role in the projection process. Optics add many advantages to the projected images, and in this section, we will explore some important optical components commonly used inside any laser projection system.

The most important optical functions are mixing the RGB colours, homogenizing the output optical field, and adjusting the size of the output image.

In a laser projection system, the RGB colors consist of three separate laser sources that must be mixed into one laser beam to form the white light. The combination of the three colors is performed by using a dichroic prism (X-cube as shown in **Figure 1-3** a), two dichroic filters (as shown in **Figure 1-3**b), or by using a three to one fiber (as shown in **Figure 1-3**c).

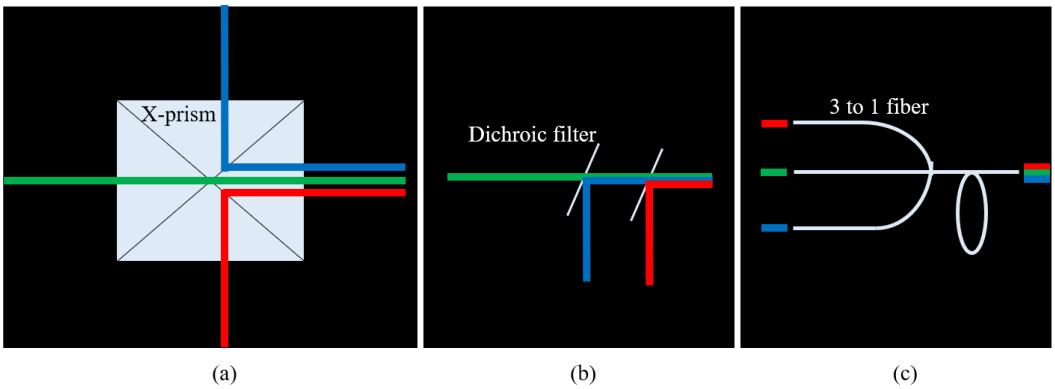

Figure 1-3: illustrate the different methods for coupling the RGB lasers: a) by X-prism, b) by dichroic filters, and c) by 3 to 1 fiber.

Second, some optical components are used to homogenize and reshape the output light field inside the light engine of a laser projector, such as a light pipe or by using a lens array as shown in **Figure 1-4**.

For the projection lens, the light will be launched from one side of the lens and will be received from the other side. According to the divergence angle of the input light, multiple reflections should happen inside the light pipe. Each reflection will form an imaginary image on the edge of the light pipe; the integration of such images will create a homogenized optical field [27]. The cross-sectional area of the light pipe can take many forms, such as circular, hexagonal, or rectangular. In other

cases, the geometry of the entrance and the exit of the light pipe may be different in order to reform the shape of the output light field.

The lens array is composed of a matrix of micro lenses. Typically, a pair of lens arrays are combined with a condenser lens to homogenize the laser light output field. Such a combination can also reshape the light field to fit the geometry of the projection pattern. The first lens array is used to transform the incident light field into many sub-focused beams. The second lens array will collimate each sub-focused beam to be parallel with one another. The condenser lens will integrate and focus all the parallel rays on to a specific area. Thus this area contains a homogenized light field that is ready to be projected by a projection lens [28].

A projection lens is used for projecting the images, controlling the focusing, and adjusting the size of the output image on a screen. The specifications of the projection lens (such as a focal lens and the diameter of its aperture) differ according to the type of application the projector was intended for.

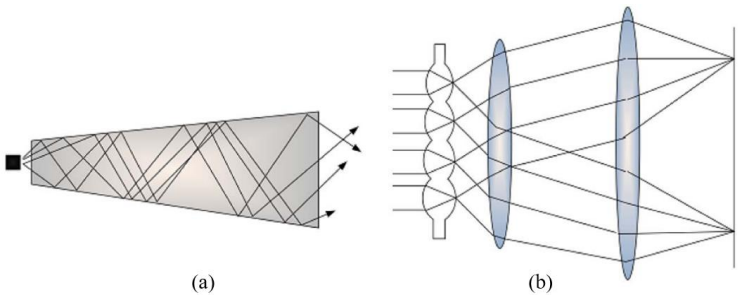

Figure 1-4: a) light pipe illumination system, and b) lens array illumination system [29].

DISPLAY PATTERN

The output projected images from laser projectors depend on four key technologies; digital light processing (DLP), liquid crystal display (LCD), liquid crystal on silicon (LCoS), and laser beam-steering (LBS). The technology of LBS is commonly used in Pico projectors.

DLP display technology

The most crucial part of DLP systems is digital mirror devices (DMD). The DMD is a micro-opto-electromechanical system (MOEMS) device. **Figure 1-5** shows a DMD chip. As shown in **Figure 1-5**, the chip surface is comprised of a rectangular array with a large number of microscopic mirrors. Each mirror has a connection with a pixel in the image that will be displayed. In **Figure 1-5**, each mirror can rotate ± 10-12° by tiny suspension system underneath. The DMD is a spatial light modulator. All the mirrors have two modes of operation, an "on" and "off" state. In any state, the laser beam is shining on the DMD chip surface and the reflected beam is projected on a screen through a projection lens. In the "on" state, the mirror face is on an angle enabling it to reflect the laser light through the projection lens, and the opposite happens in the "off" state [30]. The time taken for switching is about 20 μs from "on" to "off" [31]. **Figure 1-6** shows a simple light engine of a laser projector that is DMD based. In projectors based on lamp technology, a color wheel and color filters must be included to define the color on the image. On the other side, in LED or laser projectors, the RGB primary colours

are generated at the same time, so there is no need for a colour wheel or filters, resulting in a high optical efficiency [32].

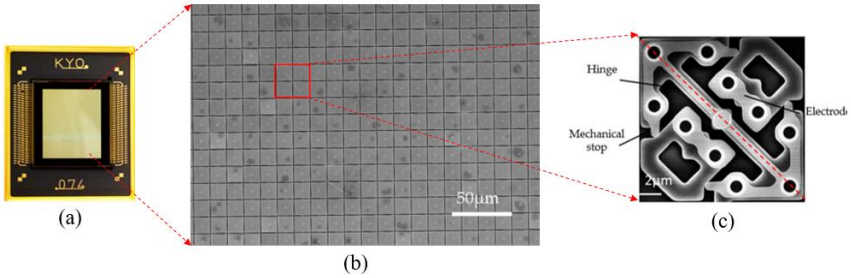

Figure 1-5: (a) DMD chip, (b) enlarged image for the DMD chip surface, and (c) enlarged mechanical actuation system under the micromirror [33].

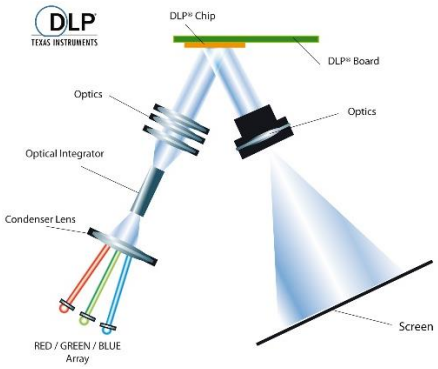

Figure 1-6: A typical Pico-projection light engine [34].

LCD display technology

In such technology, the light passes through the polysilicon LCD panel; therefore, it is identified as a transmissive technology. The LCD panel is constructed from two transparent polarized sheets. The two sheets are sandwiched together, and the gap between them is filled with a liquid containing crystals with rod-shaped. The panel contains millions of tiny cells, the opacity of each cell can be controlled by a digital electrical signal. When the cell is opaque then it will block the light from passing through the cell, by this concept, any image can be

constructed. This technology requires using a polarized light. When an electric signal applied to the crystals, it causes them to rotate the plane of polarized light. This mechanism of switching ON and OFF states can introduce 256 shades of grey (8-bit processing)[35]. Figure cc shows a laser projector engine based on laser phosphor technology. The red and yellow colors are generated from passing a blue laser light through a phosphor wheel, while the blue color is from another separate blue diode laser. Each color will be directed to pass through a separate LCD panel. The images from each panel are combined with a prism, resulting in a single image with up to 16.7 million colors.

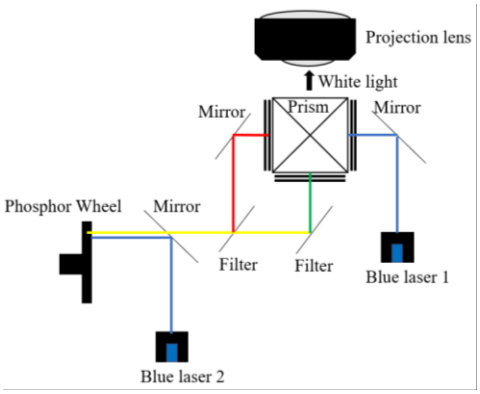

Figure 1-7: Laser projector based on laser Phosphor technology and 3LCD panel technology.

LCoS display technology

LCoS technology is a hybrid from the technology of LCD and DLP at the same time [36]. In an LCD, the modulation of light occurs by changing the polarization state of a nematic liquid crystal inside a glass panel by applying a certain amount of electric voltage. As a result, some light passes through, and the rest will not according to the polarization state of the light. In DLP technology, the

modulation of light occurs by controlling the amount of reflected light from millions of micro-mirrors. The combination between the principle of operation of LCD an the DLP let the LCoS to introduce more contrast by increasing the depth of black and white in the projected image. **Figure 1-8** shows a real image for the LCoS panel and a schematic diagram for its internal structure.

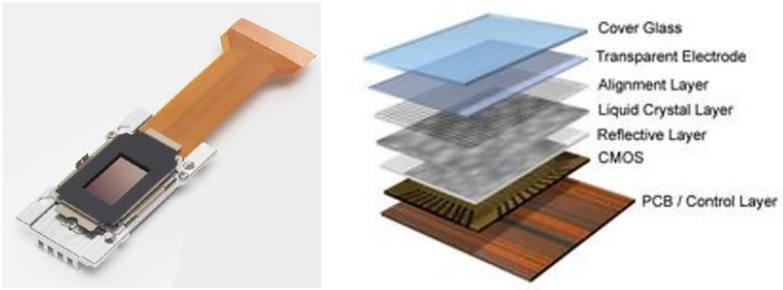

Figure 1-8: (a) LCoS module [37], and (b) schematic diagram for LCoS panel structure [38].

LBS display technology

The technology of LBS is widespread in laser pico-projectors. In this technology, each pixel of the image is formed one by one and line by line (using a raster scan motion). The raster scanning is performed by the direct scanning of the laser beam via fast scanning MEMS. (The RGB colors are controlled individually at each point). The LBS technology is affordable and assures a small size for its optical engine. Moreover, the LBS does not need a projection lens, so it is termed by a focus-free technology. **Figure 1-9** shows an image of the MEMS mirror and a conventional setup for the optical engine based on LBS technology. **Table 3-1** shows a comparison between the three display technologies: DLP, LCoS, and LBS.

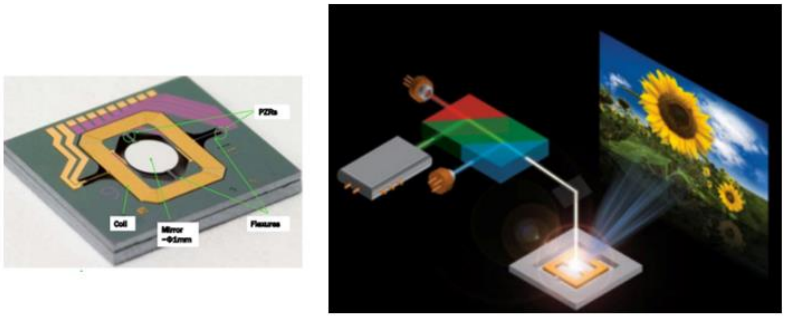

(a) (b)

Figure 1-9: (a) Laser beam scanning Bi-axial MEMS Mirror Platform [39], [40], (b) schematic diagram for pico-projector based on LBS [40].

Table 1-1: comparison between the display technologies [36].

Technology	DLP	LCoS	LBS
Key features	Reflective imaging technology using micro mirrors. RGB color delivered sequentially.	Reflective imaging technology using liquid crystal. RGB-colors delivered simultaneously.	Image scanning technology using directed laser beams. RGB color delivered simultaneously.
Advantages	Compact & small size. High contrast. No color degradation.	High resolution. No rainbow effects. Smooth pixel edges.	Focus free Low power consumption. Small size.
Disadvantages	Rainbow effect. Sharp pixel edges.	Larger size. Potential color degradation.	Laser is expensive. Speckle. Eye safety.

1.2 SPECKLE AND METHODS TO REDUCE

LASER SPECKLE

In 1960 and after introducing the first CW HeNe laser, the scholars noticed an unusual phenomenon when they illuminated some objects with highly coherent light from a laser beam: a peculiar and granular pattern would appear. Moreover, it was clear to them that such chaotic and disordered granular shapes have no apparent relationship with the macroscopic attributes of the illuminated object. These unique configurations came to be known as "laser speckle." **Figure 1-10** illustrates a typical image for laser speckle.

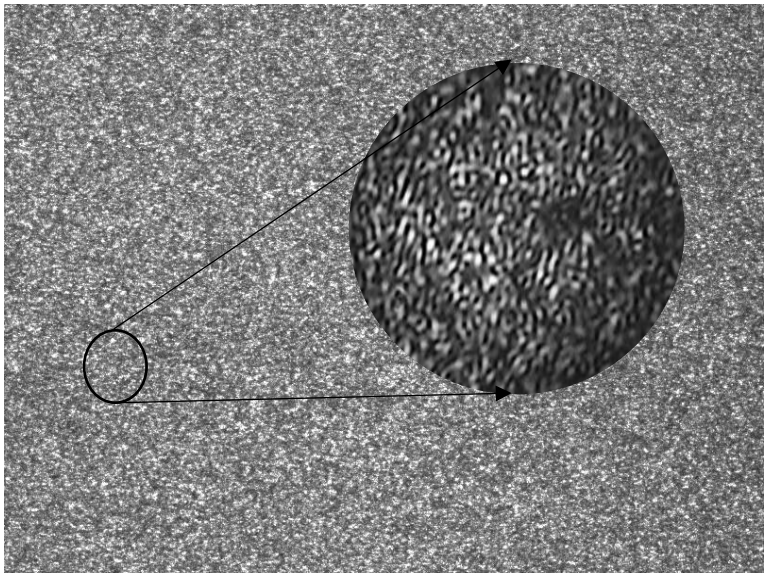

Figure 1-10: An image collected after illuminating a rough object by a coherent light.

Laser speckle originated from the high coherency of the laser light [42]. In the wavelength scale of the laser light ($\lambda \cong 0.5\ \mu m$), the microscopic attributes of the illuminated surface for an object become an important factor to consider. Thus, the surface structure on the microscopic scale is considered as a "rough" surface with random phase distribution. After coherent light is transmitted or reflected from such a rough surface, a secondary source of many coherent wavelets is formed. These output coherent wavelets are superimposed and interfere to form a random phase intensity distribution on the image plane. The human eye retina collects this information with an exposure time of 1/25 seconds (the human eye response time) and forms the laser speckle patterns.

Figure 1-11 shows the speckle formation mechanism; when a coherent electromagnetic wave (such as laser beam) illuminates a rough surface, each illuminated point on the surface act as a secondary spherical wave source (based on the diffraction theory). The output scattered light field is a result of the produced wave from each point. When the surface roughness is high enough to create a path-length difference with more than one wavelength, this leads to phase changes > 2π and the resultant light amplitude (or intensity) varies in a random way.

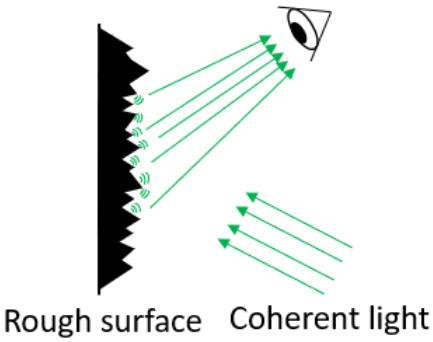

Figure 1-11: Speckle formation mechanism.

MATHEMATICAL DESCRIPTION ON LASER SPECKLE

In the context of the previous section, the scattered field of speckle noise can be expressed statistically by the sum of random phasor elements [43]. The resultant of the output field $\boldsymbol{X}$ is represented by the summation of N number of random phasors elements at the observation point as:

$$\boldsymbol{X} = Xe^{j\Theta} = \frac{1}{\sqrt{N}} \sum_{n=1}^{N} x_n \, e^{j\phi_n} \qquad (1 - 1)$$

where X is the magnitude of the complex resultant, x_n and ϕ_n are the amplitude and phase of the nth complex phasor element.

The wavefield intensity I is determined as:

$$I = \begin{cases} |\boldsymbol{X}_x|^2 + |\boldsymbol{X}_y|^2 & \text{in case of unpolarized wave} \\ |\boldsymbol{X}|^2 & \text{in case of polarized wave} \end{cases} \qquad (1 - 2)$$

The variance of $\boldsymbol{X}$ is:

$$\sigma^2 = \frac{1}{N}\sum_{n=1}^{N}\frac{x_n^2}{2} \qquad (1 - 3)$$

To describe the variation of intensity in a speckle pattern quantitatively, the speckle contrast ratio (SCR) is used. The SCR is defined as:

$$SCR = \frac{\sigma_I}{\bar{I}} = \frac{\sqrt{\bar{I^2} - \bar{I}^2}}{\bar{I}} \qquad (1 - 4)$$

Where σ_I is the standard deviation and $\bar{I}$ is the mean intensity of the output pattern. This quantitative description of the speckle by SCR is valid under the following assumptions:

A. The amplitude and phase for any specific complex phasor element are statistically independent.
B. The amplitude and phase for any two complex phasor elements are independent.
C. The distribution of a random phase (ϕ_n) is uniformly distributed over $(-\pi, \pi)$.

When the $\mathrm{SCR} = 1$, this means that the speckle patterns are fully developed. In this case, the speckle patterns consist of a large number (N) of independent phasors. When coherent polarized light illuminates a surface with enough roughness and the texture heights follow a gaussian distribution, then the output speckle patterns will be fully developed. When the $\mathrm{SCR} < 1$, this means that the speckle noise is reduced. When the $\mathrm{SCR} = 0$, this means that the patterns have constant intensity, and the SCR has been minimized.

TYPES OF LASER SPECKLE

There are two main types of laser speckle (as shown in **Figure 1-12**): (a) objective and (b) subjective speckle [44]. Both laser speckles are classified by determining the propagation method of laser light.

Figure 1-12a shows the formation of objective speckle. The laser light will propagate freely in the space after being transmitted or reflected from an optically rough surface. In the objective speckle, all elements from the illuminated objective plane contribute to form a point on the image plane. The rough object has a random phase. As a result, arbitrary interference will exist at the plane of the image and form speckle. **Figure 1-12b** shows the formation of subjective speckle. The laser light propagates through the imaging system. The term subjective is used as the speckle pattern's structure relies on the viewing system parameters, such as the aperture size or the position of the imaging system. A finite area from the objective plane forms each point on the image plane through the point spread function (PSF) area of the imaging system. Each finite area on the image plane has a random phase. Thus, this will cause arbitrary interference. This random interference causes intensity variation on the image plane, which is defined as speckle.

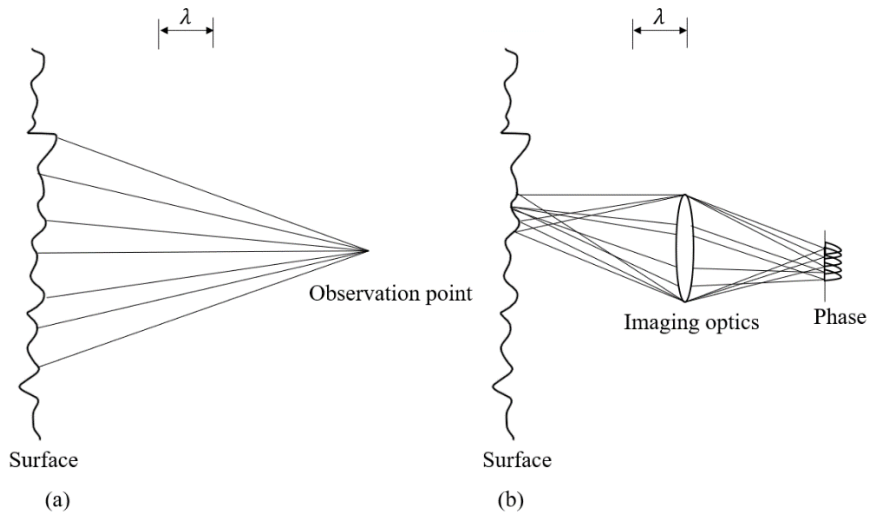

Figure 1-12: (a) objective and (b) subjective laser speckle formation [45].

Practically, there are many components that contribute to laser speckles. One of the vital elements is the material that the projector screen is made from. The screen is regarded as a very rough surface because the laser light has to be diffused with a large viewing angle. Some other optical components such as diffusers and multimode fibers inside the optical engines of a laser projector also introduce random phases. Such elements are used for light field homogenizing.

SPECKLE IN LASER PROJECTION DISPLAY

From the previous discussions, it was evident that using a laser as a light source in projection systems is superior to lamps and LEDs. Lasers offer much higher resolution, higher brightness, a better color gamut, and longer lifetime than lamps and LEDs. However, the high cost, safety issues, and some image quality issues that arise due to speckle are still the main disadvantages of laser-based

display technology. The main reason for the decrease in the output projected image quality is due to laser speckle.

Many types of research were performed to reduce the laser speckle, but the focus was on larger laser projectors such as laser cinema projectors. It is necessary to investigate factors outside of laser speckle reduction performance, such as optical efficiency, size, power consumption, reliability, and cost.

In large scale projectors such as cinema projector, many researchers were able to optimize all these parameters with different methods. However, little research has been conducted to find a suitable and optimized solution for handheld laser projectors such as mini-/pico- projectors. Such small projectors have become very important recently, and they are involved in many applications such as rear-projection televisions, near projection devices, in mobile projectors, and the automotive industry. These laser projectors have a small and compact optical light engine, so finding effective methods for reducing laser speckle is still a challenge.

HUMAN SPECKLE PERCEPTION THRESHOLD FOR STILL IMAGES FROM A LASER PROJECTION SYSTEM

A high quality and cost-efficient projection display solution can only be labelled as such if the laser speckle phenomenon goes unnoticed to a human observer. Therefore, it is imperative the value at which this phenomenon becomes otherwise unnoticeable to the human eye is known before a laser-based display system can be designed.

Fortunately, laser speckle has been widely studied and the human perception limit has been determined to be a sufficiently low speckle contrast ratio. Although the topic is generally debated some published results suggest that a speckle contrast ratio below 2% [2] or even 4% [46] would be sufficient such that a human observer would not notice any speckle patterns. The latter publication derived 4% as the lower limit based on intensity variations and speckle patterns being slightly different in terms of human perception. Another study then suggested that based on this fact a lower limit of approximately 3% would be sufficient [47].

The discrepancy in the lower limit to speckle contrast ratio can be attributed to the complexity of the experimental setup and the many variables involved. For example, to perform a standardized speckle measurement one must consider the resolution of the human eye at the objective plane, viewing distance between the observer and the screen, viewing angle, luminance, image status (fixed or video), etc.

In a normal experiment, 40 – 100 participants are selected to describe their perception of speckle patterns in an image. The participants are subject to multiple viewing angles, distances, levels of luminance, etc. The experiments are then conducted under dark and light room conditions. In conclusion, the threshold of human speckle perception is then choses at the point which less than 25% of the participants observe the speckle patterns [48], [49]. According to [50]–[53], the human eye cannot sense the speckle noise when the speckle contrast is lower than 5%.

PRINCIPLE OF SPECKLE REDUCTION

According to Goodman [44], [54], under the most ideal condition, the mean intensities of all N independent speckle patterns are the same, thus the SCR is reduced from 1 to R^{-1}, where $R = \sqrt{N}$ and is defined as the factor of reduction. If mean intensities for the independent speckle patterns in speckle-noise reduction process are not the same, however, reduction of the speckle will be introduced but in lower efficiency. Thus, if $R_1, R_{2'} R_{3'} \cdots, R_N$ are all independent reduction methods then the total reduction is $R < R_1 R_2 R_3 \cdots R_N$ [55].

As previously stated, the key to performing speckle reduction is to generate independent speckle patterns. Any speckle pattern can be modified by manipulating the three primary parameters for the illuminating laser light: wavelength, polarization, and angle. To generate independent laser speckle patterns, a diversification for the previously mentioned light parameters must exist. Most of the reduction methods are relay on three method, i.e. wavelength diversity (R_λ), polarization diversity (R_σ), and spatial (angular) diversity (R_Ω). The reduction by the three methods can be expressed by [56]:

$$SCR = (R_\lambda R_\sigma R_\Omega)^{-1} \qquad (1 - 5)$$

Based on the interference phenomenon, each wavelength will have a unique speckle pattern. When projecting two lasers with two different wavelengths ($\lambda_1 \neq \lambda_2$) on a screen, the speckle patterns of both lasers are uncorrelated when the

average relative phase shift formed by the screen surface is $\geq 2\pi$. It is possible to achieve the wavelength diversity by many methods: a) developing a broadband lasers, the increase of the spectral linewidth ($\Delta\lambda$) of the illuminating laser will reduce the speckle noise according to $R_\lambda = \sqrt{\Delta\lambda / \delta\lambda}$ where $\delta\lambda$ is the wavelength separation, b) using a pulsed laser, as $\Delta\lambda = \lambda^2/c\Delta\tau$, c is the light speed and $\Delta\tau$ is the laser pulse width, in that method $\Delta\tau$ has to be small to increase R_λ, this can be done by generating very narrow laser pulses using Q-switching techniques, by decreasing the laser pulse width the peak power will be very high and this might be harmful for the human eye. Because of the a safety precautions, this method is rarely to be used in projection purposes, c) by using more than single laser for illumination, and the minimum wavelength separation is $\delta\lambda = \lambda^2 / 2x$, where x is the average height of the screen surface, d) a combination from (a) and (b).

In spatial (angular) diversity (R_Ω) method, the N independent patterns are generated by sequential illumination of the N sub-resolution areas on the detector resolution spot within an ~30 or 50 msec integration time (to mimic the integration time of the human eye). These independent patterns can be considered as overlapping on intensity bases (as they are generated within human eye integration time) on retina, which provide an averaged light field with reduced SCR. A considerable R_Ω can be achieved by time-varying components such as vibrating/rotating diffuser, rotating light pipe, tunable liquid lenses, vibrating/rotating screen, and rotating lens array.

The ideal SCR reduction of overlapping N independent speckle patterns with equal intensity should be $N^{-\frac{1}{2}}$. However, this case will not be valid here as the R_Ω is dependent on the geometrical optics of the system [44] and there will be a saturation of speckle reduction even when N is very large. This limitation must be considered because it will not help to decrease the SCR below the human eye limit to recognize the speckle noise. Thus, it is very important to add other methods to achieve SCR lower than 5%.

When a laser beam with certain polarization is illuminating a depolarized surface (such as most of the white printing paper), the polarization will be scrambled because of multiple scattering. Some unique surface will keep the polarization constant, so R_σ in this case will equal to unity. The output speckle configurations are independent and uncorrelated because their polarization is orthogonal to each other. In this case, the value of R_σ is equal to $\sqrt{2}$. In another situation, if a single laser beam is divided into two rays, each portion is with different coherent length (this can be done by delaying the optical path of one of them) or using two different lasers with different coherent lengths and shining them on a depolarized screen, as a result, the value of R_σ will be equal to 2, not $\sqrt{2}$. This is because of the four generated speckle configurations are independent. In some projection applications such as 3D projection, it is not allowed to use such technology because it depends on maintaining the polarization of the laser beam constant.

SPECKLE SUPPRESSION METHODOLOGIES

Speckle noise is an intrinsic property of the laser beam, so it can be reduced by modifying the origin of the laser emission itself to generate a laser beam with low speckle noise. The speckle can also be reduced by other optical methods external to the laser source as well. Usually, to introduce a SCR lower than 5%, a combination of both methods will be highly recommended. According to this, we can classify the methods as: I) modifications inside the laser source, and II) modifications outside the laser source (or optical modifications).

I. Laser speckle reduction by modifying the laser source

The speckle is reduced in [57] by broadening the output emission spectrum of a AlGaInP/GaInP quantum well laser source. This is produced by introducing unequally spaced wells. The AlGaInP/GaInP quantum well on a substrate from GaAs contains 25 emitters. The emitters are designed to be unevenly spaced on the substrate. The thermal rising on the small spaced region will cause into a shift in the emitting wavelength. The output spectrum form that designed structure is 3.7 nm. The resultant SCR is 0.05 from that method.

The emission can be broadened in diode pumping solid state (DPSS) lasers by using Tandem-Poled Lithium Niobite (TPLN) crystal as a second harmonic generator inside a DPSS laser cavity [58]. The output spectral bandwidth is 36 times broader than the periodically poled case. The output band width is 6.5 nm, and the

resulting SCR is 0.041 which is one-seven of the conventional approach for a laser projection display.

The speckle noise can be reduced by blending multiple wavelengths with a slight wavelength difference between them [59], [60]. This will generate a degree of wavelength diversity. As a result, the speckle will be reduced. In [61], a combination of 4 laser emissions (531 nm, 532 nm, 541 nm, and 543 nm) was used. The 532 nm and 543nm emissions were from a diode pumped $Nd:YVO_4$ crystal and the 531 nm and 541 nm emissions were generated by a $Nd:GdVO_4$ crystal by using second-harmonic nonlinear crystals and the proper mirror coating. When combining this output with another speckle reduction method, the SCR will be 5.6%.

The speckle noise can also be reduced by decreasing the coherence length of the output laser. In random laser cavities, the active medium is made from a disordered material. The light is trapped inside the laser cavity, while will then undertake multiple scattering events, and this will create a laser emission at different frequencies which will decrease the coherency of the output emitted laser light [62].

The SCR is reduced by a factor greater than 2 via generating multiple independent longitudinal laser modes from a diode laser by modulating the driving current [63].

Another modification of DPSS laser sources has been performed in ref. [64]. A layer of microspheres (with 80 μm diameter) is inserted inside a plane-plane resonator. The active medium is a Nd: YAG crystal. The resonator will generate a combination of gaussian and fractal transverse modes in the output laser emission, as shown in **Figure 1-13b**. By optimizing the cavity structure, microsphere diameter, and by adding an appropriate second harmonic nonlinear crystal, a many parallel-multi-microbeam, each microbeam has a unique intensity (phase) distribution. Thus, a spatial diversification (by a combination of these different output phases) will produce an output free from laser speckle [65].

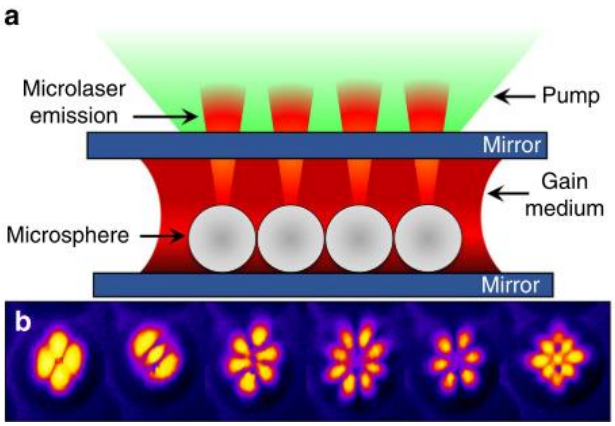

Figure 1-13: Hybrid micro laser resonators. A) Cross-sectional diagram (not to scale) of one configuration of the hybrid optical resonator. B) Images of some transverse modes associated with a sphere-stabilized micro laser [64].

II. Laser speckle reduction by optical systems

Most of these methods involve introducing a great number of independent speckle patterns within the human eye integration time. This was performed by introducing a time varying component to the of the laser path.

In [66], vibration of one or more optical diffusers can reduce the laser speckle to 2.80%. The diffuser can also be rotated to reduce the SCR as shown in ref. [67], [68].

In [69], the reduction of the speckle was performed by a weak scattering static diffuser (WSSD). The WSSD is constructed from a transparent microfluidic chip (from polydimethylsiloxane (PDMS)), the chip was filled by poly (methyl methacrylate) (PMMA) nanoparticles. The liquid which contains the nanoparticles from PMMA will be dispersed by a piezoelectric micropump through built-in micro channels. Figure **1-14a** shows the microfluidic chip, and Figure **1-14b** shows a proposed projection setup to measure the SCR. The lowest SCR is 0.04.

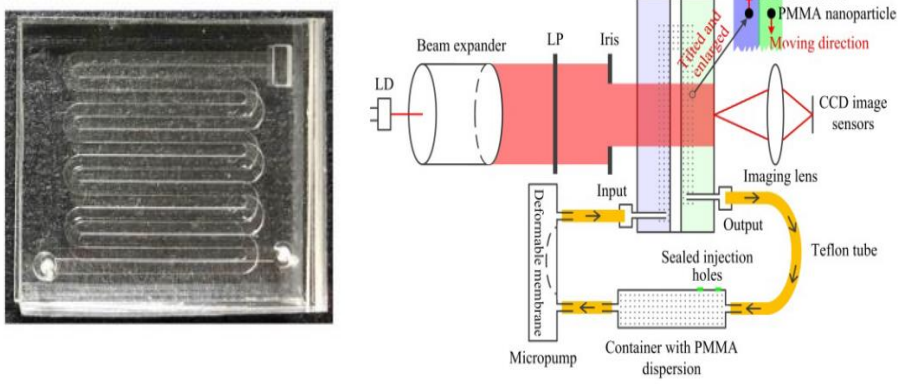

Figure 1-14: Illustration for a) microfluidic device, and b) the test setup for the device [69].

In [70], a rotation of the light pipe component can suppress to the speckle noise to be lower than 5%.

A diffraction optical element (DOE), in 1D [71] or 2D [72] form, on a loop of flexible film can reduce the speckle noise. The entrance light is diffracted into

different orders (denoted as 0, ±1) as in **Figure 1-15**. The thickness of the cell modulator must satisfy h $(n_0 - 1) = \lambda/2$ where λ is the wavelength of laser and n_0 is the material of the modulator index of refraction. The minimum SCR is < 2.6% as reported in ref.[71], [72].

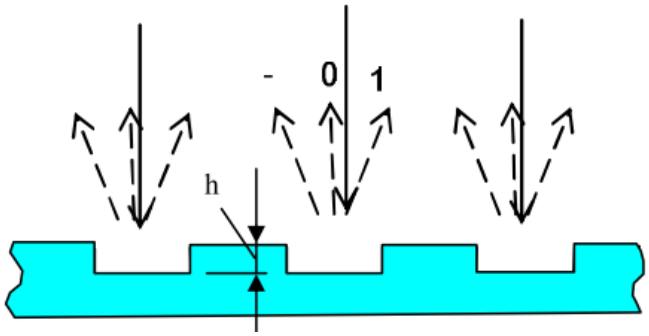

Figure 1-15: demonstration of DOE [62]

When light passes through a multimode fibre (MMF), the time taken by the light to move inside the fibre until reaching the end is determined by the propagation time. The longest time for propagation occurred when the light rays totally reflected inside the core of the fibre, which happens when the light was reflected at a critical angle from the interface between the core and cladding of the fibre. In [73], the MMF was used in the projection system, and the resulting SCR was 4.7%.

In [51], the speckle noise can be reduced by changing the focal lens of a tunable liquid lens. The liquid lens is constructed from two layers of an elastic polymer membrane as shown in **Figure 1-16**. A voice coil actuator can apply force to the elastic membrane which will change the curvature of the membrane. The change of the curvature will change the position of the focal point of the lens. In

Figure 1-17, the laser will pass through a tunable lens and then it will be projected on to an optical diffuser.

By applying a repetitive electrical signal on the voice coil actuator, it will modulate the output spatial phase of the laser beam after the optical diffuser. Eventually, the SCR after using the test setup in **Figure 1-17** will be lower than 0.05 [51].

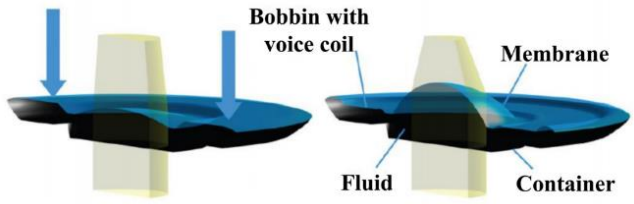

Figure 1-16: Illustration of the liquid lenses operation and construction [74].

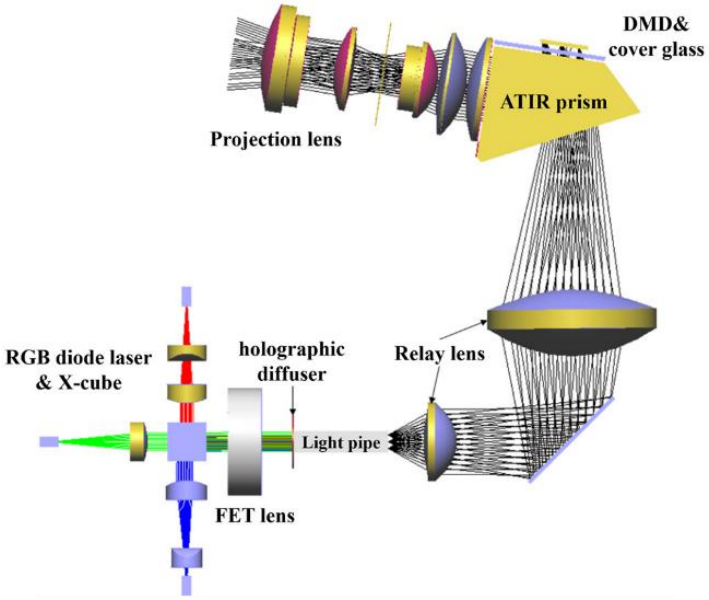

Figure 1-17: Schematic diagram of a projection system based on liquid lenses [51].

In [75], the speckle noise is reduced by using a deformable mirror shown in **Figure 1-18**.

The deformable mirror is a mirror which is controlled by selectively deforming the surface of the mirror. The mirror surface is made of an elastic membrane (elastic polymer). The deformation is applied by deploying many independent voice coil actuators beneath the membrane surface. The rate of change of these actuators is in the range of kHz. As a result, the vibration of such actuators at high speed will generate different phases for the mirror surface. As a result, the reflected laser light from such mirrors will have many uncorrelated speckle patterns. Thus, the integration of such patterns will reduce the SCR in the projected image in a projection system to 0.0236 [76].

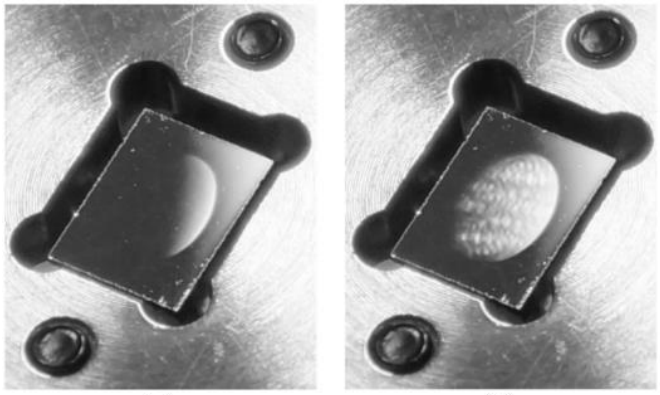

Figure 1-18: real image for deformable mirror a) under no control, and b) under control [77].

1.3 RESEARCH OBJECTIVES

MOTIVATION

While many speckle reduction techniques can be used to reduce the speckle noise, it is still a challenge in the case of mini- or pico- laser projectors. The brightness and size limits of such projectors are significant issues in the field of personal or mobile laser projectors. Hence most conventional laser speckle reduction methods are not suitable for mini- or pico- laser projectors due to the size limitations. Moreover, the cost is very important factor to help in commercializing handheld laser projectors, thus finding an affordable and practical solutions is still a challenge.

OBJECTIVE

The objective of this PhD work is investigation, application and characterization of methods for speckle suppression in a field of handheld laser projection system (mini- and pico- projectors).

OUTLINES

In general, any optical engine of any laser projection system is composed of a laser source followed by, in order, optics (RGB color combiner, homogenizer, and relay or field lenses), image generator module, and a projection lens. In our work, two different approaches are examined for speckle suppression.

I. The first approach (Chapter 2 & First published paper) depends on the concept of wavelength diversity:

This is achieved by modifying the design of the laser source to generate multiple output lasing wavelengths from the same laser cavity. The benefits of using multi-output lasering wavelengths at the same time from the same source are low speckle noise, increasing the optical efficiency, small size, and simplified integration within a projector. The DPSS laser with a single active medium usually emits a single wavelength laser with a narrow linewidth. The high coherence of the output laser will increase the speckle noise effect. The multi-output wavelength from a DPSS laser has a role of increasing the overall linewidth of the output emission by blending all the output lasers together. The dual output emission is the most preferable type from multi emission laser, as the output power level in dual-mode emission can be controlled to a certain degree depending on the production technique it. DPSS lasers that utilize cascaded active mediums are preferable. It can be tailored to generate specific output wavelengths at the same time without any mode competition inside the same cavity with a wavelength difference more than 1 nm. The output power can be controlled mechanically to let the ratio of the output power at each wavelength equal to 1. This is also very important from the point of speckle-noise reduction, because when the power ratio is close to 1, the SCR will be multiplied by factor $1/\sqrt{2}$.

In Chapter 2, the cavity is designed based on end pumping two crystals; the first crystal is $Nd:YVO_4$ and the second one is $Nd:GdVO_4$. The cavity parameters have been optimised to achieve a high optical efficiency, compact structure, high stability, and low SCR laser source. The output lasers from the cavity were in the NIR band (1062.4 nm and 1063.8 nm) with optical-to-optical (O-O) efficiency 37% and 48% for parallel and perpendicular polarisation, respectively. So, they need a uniquely designed PPLN crystal to serve as a second harmonic crystal to generate green laser light for projection applications.

II. The second approach (Chapter 3 & Second published paper) for speckle suppression is considered an optical solution by introducing the concept of angular diversity for anti-speckle technology:

Our new method was based on vibrating a simple lens (with small focal length) in front of a green laser source. A commercial CD/DVD pickup lens module is used to vibrate the lens from 30 Hz to 130 Hz in a one direction (1D), then followed by a diffuser, beam homogeniser, and projection lens. The laser beam scans the lens' curvature; thus, the laser beam is deflected to form a bright line on the optical diffuser. Each point on the bright line on the diffuser will be considered as an uncorrelated pattern. The integration of these patterns under the human eye integration time reduces the speckle noise. This provides small size, low noise, low power consumption, simple drive electronics and simplified integration within a projector. The study is performed by using a single DPSS

laser (at 532 nm) and a single laser diode (LD) (at 520 nm). The device (vibrating lens and diffuser) provides up to 20.1% and 41.7% of speckle suppression for a DPSS laser and LD, respectively. The overall speckle reduction efficiency of the system (vibrating lens, diffuser, light-pipe, and projection lens) is 75.6% and 81.25% for the DPSS laser and LD laser, respectively. It is shown experimentally that speckle contrast can be reduced to 0.15 for a single DPSS laser and to 0.07 for LD. Although the reduction efficiency is high, the output SCR is still higher than the human eye perception threshold for speckle noise (0.05).

III. The third approach (Chapter 4 & third published paper) is considered as an optimization for the second approach:

Eventually, different speckle suppression methods such as wavelength diversity and angular diversity are applied in a real laser pico-projection system . The wavelength diversity is achieved by blending 532 nm with 520 nm, and the angular diversity is performed by vibrating two lenses in two perpendicular directions (2D). The study has been done for the green laser because it is the most sensitive colour to the human eye. A speckle contrast of 0.04 is attained for combined green lasers in the projection system.

1.4 THESIS ORGANIZATION

This section is summarizing the contents of each chapter in this dissertation:

- **Chapter 1** sheds light on the background behind the subject of this research, the objectives' outlines, and the general overview of the thesis' order.
- **Chapter 2** presents an overview of the technique of end-pumping of solid-state lasers (EPSSL) for two-cascaded laser crystals (2CLC). The main topic is about increasing the O-O efficiency of the EPSSL for 2CLC. The output of our modified design results in increasing the O-O efficiency by 20 %. The instability of the output power was 0.4% showing a great performance for the output laser. The output SCR is reduced as well from 70% to 53.9%. Our design is promising as a compact laser source for small size projectors.
- **Chapter 3** presents the problem of speckle-noise and its negative effect on laser projection. It also shows the need to find a practical solution to reduce the speckle noise in the small light engines of handheld projectors. In this chapter, a new method was developed to be fit on to such small light engines. The method is based on introducing angular and spatial diversity to the green laser sources such as DPSS and LD sources. Eventually, the output results show that our technique is promising to achieve low SCR, but it never achieved an SCR lower than the human eye limits for avoiding the speckle noise effect entirely (<5%).
- **Chapter 4** presents the development of a new method to reduce the speckle noise which is presented previously in Chapter 3. The method was

upgraded by increasing the diversity from 1D to 2D scanning. Moreover, the green laser source was a combination of two laser sources (DPSS and LD sources) with optimized power ratios. The optimization for the power ratios was intended to reduce the SCR and improve the colour quality of projected images. The upgrade has been performed by using a real pico-projector engine. The output SCR is < 5% which is lower than the human eye perception limit for speckle noise.

- **Chapter 5** provides a summary of this research, the overall conclusions, and suggestions for future work.

It is worth noting that Chapters 2 through 4 represent standalone manuscripts that are already published, or submitted; nonetheless, these chapters together represent a consistent research body, as outlined in the dissertation introduction. However, some overlap might exist for the completeness of each standalone chapters/manuscripts.

1.5 NOTATIONS

x_n: amplitude of the *n*th complex phasor element.

ϕ_n: phase of the *n*th complex phasor element.

σ_I: standard deviation

$\bar{I}$: mean intensity of the output pattern

ϕ_n: distribution of a random phase

R_λ: wavelength diversity

R_σ: polarization diversity

R_Ω: spatial (angular) diversity

Greek Letters:

$\Delta\lambda$: spectral linewidth of the illuminating laser

$\Delta\tau$: laser pulse width

$\partial\lambda$: minimum wavelength separation

1.6 ACRONYMS

LEDs: light-emitting diodes

RGB: red, green, and blue

DLP: digital light processing

LCoS: liquid crystal on silicon

LBS: laser beam-steering

DMD: digital mirror devices

MOEMS: micro-opto-electromechanical system

LCD: liquid crystal display

$\boldsymbol{X}$**:** The resultant of the output field

N: number of random phasors elements

X: magnitude of the complex resultant

SCR: the speckle contrast ratio

PSF: point spread function

R: the factor of reduction

C: light speed

FWHM: full width half maximum

TPLN: Tandem-Poled Lithium Niobite crystal

WSSD: weak scattering static diffuser

PDMS: polydimethylsiloxane

PMMA: poly methyl methacrylate nanoparticles.

DOE: diffraction optical element

MMF: a multimode fibre

DPSS: diode pumped solid-state

1D: one-dimensional direction

LD: laser diode

2D: lenses in two perpendicular directions

EPSSL: end-pumping of solid-state lasers

2CLC: two-cascaded laser crystals

O-O: optical-to-optical efficiency

1.7 REFERENCES

[1] C. H. Townes, "The first Laser," *press.uchicago.edu*. [Online]. Available: http://www.press.uchicago.edu/Misc/Chicago/284158_townes.html.

[2] M. S. Brennesholtz and E. H. Stupp, *Projection Displays*, Second edi., vol. 19. John Wiley & Sons, 2008.

[3] U. Weichmann *et al.*, "UHP lamps for projection systems: getting always brighter, smaller, and even more colorful," *In Liquid Crystal Materials, Devices, and Applications X and Projection Displays X*, vol. 5289, no. May 2004, pp. 255–266, 2004, doi: 10.1117/12.541159.

[4] X. Yu, Y. L. Ho, L. Tan, H. Huang, and H. Kwok, "LED-Based Projection Systems," vol. 3, no. 3, pp. 295–303, 2007.

[5] S. Yeralan, D. Doughty, and R. Blondia, "Advantages of using high-pressure short-arc xenon lamps for display systems," *International Society for Optics and Photonics*, vol. 5740, no. April 2005, pp. 27–35, 2005, doi: 10.1117/12.590713.

[6] X. Compact and A. Lamps, "Xenon Compact Arc Lamps," *Journal of the Optical Society of America*, vol. 4, no. 6, pp. 385–388, 1951.

[7] U. Weichmann *et al.*, "Light-sources for small-etendue applications: a comparison of xenon- and UHP lamps," *In Projection Displays XI*, vol. 5740, no. April 2005, pp. 12–26, 2005, doi: 10.1117/12.590172.

[8] G. Derra *et al.*, "UHP lamp systems for projection applications," *Journal of Physics D: Applied Physics*, vol. 38, pp. 2995–3010, 2005, doi: 10.1088/0022-3727/38/17/R01.

[9] K. Kawai and M. Matsumoto, "Short-arc metal halide lamp suitable for projector application," *Projection Displays*, vol. 2407, no. April 1995, pp. 23–35, 2004, doi: 10.1117/12.205906.

[10] G. Harbers, S. J. Bierhuizen, and M. R. Krames, "Performance of High Power Light Emitting Diodes in Display Illumination Applications," *Journal of Display Technology*, vol. 3, no. 2, pp. 98–109, 2007.

[11] K. Beeson, S. Zimmerman, W. Livesay, R. Ross, C. Livesay, and K. Livesay, "61 . 5 : LED-Based Light-Recycling Light Sources for Projection Displays Overview of Light-Recycling Cavities," *SID Symposium Digest of Technical Papers*, vol. 37, pp. 1823–1826, 2006.

[12] N. Narendran and Y. Gu, "Life of LED-Based White Light Sources," *Journal of display technology*, vol. 1, no. 1, pp. 167–171, 2005.

[13] T. Watanabe, K. Nakamura, S. Kawami, Y. Fukuda, and T. Tsuji, "Optimization of driving lifetime durability in organic LED devices using Ir complex," *Organic Light-Emitting Materials and Devices IV*, vol. 4105, no. February 2001, pp. 175–182, 2001, doi: 10.1117/12.416892.

[14] F. Fournier, S. Member, and J. Rolland, "Design Methodology for High Brightness Projectors," in *Journal of Display Technology*, 2008, vol. 4, no. 1, pp. 86–91.

[15] J. Kuo, H. Wu, and G. Lee, "Optical projection display systems integrated with three-color-mixing waveguides and grating- light-valve devices," *Optics express*, vol. 14, no. 15, pp. 217–219, 2006.
[16] R. G. B. Led, M. H. Keuper, G. Harbers, and S. Paolini, "26.1: RGB LED Illuminator for Pocket-Sized Projectors," *SID Symposium Digest of Technical Papers*, vol. 35, pp. 943–945, 2004.
[17] C. J. Joshi, "14 . 4 L : Late-News Paper : Development of Long Life , Full Spectrum Light Source for Projection Display," *SID Symposium Digest of Technical Papers*, vol. 38, no. c, pp. 959–961, 2007.
[18] and A. M. Niven, Greg, "Trends in laser light sources for projection display," *Proceedings of the 13th International Display Workshops LAD2*, vol. 2, 2006.
[19] U. Steegmüller *et al.*, "Visible lasers for mobile projection," *Proceedings of SPIE*, vol. 7001, no. April 2008, pp. 70010D-70010D–8, 2008, doi: 10.1117/12.781082.
[20] H. Sugiura, T. Sasagawa, A. Michimori, and E. Toide, "56 . 3 : 65-inch , Super Slim , Laser TV with Newly Developed Laser Light Sources Development of Laser TV 65-inch Super Slim Laser TV," *In SID Symposium Digest of Technical Papers*, vol. 39, pp. 854–857, 2008.
[21] M. Sakamoto, R. R. Craig, J. G. Endriz, M. Sakamoto, R. R. Craig, and J. G. Endriz, "Highly reliable high-power cw AlGaAs (808 nm) 1-cm bar laser diodes for Nd: YAG pump application.," *Solid State Lasers and Nonlinear Crystals*, vol. 2379, no. April 1995, pp. 130–136, 1995, doi: 10.1117/12.206460.
[22] J. C. Brazas, M. W. Kowarz, J. C. Brazas, and M. W. Kowarz, "High-resolution laser-projection display system using a grating electromechanical system (GEMS)," *MOEMS Display and Imaging Systems II*, vol. 5348, no. January 2004, pp. 65–75, 2019, doi: 10.1117/12.531101.
[23] Christie, *Setting the stage for the next-generation of visual events*. 2019.
[24] Aaxa, *World's Smallest 20 lumen Pico Projector*. 2019.
[25] Delen, *Mini Beamer Laser projector*. 2019.
[26] W.-F. Hsu and I.-L. Chu, "Speckle Suppression By Integrated Sum of Fully Developed Negatively Correlated Patterns in Coherent Imaging," *Progress In Electromagnetics Research B*, vol. 34, no. January 2011, pp. 1–13, 2011, doi: 10.2528/PIERB11070601.
[27] J. Poyet and Y. Lutz, "Light pipe design method and stepper experimentation for interference effects reduction in laser illumination," vol. 55, no. 7, pp. 1–7, 2018, doi: 10.1117/1.OE.55.7.075103.
[28] S. Hwang, T. Kim, J. Lee, and T. J. Yu, "Design of square-shaped beam homogenizer for petawatt-class Ti:sapphire amplifier," *Optics Express*, vol. 25, no. 9, p. 9511, 2017, doi: 10.1364/oe.25.009511.
[29] F. Chen, Z. Qin, S. Zhao, K. Wang, and S. Liu, "Integral freeform illumination lens design of LED based pico-projector," *Applied Optics*, vol. 52, no. 13, p. 2985, 2013, doi: 10.1364/ao.52.002985.

[30] B. Lee, "Introduction to digital micromirror device (DMD) technology," *readkong.com*. [Online]. Available: https://www.readkong.com/page/dmd-101-introduction-to-digital-micromirror-device-dmd-3201197.
[31] C. Tew *et al.*, "Electronic control of a digital micromirror device for projection displays.," *Proceedings of IEEE International Solid-State Circuits Conference-ISSCC'94*, vol. 1150, pp. 130--131, 1994.
[32] and S. P. Harbers, Gerard, Matthijs Keuper, "Performance of high power LED illuminators in color sequential projection displays.," *Proc IDW*, vol. 3, pp. 1585–1588, 2003.
[33] C. Jiang, D. Hu, and Y. Lu, "Digital micromirror device (DMD)-based high-cycle torsional fatigue testing micromachine for 1D nanomaterials," *Micromachines*, vol. 7, no. 3, pp. 1–9, 2016, doi: 10.3390/mi7030049.
[34] R. Wilson, "Designing MEMS-based DLP pico projectors," *electronicsweekly.com*, 2014. [Online]. Available: https://www.electronicsweekly.com/news/products/displays-2/designing-mems-based-dlp-pico-projectors-2014-07/.
[35] Diffen, *DLP vs. LCD Projector*. 2019.
[36] B. Swetha, *LCD Vs. LCoS: Projector Technology Face-off*. 2019.
[37] santec, "Liquid crystal," *santec.com*, 2019. [Online]. Available: https://www.santec.com/en/about/coretechnology/lc.
[38] lcd-parts, "Polarizer," *lcd-parts.com*, 2019. [Online]. Available: http://www.lcd-parts.com/polarizer.aspx.
[39] J. Funk, "Pico projector," *slideshare.net*, 2012. [Online]. Available: https://www.slideshare.net/Funk98/pico-projector-12565671.
[40] J. Honkanen, "MEMS-based Laser Beam Scanning Technology Platform; Basis for Applications from Displays to 3D Sensors and 3D Printers," *slideshare.net*. [Online]. Available: https://www.slideshare.net/Jari512/memsbased-laser-beam-scanning-technology-platform-basis-for-applications-from-displays-to-3d-sensors-and-3d-printers.
[41] M. Brown and H. Urey, "MEMS Microdisplays," *Handbook of Visual Display Technology*, pp. 2067--2080, 2012, doi: 10.1007/978-3-642-35947-7.
[42] Ed. Dainty, J. Christopher, "Laser speckle and related phenomena.," *Springer science & business Media*, vol. 9, 2013.
[43] J. W. Goodman, *Speckle Phenomena in Optics: Theory and Applications*. Roberts and Company Publishers, 2007.
[44] J. W. Goodman, "Statistical properties of laser speckle patterns," in *Laser speckle and related phenomena*, Springer, 1975, pp. 9–75.
[45] A. E. Ennos, "Speckle Interferometry," in *Laser Speckle and Related Phenomena*, J. C. Dainty, Ed. Berlin, Heidelberg: Springer Berlin Heidelberg, 1975, pp. 203–253.
[46] L. Wang, T. Tschudi, T. Halldórsson, and P. R. Pétursson, "Speckle reduction in laser projection systems by diffractive optical elements," *Applied Optics*, vol. 37, no. 10, pp. 1770–1775, 1998, doi: 10.1364/AO.37.001770.

[47] Y. M. Lee, D. U. Lee, J. M. Park, S. Y. Park, and S. G. Lee, "P-45: A Study on the Relationships between Human Perception and the Physical Phenomenon of Speckle," *SID Symposium Digest of Technical Papers*, vol. 39, no. 1, p. 1347, 2008, doi: 10.1889/1.3069394.
[48] A. R. Reibman, S. Kanumuri, V. Vaishampayan, and P. C. Cosman, "Visibility of individual packet losses in MPEG-2 video," *Proceedings - International Conference on Image Processing, ICIP*, vol. 1, pp. 171–174, 2004, doi: 10.1109/ICIP.2004.1418717.
[49] S. Roelandt *et al.*, "Human speckle perception threshold for still images from a laser projection system," *Optics Express*, vol. 22, no. 20, p. 23965, 2014, doi: 10.1364/oe.22.023965.
[50] J. W. Pan and C. H. Shih, "Speckle noise reduction in the laser mini-projector by vibrating diffuser," *Journal of Optics (United Kingdom)*, vol. 19, no. 4, p. 045606, 2017, doi: 10.1088/2040-8986/aa608d.
[51] C. Lo and J. Pan, "Speckle reduction with fast electrically tunable lens and holographic diffusers in a laser projector," *Optics Communications*, vol. 454, no. July 2019, p. 124301, 2020, doi: 10.1016/j.optcom.2019.07.063.
[52] S. Tu and H. Y. Lin, "Speckle Contrast Reduction with Multi-Projection Units for a MEMS Scanning Laser Projector Shih-Yu Tu * and Hoang Yan Lin *," pp. 1733–1736, 2015.
[53] J.-W. Pan and C.-H. Shih, "Speckle reduction and maintaining contrast in a LASER pico-projector using a vibrating symmetric diffuser," *Optics Express*, vol. 22, no. 6, p. 6464, 2014, doi: 10.1364/oe.22.006464.
[54] J. W. Goodman, "Some fundamental properties of speckle," *Journal of the Optical Society of America*, vol. 66, no. 11, p. 1145, 1976, doi: 10.1364/josa.66.001145.
[55] J. I. Trisnadi, "<title>Speckle contrast reduction in laser projection displays</title>," *Projection Displays VIII*, vol. 4657, no. April 2002, pp. 131–137, 2002, doi: 10.1117/12.463781.
[56] J. I. Trisnadi, "Speckle contrast reduction in laser projection displays.," *Projection Displays VIII*, vol. 4657, no. April 2002, pp. 131–137, 2002, doi: 10.1117/12.463781.
[57] A. Furukawa *et al.*, "Effective speckle reduction in laser projection displays," *Emerging Liquid Crystal Technologies III*, vol. 6911, no. January 2008, p. 69110T, 2008, doi: 10.1117/12.760860.
[58] N. E. Yu *et al.*, "Speckle noise reduction on a laser projection display via a broadband green light source," *Optics Express*, vol. 22, no. 3, p. 3547, 2014, doi: 10.1364/oe.22.003547.
[59] S. Li, R. V. Roussev, D. V. Kuksenkov, W. A. Wood, and C. M. Lynn, "Multiple-wavelength synthetic green laser source for speckle reduction," *Nonlinear Frequency Generation and Conversion: Materials, Devices, and Applications X*, vol. 7917, no. February 2011, p. 79170B, 2011, doi: 10.1117/12.887545.

[60] G. Zheng *et al.*, "Laser digital cinema projector," *IEEE/OSA Journal of Display Technology*, vol. 4, no. 3, pp. 314–318, 2008, doi: 10.1109/JDT.2008.924163.
[61] et al. Yanagisawa T , Shohda F , Akino Y , Ikeda K , Shen Z , Yamamoto S, "De- speckle effects resulted by wavelength multiplexing of intra-cavity solid-state green lasers," in *Laser display and lightning conference Japan*, 2015.
[62] B. Redding, M. A. Choma, and H. Cao, "Speckle-free laser imaging using random laser illumination," *Nature photonics*, vol. 6, no. June, p. 355, 2012, doi: 10.1038/NPHOTON.2012.90.
[63] I. Yilmazlar and M. Sabuncu, "Speckle noise reduction based on induced mode Hopping in a semiconductor laser diode by drive current modulation," *Optics and Laser Technology*, vol. 73, pp. 19–22, 2015, doi: 10.1016/j.optlastec.2015.04.014.
[64] J. A. Rivera, T. C. Galvin, A. W. Steinforth, and J. G. Eden, "Fractal modes and multi-beam generation from hybrid microlaser resonators," *Nature Communications*, vol. 9, no. 1, pp. 1–8, 2018, doi: 10.1038/s41467-018-04945-8.
[65] J. G. Rivera, Jose A and Steinforth, Austin and Eden, "Low-speckle light source and imaging devices with micro-refractive element stabilized laser array," 2019.
[66] J.-W. Pan and C.-H. Shih, "Speckle reduction and maintaining contrast in a LASER pico-projector using a vibrating symmetric diffuser," *Optics Express*, vol. 22, no. 6, p. 6464, 2014, doi: 10.1364/OE.22.006464.
[67] K. Suzuki and S. Kubota, "Understanding the exposure-time effect on speckle contrast measurement for laser projection with rotating diffuser," *Optical Review*, vol. 26, no. 1, pp. 145–151, 2018, doi: 10.1007/s10043-018-0467-7.
[68] T. Stangner, H. Zhang, T. Dahlberg, K. Wiklund, and M. Andersson, "Step-by-step guide to reduce spatial coherence of laser light using a rotating ground glass diffuser," *Applied Optics*, vol. 56, no. 19, p. 5427, 2017, doi: 10.1364/ao.56.005427.
[69] Z. H. T. Ong, W. E. C. Heng, S. U. J. Ia, and X. Uyuan, "Weak-scattering static diffuser by fast pumping dispersed-nanoparticles in a long distance using microfluidic flows for efficient laser speckle reduction," vol. 26, no. 16, pp. 20270–20280, 2018, doi: 10.1364/OE.26.020270.
[70] M. Sun, "Speckle suppression with a rotating light pipe," *Optical Engineering*, vol. 49, no. 2, p. 024202, 2010, doi: 10.1117/1.3314310.
[71] A. Lapchuk *et al.*, "Very efficient speckle suppression in the entire visible range by one two-sided diffractive optical element," *Appl. Opt.*, vol. 56, no. 5, pp. 1481–1488, 2017, doi: 10.1364/AO.56.001481.
[72] Q. Xiong *et al.*, "Experimental demonstration of a flexible DOE loop with wideband speckle suppression for laser pico-projectors," *Optics Express*, vol. 26, no. 20, p. 26188, 2018, doi: 10.1364/oe.26.026188.
[73] Q. Ma, C. Q. Xu, A. Kitai, and D. Stadler, "Speckle reduction by optimized multimode fiber combined with dielectric elastomer actuator and lightpipe

homogenizer," *Journal of Display Technology*, vol. 12, no. 10, pp. 1162–1167, 2016, doi: 10.1109/JDT.2016.2568458.

[74] Optotune, "Electrically tunable large aperture lens EL-16-40-TC-VIS-20D," 2016. .

[75] T.-K.-T. Tran, X. Chen, Ø. Svensen, and M. N. Akram, "Speckle reduction in laser projection using a dynamic deformable mirror," *Optics Express*, vol. 22, no. 9, p. 11152, 2014, doi: 10.1364/OE.22.011152.

[76] H.-A. Chen, J.-W. Pan, and Z.-P. Yang, "Speckle reduction using deformable mirrors with diffusers in a laser pico-projector," *Optics Express*, vol. 25, no. 15, p. 18140, 2017, doi: 10.1364/OE.25.018140.

[77] F. Shevlin and D. Ph, "Speckle Reduction With Multiple Laser Pulses Dyoptyka device for speckle reduction : phase randomizing deformable mirror," in *2nd Laser Display Conference (LDC'13)*, 2013.

Chapter 2

EFFICIENT DUAL-WAVELENGTHS CONTINUOUS MODE LASERS BY END-PUMPING OF SERIES $Nd:YVO_4$ AND $Nd:GdVO_4$ CRYSTALS AND SPECKLE REDUCTION STUDY

ABSTRACT

In this paper, diode-pumped solid-state (DPSS) lasers based on end-pumping series $Nd:YVO_4$ and $Nd:GdVO_4$ crystals were studied. Dual-, tri-, and quad-wavelength emissions were achieved. In the dual-wavelength emission operation, an optical-to-optical efficiency (O-O) of 49.6% and the power instability was 0.4% were obtained. It is the most efficient and compact lasers operating in continuous wave mode reported to date with series crystals. Besides of this, the effect of changing power ratio between the output laser powers on speckle reduction was investigated for the first time. In addition, tri and quad wavelength emissions were achieved with a reasonable efficiency simply by optimizing the cavity parameters.

Keywords: diode-pumped solid-state; end-pumping series crystals; Dual-, tri-, and quad-wavelength emissions; Multi emission spectrum; laser speckle reductions; wavelength diversity.

2.1. INTRODUCTION

Recently, development of laser sources based on end-pumping of series laser crystals with multiple (dual/tri/quad) emission wavelengths has attracted attention due to their potential applications such as THz generation [1], precise spectroscopy [2], imaging [3], biomedical instrumentation [4], lidar [5], and nonlinear scientific research of optical mixers [6].

Many methods have been reported to achieve multi-wavelength emission such as: inserting optical selective elements (OSE) inside a cavity like etalon [7] or birefringent filter [8], by two inequivalent emitting centers coexisted inside the laser crystal [9], by angle tuning for a laser crystal [10], pumping two distinct crystals separately [11], and pumping two different crystals simultaneously [12]. For single gain medium based multi-wavelength emissions their lasing wavelengths generally share the same upper energy level which makes their mode competition become serious [13], thus, the approach of end pumping series crystals [12] is considered to be a solution. It uses two separate gain mediums and each crystal has its unique wavelength. They do not share the same upper energy levels which means no mode competition exists, thus, the stability is improved. For example, instability as low as 0.25% (the instability for each wavelength component is 1.93% and 1.23%) has been reported for a free-running dual-wavelength end-pumping series crystal laser [3]. Besides this, the technique can also be used to equate the output intensities for the dual-wavelength emission without any custom-designed mirrors or inserting

any OSEs. The dual-wavelength emissions from two series crystals has been demonstrated using a variety of pairs of laser crystals including $Nd:YVO_4/Nd:GdVO_4$ [14], $Nd:YVO_4/Nd:KGW$ [15], $Nd:YVO_4/Nd:LuVO_4$ [15], Nd:YAG/Nd:YLF, and Nd:YLF/Nd:YLF [3]. To date, most of the reported end-pumping series crystal lasers are operated in pulsed mode, and the highest reported O-O efficiency was 33% [15].

In the meantime, end-pumping series crystal lasers have a lower laser speckle effect than general single wavelength DPSS lasers, since the laser speckle can be reduced when multiple wavelengths are blended together [16]. Laser speckle has a significant impact on several applications mentioned above. However, characteristics of laser speckle of end-pumping series crystal lasers have not been studied. Moreover, the laser performance of end-pumping series crystal lasers in the continuous wave (CW) mode, which is important in many practical applications, has not been investigated systematically.

In this paper, compact DPSS lasers based on the end-pumping series $Nd:YVO_4/Nd:GdVO_4$ crystals are investigated in detail. The characteristics of dual-, tri-, and quad-wavelengths emission are studied and discussed. Laser speckle properties of the developed lasers are studied in terms of the power ratio between the emission peaks and the number of emission wavelengths. CW mode compact lasers based on the end-pumping series $Nd:YVO_4/Nd:GdVO_4$ crystals with high O-O efficiency, high stability, and low speckle contrast ratio have been achieved.

2.2. EXPERIMENTS

DUAL-WAVELENGTH LASER SETUP

The configuration of the end-pumping series-crystals cavity is shown in **Figure 2-1a**. A plane-plane cavity structure was used in the laser system. A fiber pigtailed laser diode (LD) was used as the pumping light source. The LD had a central wavelength of 808 nm, and maximum output power of 7 W. The core diameter was 200 μm with a 0.22 numerical aperture (NA). The pumping light from the fiber was elliptically polarized, with a power ratio of approximately 2:1 between its maximum power along the vertical (π-polarization) and horizontal (σ-polarization) directions. A graded-index (GRIN) lens and a plano-convex lens were used to focus the output beam from the LD. The GRIN lens had a 1.8 mm diameter, 0.23 Pitch, 0° Face Angle, and was anti-reflection (AR) coated at 810 nm, while the plano-convex lens had a diameter of 4 mm and a focal length of 2.5 mm. This beam focusing system was used to focus the laser beam into the gain medium with a minimum beam waist (ω_0) of 120 μm.

Two crystals, the first laser crystal (LC_1) and second laser crystal (LC_2), were used as the gain mediums. LC_1 was 1-at% doped a-cut $Nd:YVO_4$ and LC_2 was 0.5-at% doped a-cut $Nd:GdVO_4$. The crystals had cross-sections of 3 mm × 3 mm and thicknesses of 2 mm and 4 mm, respectively. The input facet of LC_1 was coated with a high-reflection (HR) coating at 1064 nm and high transmission coating at

808 nm to be used as the input mirror (M_1), the output facet of LC_1 was AR coated at 1064 nm. Both facets of LC_2 were AR coated at 1064 nm & 808 nm.

The temperatures of LC_1 and LC_2 were controlled by two thermoelectric coolers independently. The output-mirror (M_2) had a reflectivity of 85 % at 1064 nm. A filter was used to block the remaining 808 nm pumping light after M_2, and a polarizing beam splitter (PBS) was employed to separate the π-polarized and σ-polarized components of the output laser beam. The laser output power was measured by a power meter, and output power stability was characterized as well. The output spectrum was captured by an optical spectrum analyzer (OSA) with a resolution of 0.1 nm.

The relative position of the two crystals is shown in **Figure 2-1b**. In the experiments, the π-polarization component of the elliptically polarized pumping light was aligned parallel with the c-axis of LC_2. The distance between the crystals in the σ-π configuration was 0.1 mm. The position of the minimum pump beam waist (z_o) was varied along the optical axis (in the z-direction) through the cavity, allowing for the control of the gain and pumping absorption efficiency of each crystal [17]. z_o=0 was defined as the input facet (or M_1) of LC_1. The pump absorption efficiency of each crystal was also controlled by altering the pumping wavelength (λ_p) which was achieved by changing the temperature of the LD.

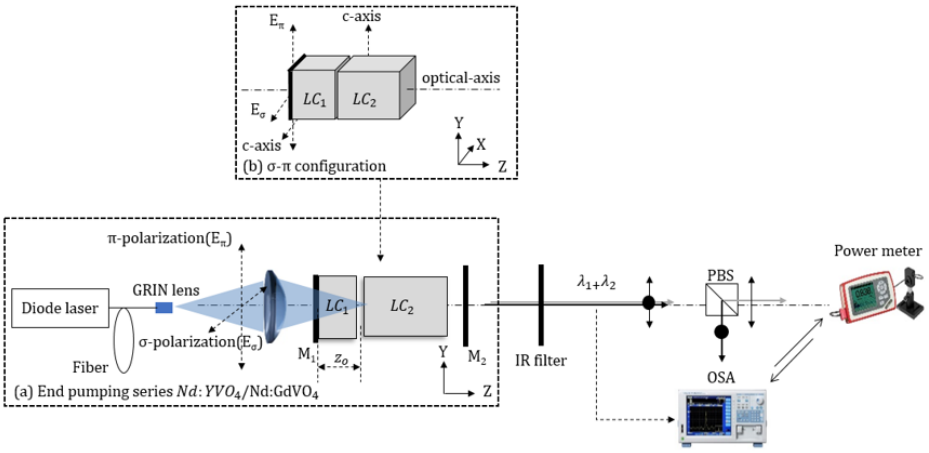

Figure 2-1: The experimental setup used in the measurements: (a) diagram for end pumping series crystals laser and (b) schematic diagram for σ-π configurations.

TRI/QUAD WAVELENGTH LASER SETUP

The experimental setup of tri-/quad-wavelengths emission was similar to the one described in the previous section. The tri-/quad-emissions were achieved by rotating LC_1 and tilting M_2 [10,17].

Figure 2-2 shows the setup of tri-/quad-wavelengths emission. **Figure 2-2a** represents a schematic diagram for the series crystals. E_π , E_σ represent the polarization directions of the pump light. θ is the tilting angle of M_2 with respect to the y-axis and ∅ is the angle of rotation of LC_1 about the z-axis. The c-axis of the two crystals was parallel to E_π.

Figure 2-2b represents the xy-view for the setup. In **Figure 2-2b**, the left subfigure represents the setup of tri-wavelengths emission (θ=0.7 mrad and ∅=0 rad), and the right subfigure represents the setup of quad wavelengths emission

(θ=0.7 mrad and ∅=0.78 rad). The distance between LC_1 and LC_2 was 0.2 mm. The length of the cavity was 18 mm. The temperature of LC_1 and LC_2 were set at 45 ℃ and 18 ℃, respectively. Tri-/quad- wavelengths started to be seen until input pump power reach 4.2 W and 4.38 W, respectively.

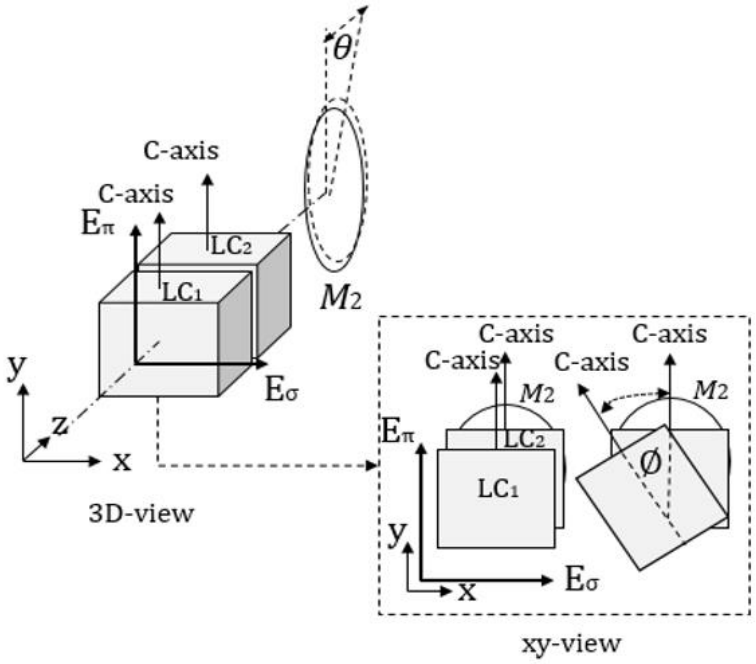

Figure 2-2: The configuration of LC_1 and LC_2 in multi wavelength emission. (a) A 3D configuration with a tilted angle of θ for M_2, and (b) xy view of the setup for tri output wavelengths emission with θ=0.7 mrad and ∅= 0 rad (left) and quad wavelengths emission (right) with θ=0.7 mrad and ∅= 0.78 rad.

THE CONFIGURATION OF SPECKLE CONTRAST IMAGING SYSTEM

Figure 2-3 shows the setup used for measuring the speckle contrast ratio (SCR). The SCR of the proposed laser systems was measured by projecting the output beam via a projection lens onto a white print paper, then using a CCD

camera (C2400 from Hamamatsu/ spectral response: 400-1800 nm) to capture the speckle-pattern. The focal length of the camera lens is 50 mm with f/16. Both the distances from projection lens to screen and screen to camera were set to be 50 cm.

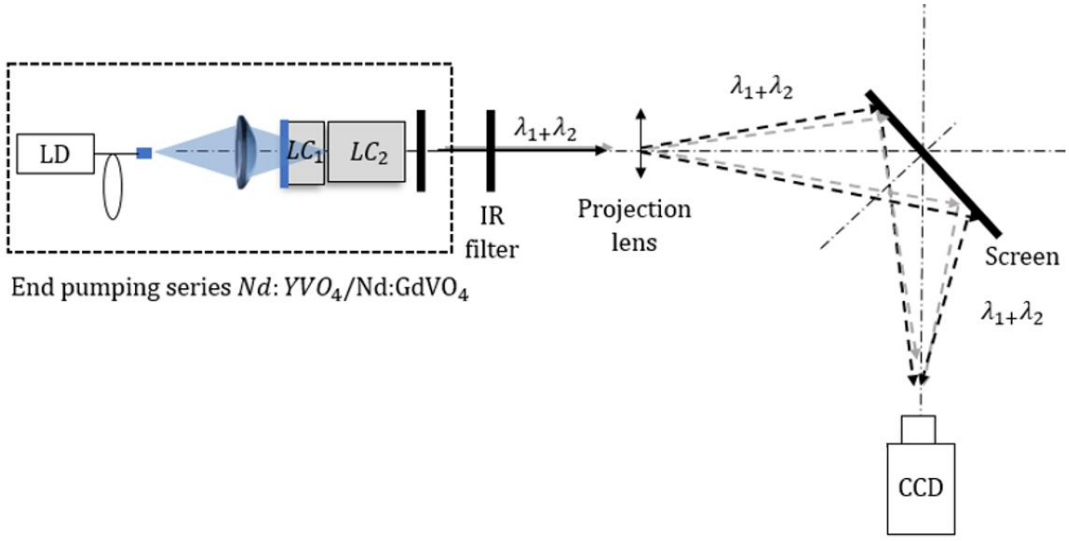

Figure 2-3: Experimental setup for speckle test.

2.3. RESULTS AND DISCUSSION

DUAL OUTPUT WAVELENGTHS

Figure 2-4a shows the single 1063.7 nm laser spectrum. **Figure 2-4b** shows spectrum at $z_o=z_{BPP}$, at which an equal output power is achieved for the two wavelengths. As mentioned in section 2.1, the lasing wavelength from LC_1 is 1063.7 nm in σ polarization (σ pol.) and 1062.4 nm from LC_2 in π polarization (π pol.).

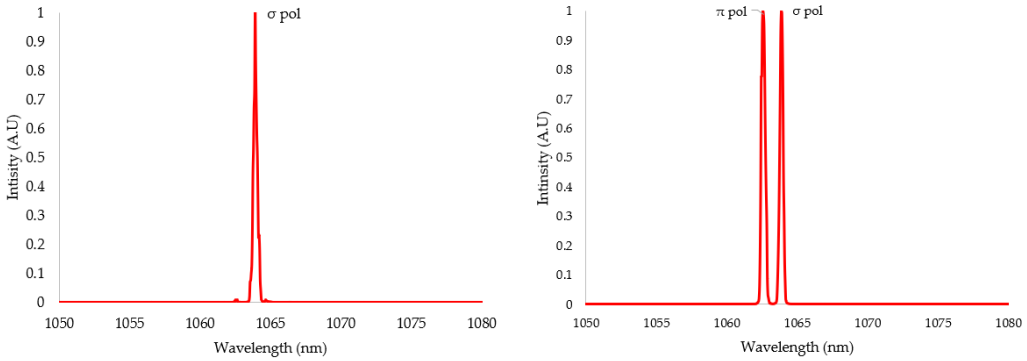

(a) (b)

Figure 2-4: (a) and (b) are the single (1063.7 nm) and dual-wavelength normalized emission spectrum respectively.

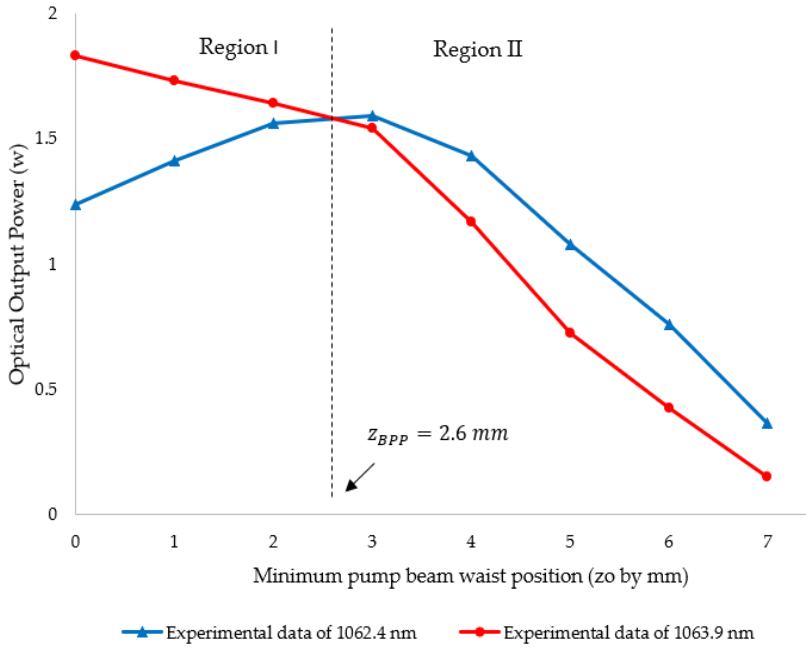

Figure 2-5: The measured output powers of 1062.4 nm (triangle up) and 1063.7 nm (dots) for σ-π configuration.

Figure 2-5 shows the change in the output power of the 1062.4 nm emissions from $Nd:GdVO_4$ (blue line with triangles) and 1063.7 nm emissions from

$Nd:YVO_4$ (red line with dots) versus the change of z_o. In the experiments, the maximum pump power was set to 6.5 W and $z_o$was adjusted to change the power ratio between two different wavelengths. In the σ-π configuration, the pumping wavelength was set at 805 nm.

Figure 2-5 is separated into Region I and Region II by the balance point position (z_{BPP}), which is defined as the position of beam waist of the pumping beam where an equal output power was achieved for the two wavelengths. The $z_{BPP}$was found to be 2.6 mm as shown in **Figure 2-5.** The total power at z_{BPP} is 3.18 W. It is worth noting that the balanced power ratio at z_{BPP} point is important for speckle reduction, which will be further illustrated in following sections.

The absorption of LC_1 controlled the amount of leaked pump power to LC_2. So, the pumping wavelength is shifted to be 805 nm (via controlling the LD temperature) because the change in pump wavelength (< 808 nm) will decrease the absorption of LC_1, resulting in a decrease in the gain in LC_1 . The same effect will happen to LC_2 as well, so that the overall O-O efficiency of such series crystal end-pumping is lowered.

The change in power ratio is related to the change of the pump beam waist position (z_o) [18]. With the increase of z_o, one can observe that 1063.7 nm laser power decreased, and 1062.4 nm laser power increased, until they become equal at $z_o=z_{BPP}$.

In **Figure 2-5**, when $z_o = 0$, the output power of 1063.7 nm laser is higher than 1062.4 nm laser because the minimum pump beam waist (ω_o) is on the input facet of LC_1, so the overlapping ratio between pump light size and laser mode size in LC_1 is large, makes the gain of LC_1 higher. In addition, only a small fraction of pump power leaked from LC_1 so that the output power of 1062.4 nm laser is smaller than the power of 1063.7 nm. By continuing to increase z_o, the pump power absorbed by LC_1 decreases, this leads to a decrease in the power of the 1063.7 nm laser and an increase in the power of the 1062.4 nm laser. This is because of the change in the overlapping ratio will be larger with respect to the mode size of LC_1 and vice versa to LC_2. In region II, when $z_o$is close to z_{BPP}, ω_o will be much closer to the 1st edge of LC_2, thus the power of 1062.4 nm laser increased while the power of 1063.7 nm laser decreased.

The output power of dual wavelengths emissions (when $z_o$was fixed at z_{BPP}) are shown in **Figure 2-6**. Based on the total power presented in **Figure 2-6**, the maximum O-O efficiency was 49.6% (51.7% after compensating IR filter and PBS losses) and, the slope-efficiency was 61% for the linear best fit (dotted blue line) which is shown in **Figure 2-7**. To the best of our knowledge, this is the highest efficiency achieved by dual-wavelength laser for σ-π configuration.

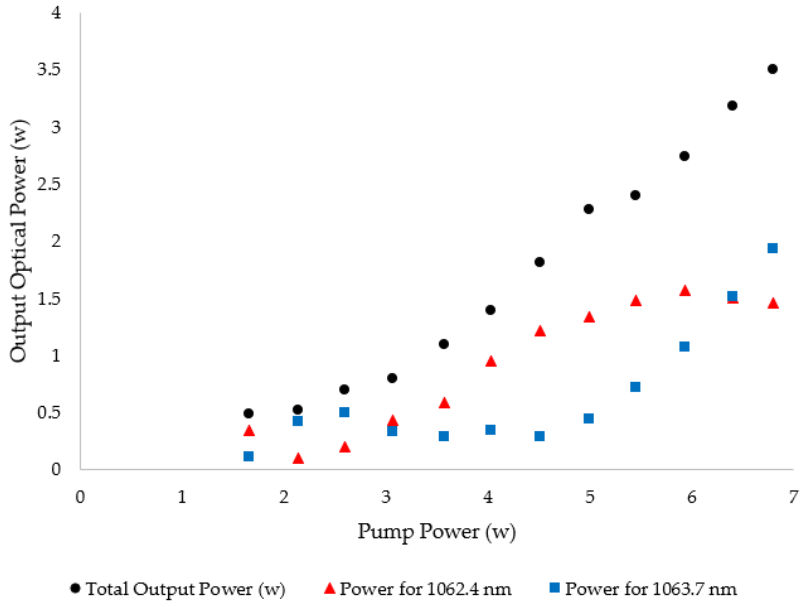

Figure 2-6: The measured output power versus pump power for σ-π configuration, where the total output power, output power for 1062.4 nm, and 1063.7 nm are represented by black dots, red triangle up, and blue square, respectively.

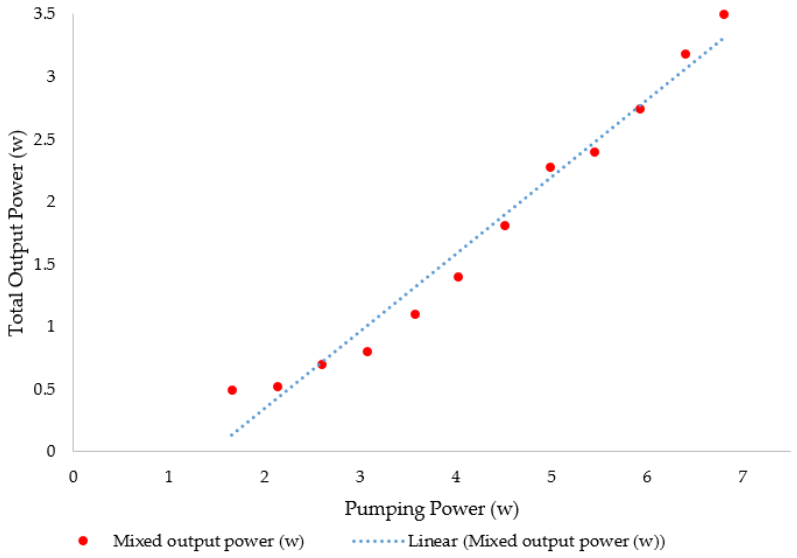

Figure 2-7: The measured total output power versus input pump power for σ-π configuration.

In addition, the O-O efficiency for π-π configuration has been studied. In that configuration, the c-axis of LC_1 is parallel to the c-axis of LC_2. Because of the absorption coefficient of LC_1 in π polarization is 4 times higher than σ polarization , the input pumping wavelength was further shifted to 804 nm to further decrease the pump power absorption of LC_1 (pump power was 7.7 W). The temperature of LC_1 and LC_2 was 45℃ and 18℃, respectively. 2.72 W total output power was achieved at z_{BPP}= 2.5 mm. The O-O efficiency was 35%.

The output power stability of dual-wavelength emission at the balance power point (BPP) was also studied. A power meter was used to record the power fluctuations over 1200 seconds in 1 second intervals. The power fluctuations of the total power and each polarization component were recorded and analyzed. According to the method presented in ref. [19], the power instabilities for both wavelengths blended together is 0.4%, while it is 1.9% for 1063.7 nm components and 1.12% for 1062.4 nm. The low power instability is mainly due to the fact that the two output wavelengths are from different crystals, and the mode competition is negligible in this type of laser [15]. The laser beam quality was measured by the knife-edge method in case of dual emission; the M^2 was factor < 1.2 for 1062.4 nm and 1063.7 nm, separately.

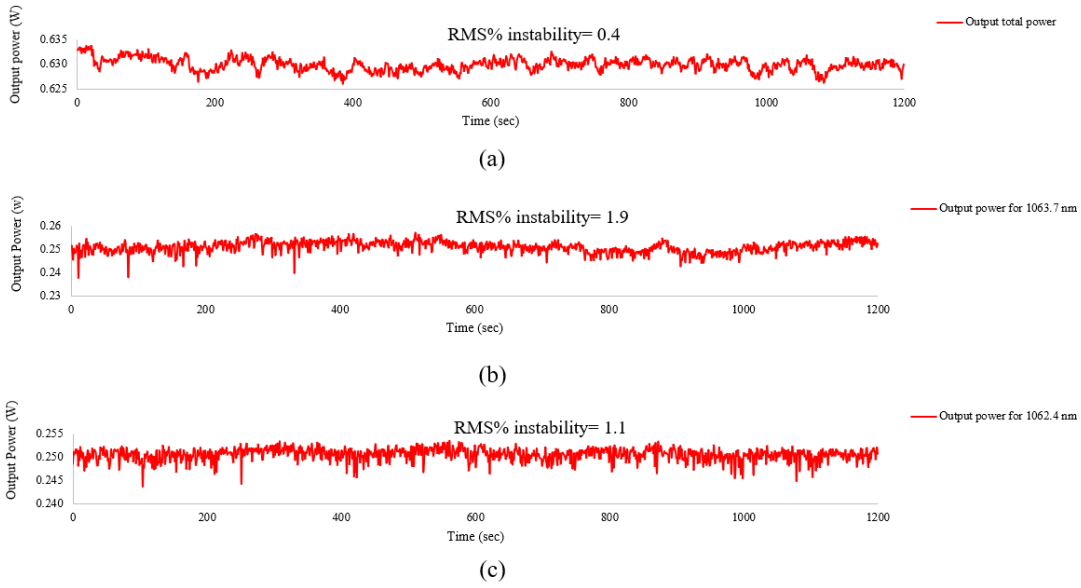

Figure 2-8: The measured (a) total power for σ-π configuration, (b) power of 1063.7 nm in σ- polarization, (c) power of 1062.4 nm in π- polarization.

As mentioned in the introduction part, when multiple wavelengths are emitted from the same laser, the overall speckle produced by this laser is lower compared to the conventional single wavelength lasers. This can greatly improve the light source quality for multiple applications described earlier. Thus, the speckle level of this laser was studied as well. The captured images of speckle patterns are shown in **Figure 2-9**, according to the measurement method reported in [19], the SCR from the single- and dual-wavelength laser was 70% and 53.9%, respectively.

Figure 2-9a, b shows the measured speckle images for 1063.7 nm and dual-wavelength emissions at z_{BPP}, respectively. The setup described in section 2.3 was used to capture the images.

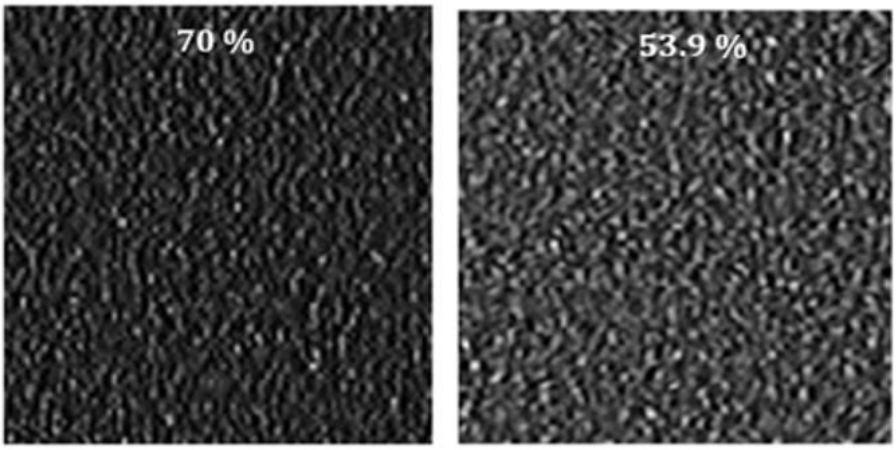

(a) (b)

Figure 2-9: (a) Single-wavelength speckle image, (b) dual-wavelength speckle image.

The SCR dependence with a different power ratio of two wavelengths was studied as well. **Figure 2-10** shows the SCR variation under different power ratios between 1062.4 nm and 1063.7 nm. The power ratio of the two wavelengths was changed by tuning z_o as described in the previous sections. In **Figure 2-10**, the X-axis represents power at 1063.7 nm over the total-output-power at the two wavelengths ($P_{\lambda 1}$ and $P_{\lambda 2}$ are the power of 1063.7 nm and 1062.4 nm lasers, respectively), where 1.0 means that the output emission wavelength is purely 1063.7 nm, and 0.5 (at BPP) means the output power is the same at each output wavelength. The minimum SCR of ~ 53.9 % is achieved when the power ratio of 1063.7 nm and 1062.4 nm was approximately 1:1.

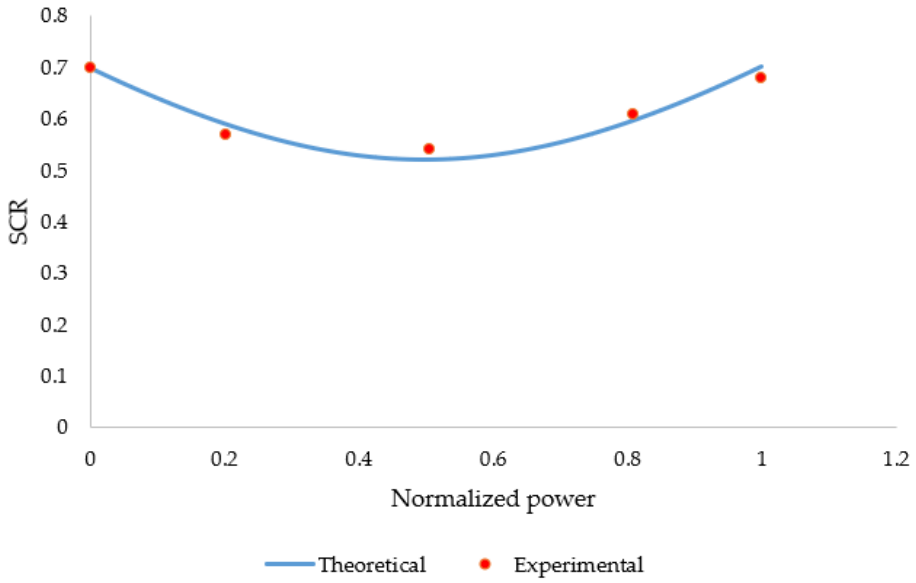

Figure 2-10: The SCR as a function of normalized power ($P_{\lambda 2}/(P_{\lambda 1}+P_{\lambda 2})$).

The experimental results matched the simulations based on the reported theoretical model [19]. In the simulations, the following parameters were used: λ_1= 1062.4 nm, λ_2= 1063.7 nm, $\Delta\lambda_1$= 0.3 nm, $\Delta\lambda_2$= 0.4 nm, $\sigma_h = 200$ µm, $\theta_i = \theta_r = 45°$, $P_{\lambda 1}= P_{\lambda 2}$= 1.5 W. Where, $\Delta\lambda_1$ and $\Delta\lambda_2$ are the linewidths for 1062.4 nm and 1063.7 nm, respectively, σ_h is the standard derivation of surface roughness fluctuation of the screen, θ_i is the incident angle of the laser beam, and θ_r is the receiving angle of camera used in the measurements. Ideally, SCR can be reduced by $1/\sqrt{N}$, where N is the number of incoherent laser wavelengths with equal output power and sufficient wavelength difference [20]. In the dual-wavelength emission with 1:1 power ratio, the expected reduction is $1/\sqrt{2}$. This agrees well with the measured results at 1:1 power ratio point.

TRI AND QUAD OUTPUT WAVELENGTHS EMISSION

By tilting the cavity output mirror, tri-wavelength emission can be achieved, and quad-wavelength emission can be achieved by further rotating the LC_1 [17,21]**.** As shown in **Figure 2-2b** in section 2.2, the left subfigure represents the setup of tri-wavelength emission (θ=0.7 mrad and $\emptyset$=0 rad), and the right subfigure represents the setup of quad-wavelength emission (θ=0.7 mrad and $\emptyset$=0.78 rad). The distance between LC_1 and LC_2 was 0.2 mm. The length of the cavity was 18 mm. The temperature of LC_1 and LC_2 were 45℃ and 18℃, respectively. **Figure 2-11a, b** shows the output spectra of tri- and quad-wavelength emission. In tri-wavelength emission, the peak wavelengths were at 1062.4 nm (π pol.), 1063.6 nm (π pol.), and 1064.6 nm (π pol.). The total output power was 1 W with an O-O efficiency of 23.8%. In quad-wavelength emission, the peak wavelengths were 1062.3 nm (π pol.), 1063.6 nm (π pol.), 1064.5 nm (π pol.), and 1066.1 nm (σ pol.). The output power was 1.55 W with an O-O efficiency of 35.4%.

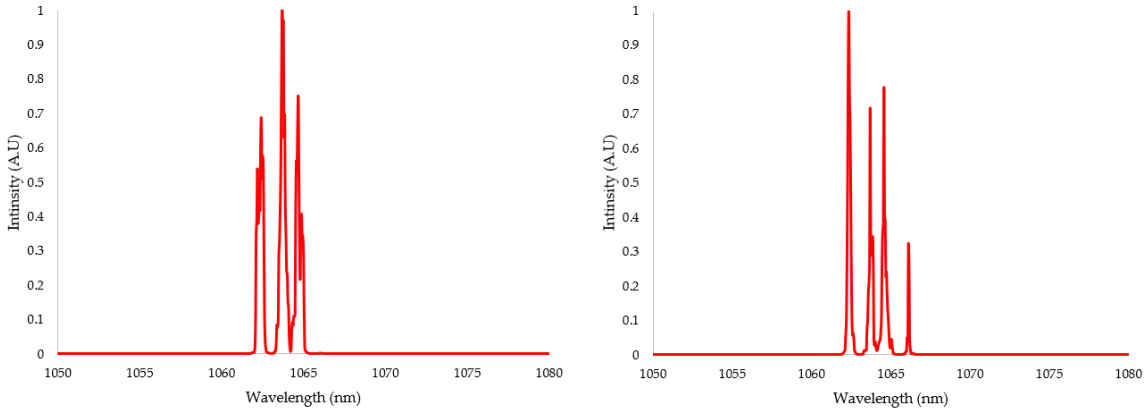

(a) (b)

Figure 2-11: The measured output spectrum of (a) tri-wavelength emission at 1062.4 nm, 1063.6 nm, and 1064.6 nm, and (b) quad-wavelength emission at 1062.3 nm, 1063.6 nm, 1064.5 nm, and 1066.1 nm.

As indicated in **Figure 1-12a, b**, the emission line are very close to each other and some of them are having the same polarization, so it was very hard to use IR filters or even PBS to isolate each individual line emission to do further investigation and measurement.

The SCR under tri- and quad-wavelength emission were measured to be 59.5% and 57.5%, respectively, which are lower than the SCR of single-wavelength emission (i.e. 70%). One can notice that these values do not follow the $1/\sqrt{N}$ relationship as described above, which can be understood as follows. First, the power levels at different emission wavelengths were not equal. According to [22], unequal power results in a limited speckle reduction effect. Second, the wavelength differences between adjacent wavelengths are not large enough, that causes co-related speckle patterns to be generated at the different wavelengths, and further limits the speckle reduction effect [19].

2.4. CONCLUSIONS

In this paper, the end pumping lasers for series crystals have been studied and optimized in the CW mode. Dual output wavelengths were achieved with O-O efficiency of 49.6% in the σ-π configuration. This is the highest efficiency reported in literature for this type of laser.

The output power instability was measured for dual wavelengths emission, 0.4% for both 1062.4 nm and 1063.7 nm blended together, 1.12% for 1062.4 nm and 1.9% for 1063.7 nm, the power instability was in between the results in [3] and [18]. In another hand, it is expected that the power instability and the spatial beam quality will be deteriorated in case of tri- and quad emission mode because the mode hopping, and competition will come to exist between the output line emissions.

The generation of tri- and quad-output wavelengths has been performed without adding any optical elements. The maximum power and O-O efficiency was 1W/23.8% and 1.55W/35.4% for tri- and quad-output wavelength emission, respectively.

SCR has been studied for this type of laser as well. It has been shown that the SCR depends on the power ratio of the two wavelengths, and a minimum SCR can be achieved when powers at each emission wavelength are equal, which agrees with the theoretical simulations.

It is worth noting that the present work provides a dynamic way to change SCR of a laser, simply by changing the position of the beam waist of the pumping beam. It is considered that lasers based on the end pumping for series crystals could be

very useful to the applications that need low laser speckle, high efficiency, and high power. As future work, the quality of the output beam should be further investigated and improved in case of dual emission to be used with the nonlinear crystals to achieve optimum conversion efficiency.

2.5. AUTHOR CONTRIBUTIONS:

Conceptualization, M.M. and; methodology, M.M. and B.Z; validation, M.M., C.J.; investigation, M.M., Q.M.; writing, review and editing, M.M.; writing, review and editing, M.M., J.K., Q.M and C.Q.X.

2.6. ACKNOWLEDGEMENTS:

The authors would like to thank the NSERC Discovery grant for the support of the project.

2.7. CONFLICTS OF INTEREST:

The authors declare no conflict of interest.

2.8. NOTATIONS

$Nd:YVO_4$:	Neodymium-doped yttrium orthovanadate
$Nd:GdVO_4$:	Neodymium doped Gadolinium Vanadate
$Nd:KGW$:	Neodymium doped Potassium-Gadolinium Tungstate
$Nd:YAG$:	Neodymium-doped yttrium aluminum garnet
$Nd:YLF$:	Neodymium-doped yttrium lithium fluoride
ω_0:	minimum beam waist
LC_1:	first laser crystal
LC_2:	second laser crystal
M_1:	input mirror
M_2:	output-mirror
z_o:	minimum pump beam waist
λ_p:	pumping wavelength
z_{BPP}:	balance point position
$P_{\lambda 1}$:	power of 1063.7 nm laser
$P_{\lambda 2}$:	power of 1062.4 nm laser
θ_i:	incident angle
θ_r:	receiving angle

Greek Letters:

-- --

2.9. ACRONYMS

DPSS	diode-pumped solid-state
LD	laser diode
SCR	speckle contrast ratio
MEMS	micro-electro-mechanical systems
CW	Continuous wave
NA	numerical aperture
O-O	optical-to-optical
THz	Tera Hertz
OSE	optical selective elements
CCD	Charged Coupled camera
GRIN	graded-index lens
AR	Anti-reflection
HR	high reflection
PBS	polarizing beam splitter
OSA	optical spectrum analyzer

N	number of incoherent laser wavelengths
RMS	Root mean square

2.10. REFERENCES

[1] Liu Y, Zhong K, Mei J, Wang M, Guo S, Liu C, Xu D, Shi W and Yao J 2017 Compact and flexible dual-wavelength laser generation in coaxial diode-end-pumped configuration *IEEE Photonics Journal* **9**

[2] Ding Y J 2014 Progress in terahertz sources based on difference-frequency generation [Invited] *Journal of the Optical Society of America B* **31** 2696–2696

[3] Liu Y, Zhong K, Mei J, Liu C, Shi J, Ding X, Xu D, Shi W and Yao J 2017 Compact and stable high-repetition-rate terahertz generation based on an efficient coaxially pumped dual-wavelength laser *Optics Express* **25** 23368–75

[4] Genina E A, Bashkatov A N, Simonenko G V, Odoevskaya O D, Tuchin V V and Altshuler G B 2004 Low-intensity indocyanine-green laser phototherapy of acne vulgaris: Pilot study *Journal of Biomedical Optics* **9** 828–828

[5] Chen Y F, Chen Y S and Tsai S W 2004 Diode-pumped Q-switched laser with intracavity sum frequency mixing in periodically poled KTP *Applied Physics B* **79** 207–10

[6] Son S N, Song J J, Kang J U and Kim C S 2011 Simultaneous second harmonic generation of multiple wavelength laser outputs for medical sensing *Sensors* **11** 6125–30

[7] Shen B, Jin L, Zhang J and Tian J 2016 Simultaneous tri-wavelength laser operation at 916, 1086, and 1089 nm of diode-pumped Nd: $LuVO_4$ crystal *Laser Physics* **26** 0–4

[8] Demirbas U, Uecker R, Fujimoto J G and Leitenstorfer A 2017 Multicolor lasers using birefringent filters: experimental demonstration with Cr:Nd:GSGG and Cr:LiSAF *Optics Express* **25** 2594

[9] Maestre H, Torregrosa A J, Pereda J A, Fernández-Pousa C R and Capmany J 2010 Dual-wavelength $Cr3^+$: $LiCaAlF_6$ solid-state laser with tunable THz frequency difference *IEEE Journal of Quantum Electronics* **46** 1681–5

[10] Sirotkin A A, Vlasov V I, Zagumennyi A I, Zavartsev Y D, Kutovoi S A and Shcherbakov I A 2014 Control of the spectral parameters of vanadate lasers *Quantum Electronics* **44** 7–12

[11] Zhao P, Ragam S, Ding Y J and Zotova I B 2011 Investigation of terahertz generation from passively Q-switched dual-frequency laser pulses *Optics Letters* **36** 4818–4818

[12] Pallas F, Herault E, Roux J-F, Kevorkian A, Coutaz J-L and Vitrant G 2012 Simultaneous passively Q-switched dual-wavelength solid-state laser working at 1065 and 1066 nm. *Optics Letters* **37** 2817–9

[13] Xu B, Wang Y, Lin Z, Cui S, Cheng Y, Xu H and Cai Z 2016 Efficient and compact orthogonally polarized dual-wavelength Nd : YVO 4 laser at 1342 and 1345 nm *Applied Optics* **55** 42–6

[14] Huang Y J, Tzeng Y S, Tang C Y, Chiang S Y, Liang H C and Chen Y F 2014 Efficient high-power terahertz beating in a dual-wavelength synchronously mode-locked laser with dual gain media *Opt Lett* **39** 1477–80
[15] Huang Y J, Tzeng Y S, Cho H H and Chen Y F 2014 Effect of spatial hole burning on a dual-wavelength mode-locked laser based on compactly combined dual gain media *Photonics Research* **2** 161–161
[16] Tran T-T-K, Svensen Ø, Chen X and Nadeem Akram M 2016 Speckle reduction in laser projection displays through angle and wavelength diversity *Applied Optics* **55** 1267–1267
[17] Pallas F, Herault E, Zhou J, Roux J F and Vitrant G 2011 Stable dual-wavelength microlaser controlled by the output mirror tilt angle *Applied Physics Letters* **99** 2–5
[18] Sato Y and Taira T 2002 Spectroscopic properties of neodymium-doped yttrium orthovanadate single crystals with high-resolution measurement *Japanese Journal of Applied Physics, Part 1: Regular Papers and Short Notes and Review Papers* **41** 5999–6002
[19] Ma Q and Xu C Q 2017 Wavelength blending with reduced speckle and improved color for laser projection *Optics and Lasers in Engineering* **97** 27–33
[20] Akram M N and Chen X 2016 Speckle reduction methods in laser-based picture projectors *Optical Review* **23** 108–20
[21] Chen H, Huang Y, Li B, Liao W, Zhang G and Lin Z 2015 Efficient orthogonally polarized dual-wavelength Nd:$LaMgB_5O_{10}$ laser *Optics Letters* **40** 4659–4659
[22] Wang D Z, Yan B X, Bi Y, Sun D H, Sang Y H, Liu H, Kumar A and Boughton R I 2014 Three-wavelength green laser using intracavity frequency conversion of Nd:Mg:$LiTaO_3$ with a MgO: PPLN crystal *Applied Physics B* **117** 1117–21.

Chapter 3

LASER SPECKLE REDUCTION UTILIZED BY LENS VIBRATION FOR LASER PROJECTION APPLICATIONS.

ABSTRACT

In this paper, a compact speckle reduction method utilizing vibrating lenses for laser beam scanning is proposed and demonstrated. The maximum speckle reduction efficiency was found to be 75.6% and 81.25% for a 532 nm diode-pumped solid-state (DPSS) laser and a 520 nm laser diode (LD), respectively. The minimum speckle contrast ratio observed using our method was 0.11 for the DPSS laser and 0.06 for the LD. The proposed method can provide speckle reduction with minimal power requirements, a low implementation cost, and no bending for the optical path of the laser beam. Additionally, this method is promising to withstand high-power lasers for use in high lumen laser projectors by optimizing the lens parameters. The demonstrated technique has a small form factor while simultaneously demonstrating a high degree of speckle reduction, which shows potential for speckle reduction in mini- and pico- laser projector applications.

Keywords: speckle reduction, vibrating lens, laser displays, pico-projectors

3.1. INTRODUCTION

In recent years, there has been rapid growth in projection-based technology. During this time, lasers have emerged as a flexible new light source for projection applications. Traditionally, projectors have been based on broadband light sources like ultra high-pressure mercury lamps and Xenon lamps. While these light sources are useful, they also have many drawbacks which include high power consumption, generation of copious amounts of heat, and a short lifetime.

Compared to the previously mentioned light sources, there are many advantages to using lasers as a light source: they have a smaller divergence angle, a wider color gamut, higher brightness, and a longer lifetime versus traditional sources [1]. Laser projectors have shown to be capable of a wide variety of applications that are seen frequently in day-to-day life, such as: conference rooms [2], home theaters [3], cinemas [4], and pico-projectors [5]. However, one of the main issues with laser light sources and the resulting image quality is laser speckle [6]–[8]. When projecting laser light (which is a highly coherent light source) on to a rough surface, granular bright and dark patterns will be generated. These patterns are a result of constructive and destructive interference between the reflected laser light from the rough surface (such as a projector screen). These patterns will reduce the image quality and as a result, it is desirable to suppress them for display-based applications.

Generally, the speckle contrast ratio (SCR) is a metric used to describe the amount of speckle present in an image. It can be calculated using the formula [9]:

$$SCR = \sigma_I / \langle I \rangle \quad (3\text{-}1)$$

Where σ_I is the standard derivation of intensity fluctuation of a speckle pattern and $\langle I \rangle$ is the average or mean intensity. The SCR is a value between 0 and 1; 0 represents an image free from speckle and 1 represents the maximum amount of speckle is present in the image. The threshold for human perception of speckle is 5% or 0.05; below this value, the image will appear free from speckle to a human observer [10].

There are multiple methods that have been proposed to reduce the SCR to a value where it is no longer visible to the human eye. One of the most important speckle reduction methods is to superpose multiple independent speckle patterns with the same intensity within the integration time of human eye [11]. This will produce a more uniform light field with lower speckle. The majority of methods used to generate multiple speckle patterns are based on mechanical movements, which include vibrating or rotating the light pipe found in many projectors [12], vibration of the diffuser element [13], vibrating the projector screen [14], and rotating/vibrating micro lens arrays [15], [16].

Technology based on these mechanical methods suffer from drawbacks such as being bulky and taking up valuable space, generating noise due to the

required actuators, and high-power consumption. These are all unwanted side effects that will reduce the stability of the system, and it is the goal to design the system in such a way as to mitigate them as much as possible for use in practical applications.

Another more recent development is micro-electro-mechanical systems (MEMS) scanning mirrors which have been studied and proposed as a method for speckle reduction. In this method, the laser beam is incident on the MEMS system, which is then tilted in one or two-dimensions, resulting in reflected beams with varying angles capable of high frequency scans. In most cases, the reflected beams will then pass through one or more diffuser elements to be collected by homogenization components. The reflected beams are capable of generating multiple different speckle patterns in a short time period (relative to the integration time of the detector), which reduces the overall laser speckle of the system.

The MEMS method has been demonstrated to be very effective regarding speckle reduction [17], [18]. However, it also has several draw backs that have been observed, one of which is that the optical path of the system must be bent. This can result in design complications for compact systems such as pico-projectors. Additionally, the laser beam diameter is limited by the small reflection surface area of the MEMS devices. So, if the power of the laser source is increased this mean that the power density of the laser beam will be increased, this unfortunately can destroy the mirrors. Based on this, the author in [1] designed a large size 2D MEMS mirror with diameter 6.5 mm instead of 2 mm in [19].

In this paper, an alternative method that makes use of a lens vibrating in one dimension (1D) to produce a laser scan capable of reducing the speckle contrast ratio is proposed and demonstrated. For proof of concept, the lens vibration was performed using an optical CD/DVD pickup actuator. In our experiments, we adopted a simple optical setup to test the speckle reduction efficiency. The amplitude of the scanned laser beam as a function of the module's vibration frequency and amplitude has been measured. Two different green lasers (a DPSS laser and a LD) were used in the experiment as the light source. The proposed setup has been optimized for speckle reduction by inserting a condensing lens, which serves to further minimize the speckle contrast ratio (SCR) and to collect all light for preventing more optical loss.

3.2. EXPERIMENTAL SETUP

Figure 3-1 illustrates a proposed setup to test the speckle reduction efficiency of an integrated lens vibrating module (LVM). In **Figure 3-1**, two different types of green laser sources were used in the experiments: A frequency doubled DPSS laser at 532 nm with a linewidth of 0.1 nm and a semiconductor LD at 520 nm with a linewidth of 1.2 nm.

In **Figure 3-1a**, the laser beam starts by passing through a single LVM. The LVM used here was an optical CD/DVD pickup actuator. After the LVM module, the laser beam illuminated an optional optical diffuser that is immediately followed by a light pipe. The output of the light pipe was then projected on to a screen and

then resulting image was captured by a CCD camera. It is worth noting that, for simplicity, there is no display panel in the system. Should a display panel be required, it can be placed after the light pipe with an accompanying relay lens if necessary.

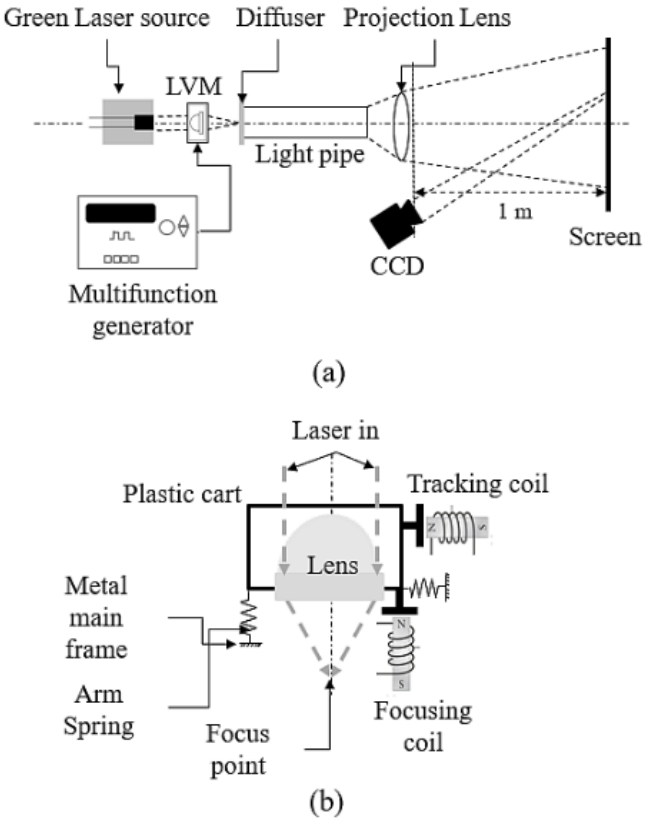

Figure 3-1: A schematic diagram for (a) proposed setup for speckle reduction, (b) a CD/DVD-pickup actuator.

Figure 3-1b shows a schematic diagram of the optical CD/DVD pickup actuator that comprises the LVM in the experiment. The vibrating module consists of a small plastic cart containing two wound copper coils: a) the focusing coil, which can move the lens parallel to the direction of light propagation (which

controls the focusing distance of the lens), and b) the tracking coil, which can move the lens perpendicular to the light propagation direction [20]. There are magnets inside both coils, allowing the coils to move at a high frequency when provided with an external alternating driving signal. The cart itself was suspended on a main metal frame by a set of suspension wires, which act as springs.

The lens is made of acrylic, and it is uncoated. The transmission efficiency is 93.3% for the green laser used in the experimental setup. The diameter and focal length of the lens are 4.5 mm and 4 mm, respectively. The measured divergence angle of the laser beam after the lens is 3.4 rad. As will be shown below, the lens can tolerate a laser input power of 1.5 W for at least 1 hour. The scanning angle θ_s at the diffuser surface is calculated using the formula $-u/f$, where u is the displacement (or amplitude of vibration) of the scanning lens and f is the focal length of the vibrating lens. The lens vibration was controlled by applying a signal from a multifunction generator (MFG) to the tracking coil of the module. If the signal voltage is varied, the lens will be vibrated with different amplitudes that will cause the laser beam to diverge over a wide range of angles. When the output light illuminates the diffuser, different speckle patterns will be generated at a high frequency. This results in reduced speckle on the projector screen, increasing image quality.

In order to achieve improved speckle reduction, it is necessary to optimize the vibration of the LVM. **Figure 3-2** shows an experimental setup used to

characterize the LVM. In **Figure 3-2a**, a collimated laser source was placed in front of the LVM. A 50X microscopic lens (ML) was used after the LVM to image the object plane that corresponds to the laser source. The output from the microscopic lens was projected on to a white paper screen with a ruler overlay to facilitate measuring distance. The distance between the microscopic lens and the screen was d=1 m. A CCD camera was placed behind the screen to capture the resulting laser spot on the screen. On the left side of **Figure 3-2b**, the resulting bright point indicates the LVM is in the "off" state, and a bright-line on the right side which indicates that LVM is in the "on" state. As shown in the **Figure 3-2**, by measuring the bright line length at the screen and taking the magnification of the ML into consideration, the actual scanning amplitude at the focal plane of the LVM can be determined.

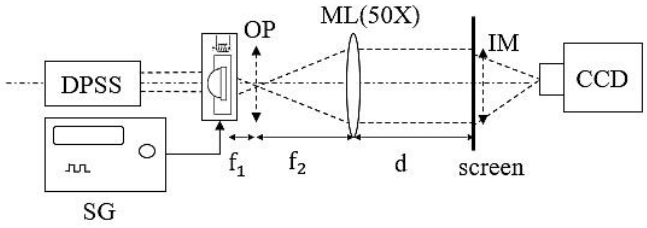

(a)

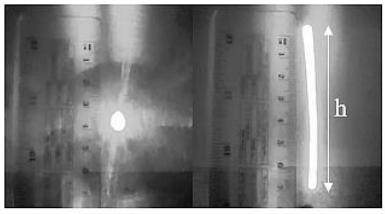

(b)

Figure 3-2: (a) A schematic diagram for the amplitude characterization setup, where ML: microscopic lens, $\mathbf{f_1}$ and $\mathbf{f_2}$: the focal length of the LVM lens and the

ML respectively, the screen, and h: bright line length, and (b) observed screen images from the CCD camera.

Figure 3-3 shows the relationship between the amplitude and the frequency of lens vibration under different driving voltages (peak values). In **Figure 3-3**, the x-axis is the vibration frequency (Hz) of the tracking actuator, and the y-axis is the measured vibration amplitude (mm). The applied signals were square waves and each peak voltage is displayed as a different data set. In the experiments, the LVM was operated at 70 Hz with a driving voltage of 1.5 V. These frequency and voltage values were selected because they provide vibration amplitudes close to the maximum amplitude allowed by the physical dimensions of the LVM housing, while limiting overall power consumption. According to the experimental results, the vibration amplitude of the LVM at 70 Hz/4 V is calculated to be 1.12 mm.

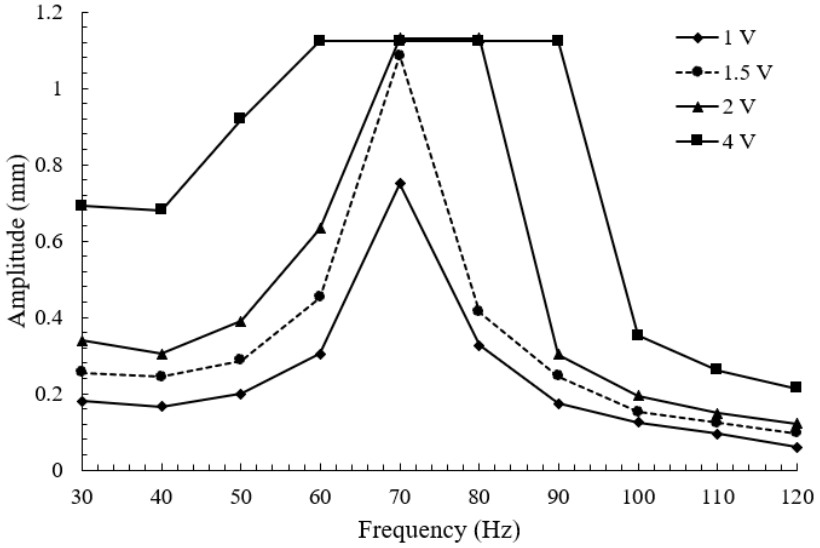

Figure 3-3: LVM response curves under a range of driving voltages.

As shown in **Figure 3-1** the laser passes through the LVM and is then launched into a diffuser with a divergence angle of 24°. A light pipe with a hexagonal cross-section was placed after the diffuser. The light pipe had a diameter of 10 mm and a length of 15 mm.

A projection lens with a focal length of 25 mm was then used to image the output of the light pipe on a depolarized screen and the F-number was 8. A high-resolution CCD camera (DCU224M from Thorlabs) with a pixel size of 5.86 μm × 5.86 μm was used to capture the image on the screen. The plane which contains both the projection lens and the CCD camera is located 1 m from the the screen. The integration time of the CCD camera was set to be 50 msec to mimic the response time of the human eye [21], while the camera lens had a focal length of 50 mm and the F-number was 11 [1]. The resulting output image was an 8-bit grayscale image. The CCD was operated in the linear region, and the experiment was performed in a dark room to avoid any background light.

3.3. RESULTS AND DISCUSSION

The general idea of the method is to utilize a fast scanning laser beam to produce a high degree of spatial diversity that will reduce the SCR of the system. After the laser reaches the lens of the LVM, the laser beam will be focused to a bright spot at the focus plane of the LVM. If a driving signal is applied to the tracking coil, the LVM and thus the output laser beam will oscillate, resulting in

one-dimensional (1D) scanning which creates a scanning line due to the vibrating lens.

When the lens is vibrated at a high frequency (> 25 Hz), the human eye will no longer be able to observe the individual laser spots on the screen due to the integration time of the retina, and a line is observed instead. The output beam is then incident on the optical elements after the LVM at different angles, which will produce a variety of speckle patterns. Should these patterns overlap, it will generate a more uniform light field with reduced SCR.

It is worth noting that similar speckle reduction methods have been realized by utilizing a MEMS scanning mirror, where a single laser spot was scanned to form bright laser lines [17]. One of the differences between the proposed method and the MEMS scanning mirror is that the proposed method produces an output beam cone with large solid angle, while the MEMS scanning method instead provides a single laser beam with a small divergence angle. In the LVM method, the shape of the beam after the LVM acts as a point source, which introduces a higher number of illumination angles to the following optics. This is important in speckle reduction as increasing spatial diversity (the difference in the illumination angles) has potential to generate more independent speckle patterns, which will reduce the SCR of the system.

Another difference between the proposed method and MEMS method is that, in the MEMS scanning method, the optical path of the system must be bent in

order to use the MEMS mirror. This has potential design issues for highly compact optical system such as pico-projectors. However, in the proposed method, the light path can be arranged in a straight line without any required folding or bending, which is convenient for highly compact projection engine designs.

In addition to these benefits, the optical pickup actuators are a mature product which have been widely used in CD players, resulting in the module being available at a low cost. The module also has a high degree of stability compared to other speckle reduction methods.

SPECKLE REDUCTION EFFICIENCY OF THE VIBRATING LENS

In order to determine the speckle reduction efficiency of the proposed system, the intial value of the SCR (SCR_i) of the laser sources must first be measured. The SCR_i for both type of green laser sources were measured via a direct projection of the green laser beam onto a depolarized screen through a projection lens, with no speckle reduction systems in place (consisting of only the laser source and the projection lens). The distance between the laser source (DPSS or LD) and the projection lens is 2.5 cm. Thus, the speckle reduction efficiency is calculated with respect to SCR_i of the laser beam and the SCR after the lens vibration (SCR_v) as: $(SCR_i - SCR_v)/SCR_i$.

The measured speckle patterns are presented in **Figure 3-4.** The SCR_i of the DPSS laser/ LD are 0.45 and 0.32, respectively. The SCR of the LD was lower than the DPSS laser due to the linewidth of the LD being 1.2 nm, while for the DPSS

laser the linewidth is roughly 0.1 nm. A broader linewidth will provide more wavelength diversity, and this results in a lower SCR [22].

The detailed speckle reduction experiments were conducted using the setup illustrated in **Figure 3-1**. Two different cases are presented here: a) without a diffuser after the LVM and b) with a diffuser after the LVM.

The measured results are presented in **Figure 3-4**. **Figure 3-4b** demonstrates the results when no diffuser was present, and **Figure 3-4c** corresponds to the case where a diffuser was included in the optical setup. The images on the left are the results from using the DPSS laser as the light source and the images on the right are the results from using the LD as the light source. Measurements were taken both when the LVM was off and when the LVM was on, as indicated in **Figure 3-4**. **Table 3-1** summarizes the SCR values in all cases.

Table 3-1: The SCR values.

	DPSS			**LD**		
SCR in case:	SCR_i	LVM "OFF"	LVM "ON"	SCR_i	LVM "OFF"	LVM "ON"
	0.45			0.32		
Without diffuser		0.33	0.22		0.14	0.09
With diffuser		0.19	0.15		0.12	0.07

It can be observed that when diffuser was not used and the LVM was off, the SCR of the system is 0.33 and 0.14, for the DPSS laser and LD respectively. When the LVM was turned on, the SCRs drop to 0.22 and 0.09 respectively. Compared to the SCR_i, the speckle reduction efficiencies are (0.45-0.22)/0.45=51% and (0.32-0.09)/0.32=72%, for the DPSS laser and LD, respectively.

When the diffuser was added into the system, even lower SCRs were achieved. The rough surface of the diffuser results in many uncorrelated speckle patterns when illuminated by the laser. The light pipe that follows the diffuser results in further overlap between the various speckle patterns and this provides a more uniform light field.

The lowest SCR values observed were 0.15 for the DPSS laser and 0.07 for the LD, which is close to the threshold of speckle free projection (< 0.05 or 5%). The corresponding speckle reduction efficiencies are 67% and 78% respectively.

The speckle reduction mechanism of the LVM is straightforward. As the lens vibrates, the output laser beam expands from a single focused spot into a laser line. This is combined with the light pipe that follows the LVM, which will provide better spatial diversity as a result of laser illumination from different angles. This results in a lower overall SCR for the produced image.

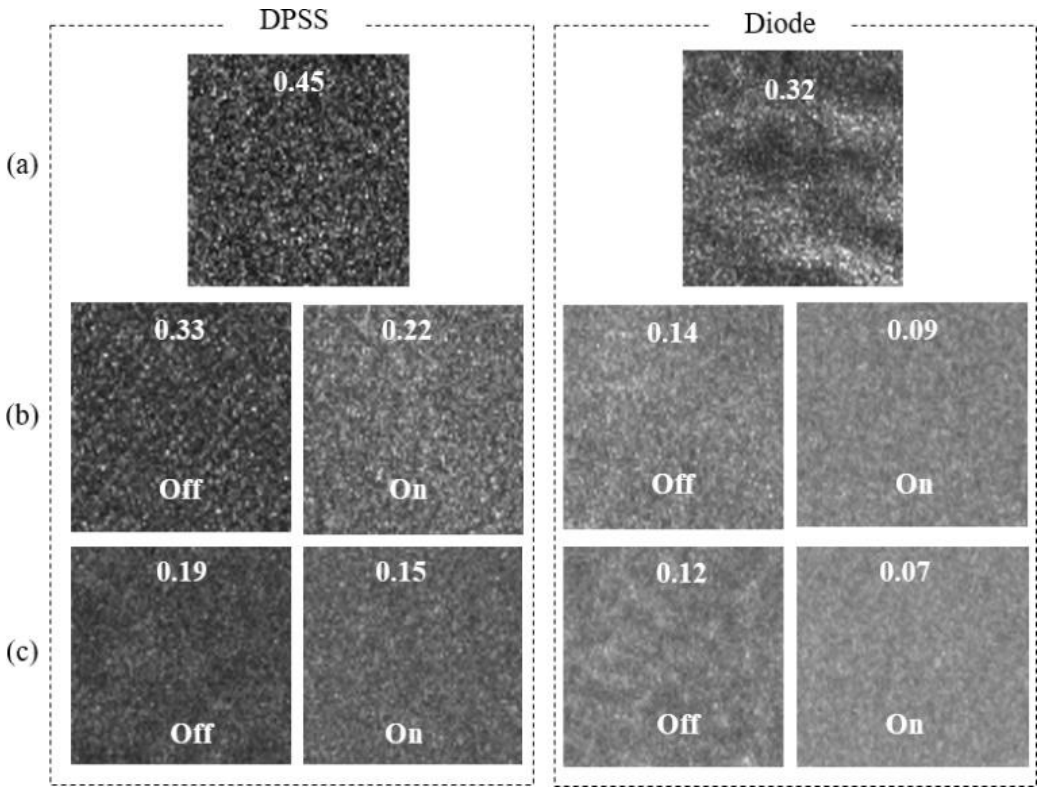

Figure 3-4: Speckle images and SCR values for (a) initial speckle image of DPSS/LD, (b) proposed setup in **Figure 3-1** without diffuser, and (c) proposed setup in **Figure 3-1** with diffuser, where off means no applied signal and on means an applied square wave with 70 Hz and 1.5 V.

OPTIMIZING THE SETUP WITH A CONDENSING LENS

In order to further increase the speckle reduction efficiency of the proposed method, an extra condensing lens was used after the LVM. The condensing lens can increase the length of the laser scan line on the diffuser, which implies an increase in the number of uncorrelated speckle patterns. As a result, a lower SCR will be achieved.

The condensing lens that was used had a 30 mm focal length and 25.5 mm diameter. The distance between the LVM and the condensing lens was 40 mm, and

the distance between the condensing lens to the light pipe was 35 mm. The setup of the experiment is shown in **Figure 3-5**. The condensing lens has a large diameter which will collect all output light from the LVM and avoid any extra optical power loss during lens scanning. In the experiment, it was observed that the output beam from the LVM always fell within the entrance pupil of the condensing lens. This resulted in no meaningful optical loss when the condensing lens was introduced in to the system.

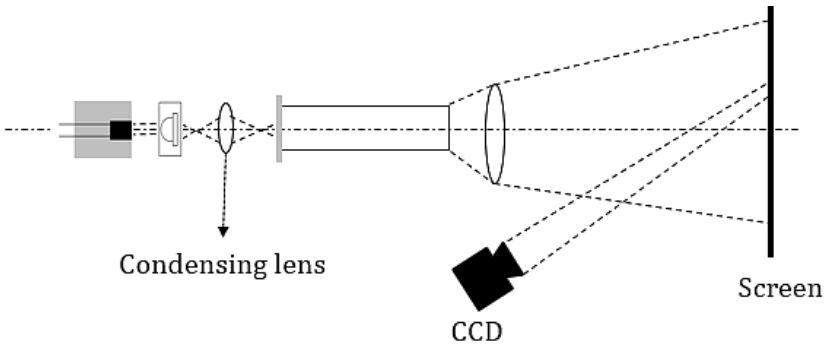

Figure 3-5: Experimental setup with a condense lens in the system.

Figure 3-6 shows the relation between the SCR and the lens vibration frequency for different peak voltage values when the condensing lens was introduced to the system. It was noted that the SCR values produced with the condensing lens for the DPSS and LD were lower compared to the setup without the condensing lens. The minimum speckle contrast values were achieved at a vibration frequency of 70 Hz for both the DPSS and LDs. Moreover, the speckle noise increases with the vibration frequency after 90 Hz as shown in **Figure 3-6**. This is because the amplitude of vibration is effectively much lower at high frequencies.

It was observed that the SCR values from 60 to 80 Hz are very close to each other. This was because the amplitudes of vibration of the LVM in **Figure 3-3** in this frequency range are also close to each other. The general trend of the two curves in **Figure 3-6a, b** shows the minimum SCR value between the 60 to 80 Hz frequency range. This can be explained by considering that a large vibration amplitude produces more speckle patterns which leads to a higher degree of speckle reduction.

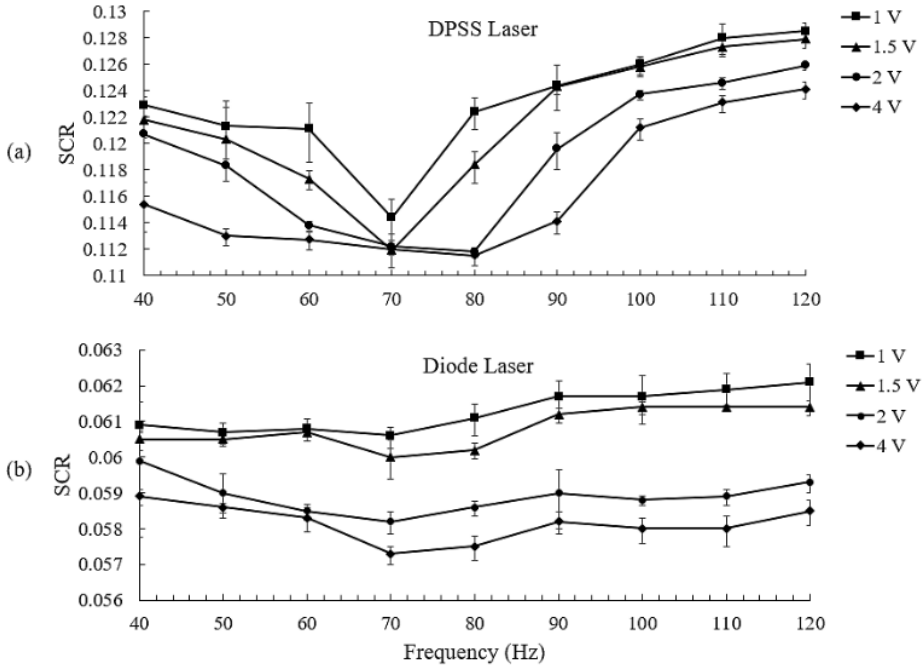

Figure 3-6: The SCR versus frequency for the range of driving voltages (1 V, 1.5 V, 2 V, and 4 V) for: (a) DPSS, and (b) LD source.

Figure 3-7 shows the images corresponding to the minimum speckle values, as well as the resulting speckle values that were achieved for the DPSS and LDs. The minimum SCR was 0.11 & 0.06 for the DPSS & LDs, respectively, with

an applied square signal peak voltage 4 V at 70-80 Hz. This resulted in a speckle reduction efficiency of 75.60% for the DPSS laser and 81.25% for the LD.

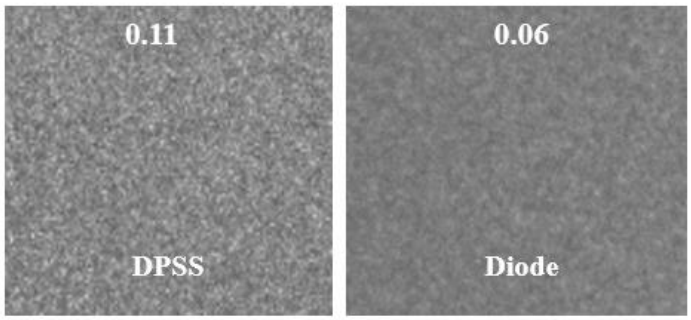

Figure 3-7: Achieved minimum SCR for: (a) DPSS, and (c) LD source.

Generally, larger voltage values produce larger vibrational amplitudes (larger scanning angles). At higher vibrational amplitudes, the speckle noise decreases further through the introduction of additional uncorrelated speckle patterns. However, larger vibrational amplitudes result in increased power consumption by the module, due to the additional power required by the voice coil to increase the electromagnetic force generated for vibration. Moreover, a vibrational noise exists at these large scanning amplitudes as the lens begins to collide with the physical mainframe boundaries in both scanning directions. As a result, selecting the proper voltage level should be seen as a trade-off between the SCR, noise, and power consumption.

From **Figure 3-3**, at voltage levels of 2 V and 4 V the maximum amplitude is saturated at 1.123 mm. The maximum amplitude for voltage levels of 1 V and 1.5 V are 0.7494 mm and 1.0854 mm, respectively. The minimum SCR at 70 Hz

for 4 V, 2 V, 1.5 V, and 1 V is 0.0573, 0.0582, 0.06 and 0.061, respectively. The vibrational noise reaches its maximum for voltage levels of 2 V and 4 V. Furthermore, the power consumption increases as the voltage increases, while the SCR decreases with increasing voltage prior to saturation. As a result, the optimized voltage level is 1.5 V. At 1.5 V, the SCR is 0.06 without any vibrational noise and low power consumption.

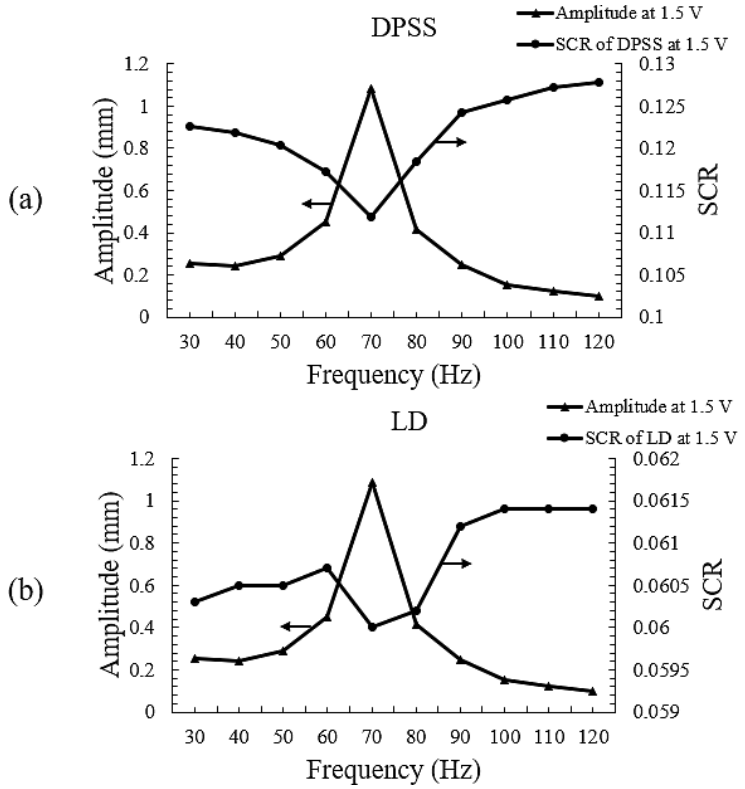

Figure 3-8: Show the relation between the amplitude, frequency, and SCR for: a) DPSS, and b) LD laser source.

Figure 3-8 shows the relation between the frequency, amplitude, and SCR for voltage level 1.5 V for each laser source type (DPSS or LD). As aforementioned

in that section, the minimum SCR is achieved at 70 Hz and with 1.0854 mm amplitude. The minimum SCR for DPSS and LD is 0.11 and 0,06, respectively.

3.4. CONCLUSIONS

In this paper, a method for speckle reduction by using vibrating lenses has been proposed and demonstrated. SCR values as low as 0.06 and 0.11 have been achieved for green LD and DPSS green laser, which correspond to a speckle reduction efficiency as high as 81.25% and 75.60%, respectively. These values were achieved by employing a vibrating lens, a diffuser, a light pipe and a condensing lens in the experimental optical setup. Although the proposed method utilizes a similar speckle reduction principle to a MEMS scanning mirror, the output laser beam from the vibrating lens has a large solid angle which provides better speckle reduction as compared to the MEMS method. It is worth noting that the proposed method can achieve effective speckle reduction with minimal power consumption (TTL digital signal levels), low cost, and no bending for the optical path of the laser beam, which is an important design consideration for compact laser projector designs. The diameter of the lens is 4.5 mm so it can withstand high laser power and it can be easily enlarged by using much larger diameter lenses with high damage threshold. The transmission of the lens can be further improved by coating the two lens surfaces by anti-reflection coating. In the present work, only one-dimensional line scanning has been demonstrated.

Our technique can also provide much lower SCR by changing some of the test setup parameters as in ref.[10] to adjust the F-number to be 1.4 and changing the distance of the screen to be 0.5 mm, thus according to [22], the decrease in F-number and the distance of the measurement will decrease the speckle contrast ratio.

It is expected that, by combining two LVM modules with vibration directions that are perpendicular to one another, a 2D laser scan would be produced. This will provide a lower SCR values, which will be examined in future work. In general, when a laser beam scans a diffuser, each point of contact between the laser beam and the diffuser produces a unique speckle pattern, where each point represents a different incident angle. For 1D scanning, a bright line (BL) is produced on the diffuser (with a repetition rate > 25 Hz). The BL consists of two identical overlapping sublines; each subline represents a different direction scanning the diffuser's surface. Thus, each subline contains several uncorrelated speckle patterns. As the speckle reduction is calculated via the integration of the uncorrelated patterns, 1D speckle reduction depends on just a single subline. In 2D scanning (such as raster or Lissajous scanning), the scanning area on the diffuser surface is substantially increased and contains a higher density of sublines. The probability of reproducing the same speckle patterns in each subline is very low, such as in 1D scanning. As a result, the speckle reduction in 2D (raster or Lissajous scanning) is expected to be much higher than in 1D scanning due to integrating a

significantly larger number of uncorrelated speckle patterns, thus introducing a larger degree of angular diversity.

3.5. ACKNOWLEDGEMENT

This project is partially supported by the NSERC Discovery grant.

3.6. NOTATIONS

h:	bright line length
f_1:	focal length of the LVM lens
f_2:	focal length of the ML
u:	the displacement

Greek Letters:

σ_I:	the standard derivation of intensity fluctuation of a speckle pattern
$\langle I \rangle$:	the average or mean intensity
θ_s:	scanning angle

3.7. ACRONYMS

CV:	Cross-validation
DPSS	diode-pumped solid-state
LD	laser diode

SCR	speckle contrast ratio
MEMS	micro-electro-mechanical systems
2D	Two dimensions
1D	one dimension
LVM	lens vibrating module
MFG	multifunction generator
ML	microscopic lens
CCD	Charged Coupled camera
TTL	digital signal levels
BL	bright line

3.8. REFERENCES

[1] Z. Tong et al., "Combination of micro-scanning mirrors and multi-mode fibers for speckle reduction in high lumen laser projector applications," Optics Express, vol. 25, no. 4, pp. 3795–3804, 2017.

[2] M. S. Brennesholtz and E. H. Stupp, Projection Displays, Second edi., vol. 19. John Wiley & Sons, 2008.

[3] J.-H. Lee et al., "Laser TV for home theater," Projection Displays VIII, vol. 4657, no. April 2002, pp. 138–145, 2003.

[4] G. Verschaffelt et al., "Speckle disturbance limit in laser-based cinema projection systems," Scientific Reports, vol. 5, no. September, p. 14105, 2015.

[5] H. C. Lin and Y. H. Lin, "An electrically tunable focusing pico-projector adopting a liquid crystal lens," Japanese Journal of Applied Physics, vol. 49, no. 10, pp. 1025021–1025025, 2010.

[6] T. K. T. Tran et al., "Design, Modeling, and characterization of a microelectromechanical diffuser device for laser speckle reduction," Journal of Microelectromechanical Systems, vol. 23, no. 1, pp. 117–127, 2014.

[7] E. J. Young, N. J. Kasdin, and A. Carlotti, "Image analysis with speckles altered by a deformable mirror," Techniques and Instrumentation for Detection of Exoplanets VI, vol. 8864, no. September 2013, p. 88640S, 2013.

[8] Z. Tong, X. Chen, M. N. Akram, and A. Aksnes, "Compound speckle characterization method and reduction by optical design," IEEE/OSA Journal of Display Technology, vol. 8, no. 3, pp. 132–137, 2012.

[9] Z. Cui et al., "Speckle suppression by controlling the coherence in laser based projection systems," IEEE/OSA Journal of Display Technology, vol. 11, no. 4, pp. 330–335, 2015.

[10] J. W. Pan and C. H. Shih, "Speckle noise reduction in the laser mini-projector by vibrating diffuser," Journal of Optics (United Kingdom), vol. 19, no. 4, p. 045606, 2017.

[11] D. V. Kuksenkov, R. V. Roussev, S. Li, W. A. Wood, and C. M. Lynn, "Multiple-wavelength synthetic green laser source for speckle reduction," no. February 2011, p. 79170B, 2011.

[12] Q.-L. Deng, B.-S. Lin, P.-J. Wu, K.-Y. Chiu, P.-L. Fan, and C.-Y. Chen, "A hybrid temporal and spatial speckle-suppression method for laser displays," Optics Express, vol. 21, no. 25, p. 31062, 2013.

[13] J. W. Pan and C. H. Shih, "Speckle noise reduction in the laser mini-projector by vibrating diffuser," Journal of Optics (United Kingdom), vol. 19, no. 4, p. 045606, 2017.

[14] S.-Y. Tu, H. Y. Lin, and M.-C. Lin, "Efficient speckle reduction for a laser illuminating on a micro-vibrated paper screen," Applied Optics, vol. 53, no. 22, p. E38, 2014.

[15] T. Mizushima et al., "L-9: Late-News Paper: Laser Projection Display with Low Electric Consumption and Wide Color Gamut by Using Efficient Green

SHG Laser and New Illumination Optics," SID Symposium Digest of Technical Papers, vol. 37, no. 1, p. 1681, 2006.
[16] J.-W. Pan and C.-H. Shih, "Speckle reduction and maintaining contrast in a LASER pico-projector using a vibrating symmetric diffuser," Optics Express, vol. 22, no. 6, p. 6464, 2014.
[17] F. Li, J. He, W. Shen, P. Zhou, H. Yu, and F. Ma, "A large size MEMS scanning mirror for speckle reduction application," Micromachines, vol. 8, pp. 539–543, 2017.
[18] T. Wang, W. Shen, S. Wu, P. Zhou, J. He, and H. Yu, "The implementation of laser speckle reduction based on MEMS two-dimensional scanning mirror," International Society for Optics and Photonics., vol. 10022, no. October 2016, p. 100222U, 2016.
[19] M. N. Akram, Z. Tong, G. Ouyang, X. Chen, and V. Kartashov, "Laser speckle reduction due to spatial and angular diversity introduced by fast scanning micromirror," Applied Optics, vol. 49, no. 17, p. 3297, 2010.
[20] E. E. Te Hwu and A. Boisen, "Hacking CD/DVD/Blu-ray for Biosensing," ACS Sensors, vol. 3, no. 7, pp. 1222–1232, 2018.
[21] Z. Tong, S. Song, S. Jia, and X. Chen, "Nonsequential Speckle Reduction Method by Generating Uncorrelated Laser Subbeams with Equivalent Intensity Using a Reflective Spatial Light Modulator," IEEE Photonics Journal, vol. 9, no. 5, 2017.
[22] N. E. Yu et al., "Speckle noise reduction on a laser projection display via a broadband green light source," Optics Express, vol. 22, no. 3, p. 3547, 2014.
[23] S. Roelandt, Y. Meuret, G. Craggs, G. Verschaffelt, P. Janssens, and H. Thienpont, "Standardized speckle measurement method matched to human speckle perception in laser projection systems," Optics Express, vol. 20, no. 8, p. 8770, 2012.

Chapter 4

SPECKLE REDUCTION BY EMPLOYING TWO GREEN LASERS AND TWO-DIMENSIONAL VIBRATION OF LENSES

ABSTRACT

A method of speckle reduction suitable for use in a laser projector was proposed in the paper. Speckle contrast ratio (SCR) reduction was achieved by combining wavelength diversity and angular diversity methods. First, wavelength diversity was demonstrated by the use of two green laser sources (a 520 nm laser diode (LD) and a 532 nm diode-pumped solid-state (DPSS) laser) at a power ratio of 4:1. Second, angular diversity was achieved via the vibration of two lenses in two orthogonal directions placed directly after the laser source. The vibrating lenses are small and do not require changes to the beam path of the laser source, allowing for more compact projector designs. The frequency of vibration of these lenses was optimized to minimize the SCR in the output image. A speckle contrast ratio of less than 4% was achieved without the use of optical diffusers, which significantly reduces optical losses. Optical transmission could be further increased with the optimization of optical coatings on the lenses. This result shows great promise for applications such as laser pico-projectors within the realm of heads-up displays (HUDs) and mobile devices.

Keywords: speckle reduction, mini-/ pico- projectors, two-dimensional vibration of lenses.

4.1. INTRODUCTION

In recent years, projection display technology has played a vital role in modern life. Projectors can often be found acting as an invaluable tool for the communication of ideas within a classroom or conference room [1]. Projectors can also function as entertainment devices within home theatres [1] or cinemas [2]. Notably, the advent of the pico-projector has brought display technology into the mobile space with great potential to revolutionize heads-up display (HUD) systems [3]. Large number of projection systems is still relying on lamps [4] and light-emitting diodes (LEDs) [5] as light sources launched into the light engines. The problems that plague these display technologies can be effectively overcome with the use of laser sources, which have increased brightness, wider color gamut, longer lifetime, and increased optical efficiency [6]. The pico-projector is a miniaturized application of this laser display technology, which has generated a great deal of interest due to its reduced size and weight. Therefore, it has become highly sought after for mobile photo/video applications [7], portable personal cinemas [8], and HUD systems [9]. To date, pico-projectors commonly use LEDs as light sources rather than lasers, and therefore using lasers as a light source would provide a significant improvement to image quality and light engine efficiency (due to a reduction in etendue).

However, it must be noted that the adoption of lasers as a light source has suffered due to a phenomenon known as laser speckle caused by the high coherency

of the laser source [10]. Laser speckle results in a noticeable decrease in output image quality and therefore, the success of laser display technology is dependent on the reduction of this effect. For the purposes of this paper, this effect will be referred to as speckle noise. Speckle noise can be calculated via the SCR which is defined as $SCR = \sigma/\bar{I}$, where σ is the standard deviation and $\bar{I}$ is the mean of the light intensity passing through the plane of the projected image.

There are several methods of suppressing speckle noise and decreasing the SCR of the laser projection system. These methods are often divided into three categories: wavelength diversity [11], angular diversity [12], and polarization diversity [13]. The effective application of one or more of these effects can reduce the SCR to less than 5%, which is the limit where the speckle effect becomes invisible to the human eye [14,15]. Due to the benefits associated with laser projection, multiple techniques have been implemented to take advantage of these speckle reduction methods. They include but are not limited to, the use of micro-electro-mechanical systems (MEMS) scanning mirrors [16,17], deformable mirrors [18], diffractive optical elements [19], and vibrating diffusers [20]. Although these techniques effectively suppress speckle noise, they can be unattractive to manufacturers due to a high cost and/or degree of complexity, as well as reduced optical and electrical efficiency [19]. Additionally, they can be relatively bulky, which can cause problems when attempting to optimize a small form factor design, such as with pico-projectors and related applications.

In this paper, we propose an effective method of speckle reduction with a low cost and a compact size, which is especially important to pico-projectors. The method is depending on the our presented idea of using single lens vibration in one dimension (1D) to reduce laser speckle noise [21] .Two cascaded lenses were inserted into the red, green blue (RGB) laser optical path. Each lens was fixed inside an optical CD/DVD pickup actuator to create what will be referred to as a lens vibrating module (LVM). The two lenses were then vibrated in the directions perpendicular to the optical axis at optimized frequencies to achieve angular diversity. In addition to speckle noise reduction, we discuss prevention of image fluctuations ("flickering") by optimizing the vibration frequencies in the proposed method. To further reduce speckle, wavelength diversity was implemented via the use of a green light source comprised of two individual green wavelengths (532 nm and 520 nm). This served a dual purpose in both reducing the speckle noise and greatly enhancing the colour gamut and brightness of the output image.

4.2. WORKING PRINCIPLE OF LVM

Figure 4-1 shows a schematic diagram of a single LVM module, which is widely used as an optical CD/DVD pickup actuator [22]. A plano-convex lens with 4.5 mm diameter and 4 mm focal length is capable of vibration in two dimensions (i.e., along the direction of the optical axis and perpendicular to the optical axis). In our experiments, only the tracking motion (i.e., the direction perpendicular to the optical axis) was used.

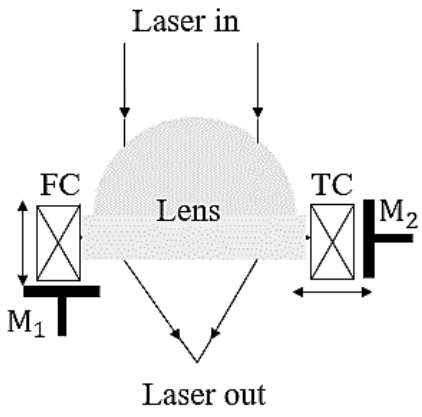

Figure 4-1: A schematic diagram for LVM, where FC: focusing coil, TC: tracking coil, M_1: is the 1st permanent magnet, and M_2: is the 2nd permanent magnet.

The vibration of the lenses is facilitated by small voice coils and small permanent magnets on the LVM frame. Under the application of a voltage across the voice coil terminals, an electromagnetic force will act against the static magnetic field from the magnets, which then manifests as a mechanical motion of the lens. The lens was transparent (no coating) and made of acrylic (or PMMA). The measured transmission efficiency of a single lens is around 90%. No obvious degradation of the transmission efficiency with an input green DPSS laser power of 1.5W for 1 hour with no obvious degradation of the lens, which means the acrylic lens is suitable for a pico-projector system which usually has low optical power. **Figure 4-2** shows the transmission efficiency of a single lens versus input of the

green DPSS laser power. The transmission efficiency is about 90%, which is almost independent of the input green DPSS laser power.

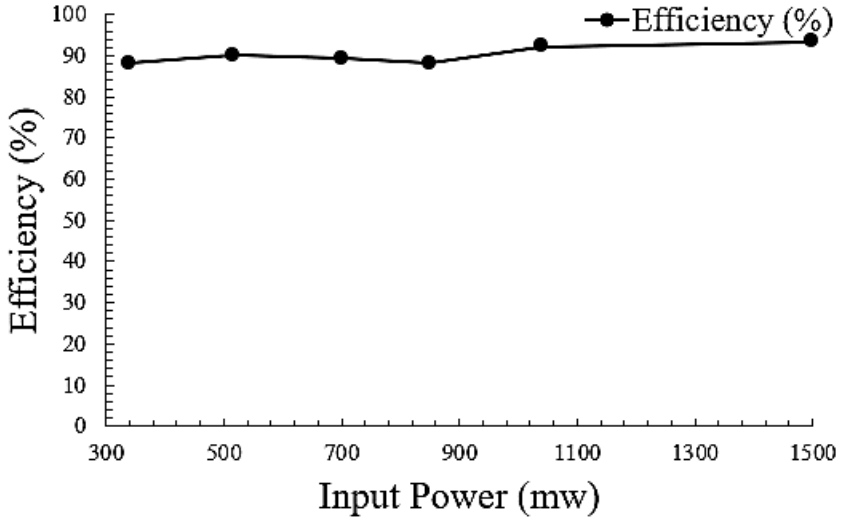

Figure 4-2: Transmission efficiency of the vibration lens versus green DPSS laser power.

4.3. CHARACTERIZATION OF THE LENS VIBRATOR MODULE (LVM)

Figure 4-3 shows a schematic diagram of the experimental setup used to characterize the amplitude of each LVM and the scanning area shape. In **Figure 4-3**, the laser source is a DPSS laser. The wavelength of the DPSS laser is 532 nm, with a linewidth of 0.1 nm. In this experiment, two LVMs with different dimensions were used (14.9 mm × 10 mm and 13 mm × 10 mm for LVM_1 and LVM_2, respectively). The tracking coil of LVM_1 was controlled by a ±3V square wave voltage from a multifunction generator, while the tracking coil of LVM_2 was controlled by a transistor-transistor logic (TTL) signal (+3.1V) from another signal generator. The lens of LVM_1 vibrates in the Y-direction and the lens of

LVM_2 vibrates in the X-direction. A high-resolution charged coupled device (CCD) camera (DCU224M from Thorlabs, pixel size 5.86 μm × 5.86 μm) was used to capture the image of the screen.

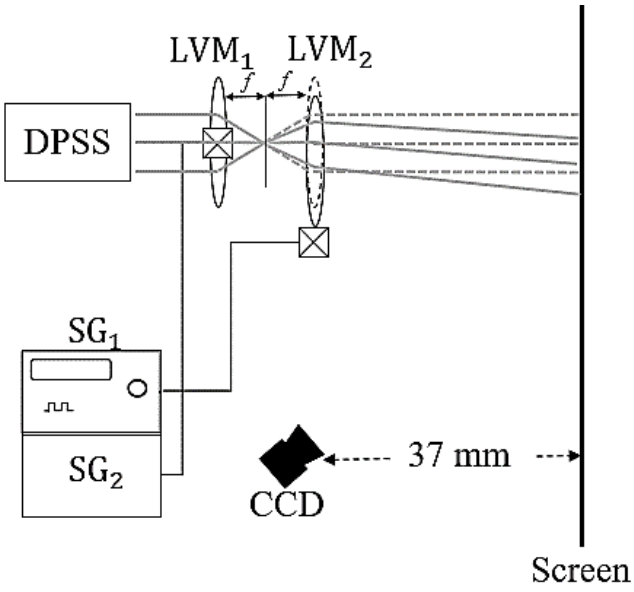

Figure 4-3: A schematic diagram for characterizing the LVM_1 and LVM_2 amplitudes.

Figure 4-4 shows images captured by the CCD camera using the test setup shown in **Figure 4-3**. In Figure **4-4**, **Figure 4-4a** represents the output image as a bright point when there are no applied signals on both LVM_1 and LVM_2.

Figure 4-4b represents the output image as a horizontal bright line when LVM_1 is "off" and LVM_2 is "on". **Figure 4-4c** represents the output image as a vertical bright line when LVM_1 is "on" and LVM_2 is "off". **Figure 4-4d** represents the output image as a bright pattern (the shape of this pattern depends on the frequency change of LVM_1 and LVM_2) when both LVM_1 and LVM_2 are "on". In this context, "on" and "off" refers to whether the aforementioned input signal(s) are

being applied. During this measurement, the amplitudes of LVM_1 and LVM_2 covered a frequency range of 30 to 130 Hz. Note, the fourth image was taken under the condition that the frequency of vibration of the two modules was not equal.

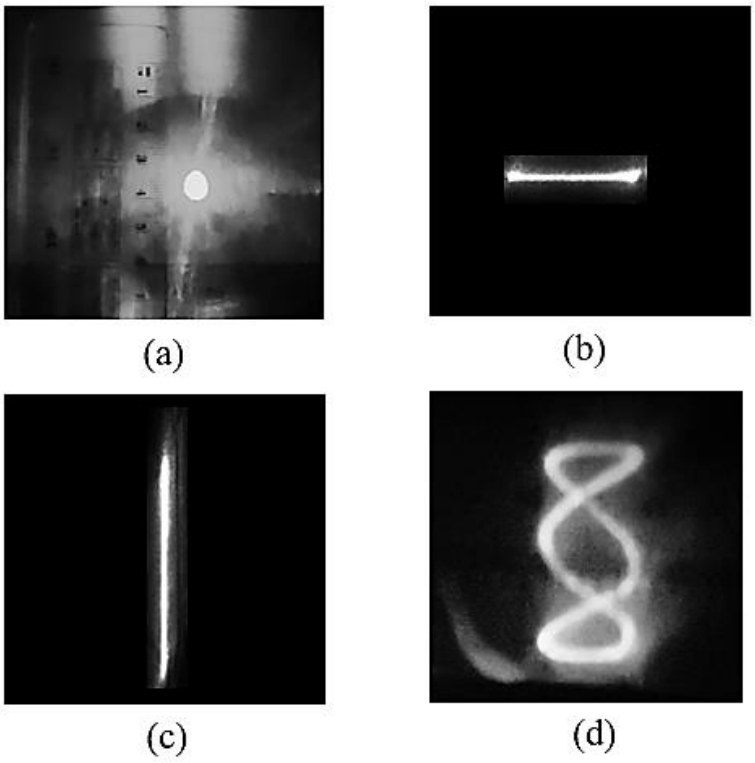

Figure 4-4: Captured grayscale images from CCD camera where (a) LVM_1 and LVM_2 are off, (b) LVM_1 and LVM_2 are off and on, respectively, (c) LVM_1 and LVM_2 are on and off, respectively, and (d) LVM_1 and LVM_2 are both on with different frequencies.

Figure 4-5 shows the relationship between the frequency of vibration and the measured amplitude on the screen. Using the distance between the LVM_{xy} and the screen (37 cm), the real values of the amplitude from the LVM_{xy} module can be estimated by considering the magnification of the lenses used. In **Figure 4-5**, the vertical and horizontal bright lines images represent the shape of the laser beam on

the screen under the effects of the vibration. The vertical and horizontal bright lines are produced by LVM_1 and LVM_2, respectively.

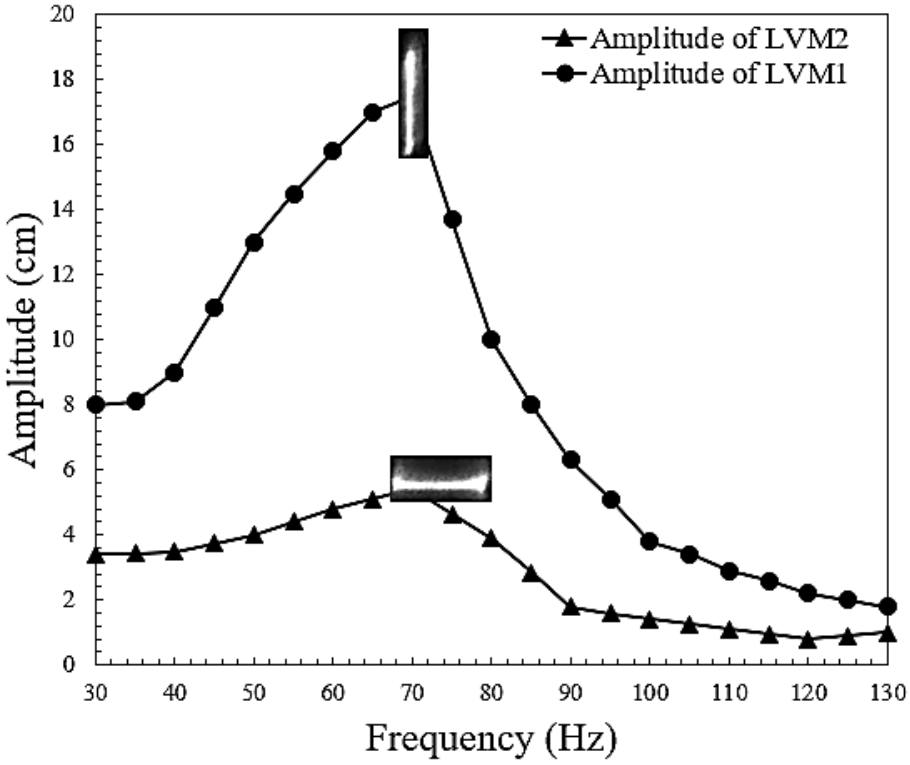

Figure 4-5: Amplitude versus frequency for the two individual vibrating lenses.

4.4. THEORETICAL BACKGROUND

The SCR is dependent on a speckle reduction factor R, which can be expressed as:

$$\mathrm{SCR} = \frac{1}{\mathrm{R}} = \frac{1}{\mathrm{R}_\lambda \mathrm{R}_\Omega \mathrm{R}_\sigma}$$

Where, R_λ, R_Ω, and R_σ are the wavelength, angular, and polarization diversity, respectively. $\mathrm{R}_\sigma = 1$ for any screen can preserve the polarization state of laser and

$R_\sigma = \sqrt{2}$ for any depolarized screen such as the white A4 paper used in this experiment. Thus, R_σ is constant in all experiments and the reduction factor R depends on the values of R_λ and R_Ω. One of the most effective method to achieve large R_Ω is by moving a diffuser in the path of laser beam [23]. As the lens array is considered a diffuser with low diffusion and high transmission efficiency [24], the motion of the laser beam across the lens array can increase R_Ω.

Also, R_Ω has an upper limit according to the solid angles of the projection lens and the detector lens [13]. So, the only remaining factor can yield a further reduction of the speckle noise is R_λ.

According to Goodman's theory [13], the R_λ of two laser wavelengths with equal intensities, Gaussian shape and wavelength separation greater than 1nm, is $R_\lambda = 1/\sqrt{2}$. However, according to [25], to achieve the minimum SCR by using two lasers with two different linewidths thus the power level of each laser is not the same. As a result, the lower values of SCR can be achieved when the power level of the laser with wider linewidth must be higher than the power level of the laser with narrower linewidth. Eventually, the total speckle reduction is a combination from the aforementioned values of $R_\lambda, R_\Omega,$ and R_σ.

4.5. PROPOSED LASER PROJECTOR LAYOUT

Figure 4-6 shows a proposed configuration for a laser projector layout. In **Figure 4-6**, the red, blue, and green laser modules are combined using a dichroic prism to complete the RGB light source. The green laser module is comprised of a

DPSS laser (532 nm) and laser diode (LD) (520 nm). The combination of the two lenses performed by using a single lens. The RGB laser light is collimated by a lens and then directed to cross two lenses (LVM_1 and LMV_2). The two lenses are vibrated in directions either perpendicular or parallel to the optical path and make up the component LVM_{xy} (as shown in **Figure 4-6**). A homogenizer module will be used to homogenize the light field. A lens system (including a pair of lens arrays) is used to reshape the light field to be rectangular. A polarizing beam splitter (PBS) is used to take the footprint image from a liquid-crystal on silicon (LCoS) panel. Finally, the output image will be projected via a projection lens. The overall length of the light engine from the dichroic prism to PBS is 70 mm. Utilizing this projection system with a laser light source shows great promise in terms of creating compact and cost-effective mini-/pico-projector systems.

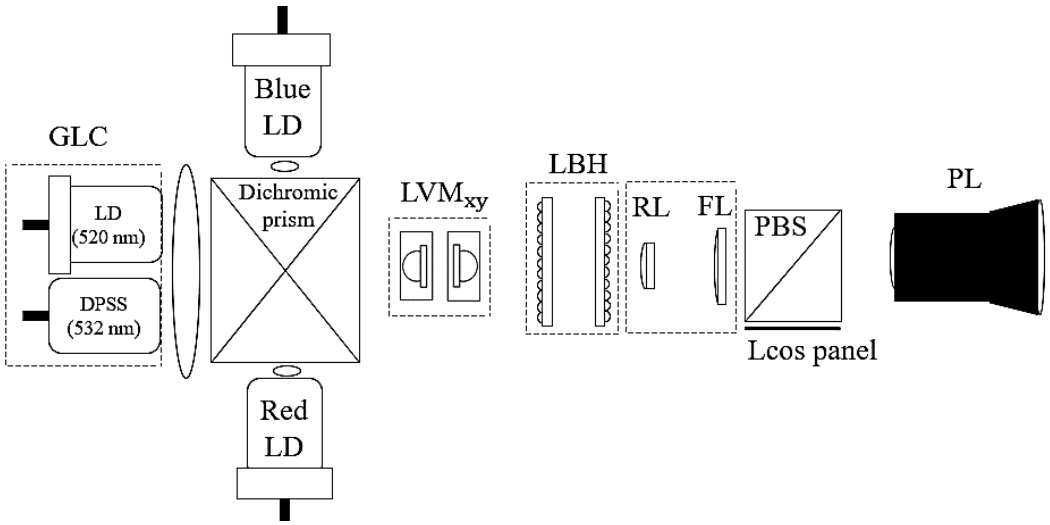

Figure 4-6: A schematic diagram of the proposed laser projector layout, where CGL is a compound green laser, LBH: laser beam homogenizer, RL: relay lens, FL: field lens and PL is the projection lens.

4.6. EXPERIMENTS AND DISCUSSIONS

SPECKLE REDUCTION CHARACTERIZATION

An experiment was performed for studying laser speckles and evaluating its reduction efficiency by using the green laser source as the human eye is most sensitive to green wavelengths, compared to both red and blue [26].

Figure 4-7 shows the experimental setup, which was used to reduce the green laser speckle noise. The laser source consisted of a green LD (NDG7475 Nichia) at 520 nm with 2 nm linewidth and a green DPSS laser at 532 nm with 0.1 nm linewidth. The green LD and DPSS laser were attached to Peltier elements, and aluminum heat sinks to maintain an operating temperature of 25°C. The two laser sources were then combined using a cubic beam-splitter. Half of the combined green laser (CGL) beam was collected by a power meter (LM10 from coherent Inc) to measure the power ratio between the two green sources.

The remaining half of the CGL was then directed to pass through two vibrating lenses (LVM_1 and LVM_2) which comprise LVM_{xy}. After LVM_{xy}, a pair of micro-lens arrays (fly-eye lenses) were used to act like a laser beam homogenizer [24]. That is, they were used to transform the initially circular cross-section of the CGL into a rectangular cross-section with uniform intensity distribution. The fly-eye lens was followed by a telecentric imaging system consisting of two lenses (L_2 and L_3) to project the rectangular CGL beam into a rectangular aperture (6.60 mm

× 5.23 mm). Finally, a projection lens with a focal length of 6.5 mm produced the output image on an A4 white paper screen.

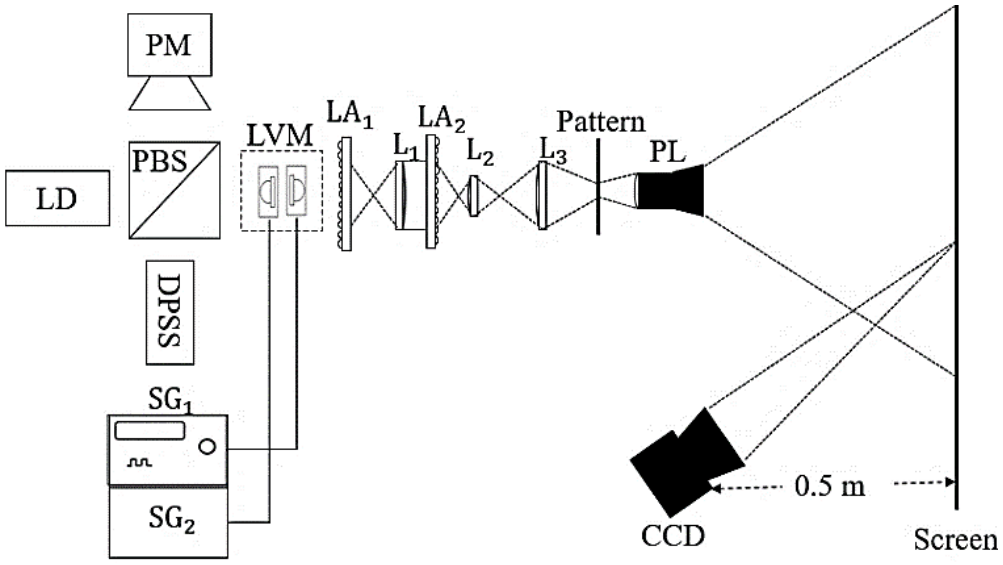

Figure 4-7: Schematic diagram of speckle reduction measurement setup, where, SG_1: is the signal generator of LVM_1, SG_2: is the signal generator of LVM_2, L_1: relay lens, L_2 and L_3: comprise the telescopic lens system.

It is well known that the measurement conditions have a significant impact on measuring the SCR, thus the measurement conditions used correspond to the human eye perception. In order to ensure an accurate SCR value, the parameters used in this work agree with the previously reported work in [16,18,27–29] to measure the SCR in a handheld laser projector such as pico-projector. The pixel size of the CCD camera is 5.2 um × 5.2 um with a resolution of 1280 × 1024 pixels. The F/# for the camera lens is 1.4. The integration time of CCD camera was chosen to be 20 ms as that is comparable to the integration time of the human eye. The focal length of the camera's lens was 25 mm. The distance between the camera and the screen was 0.5 m. The CCD camera-generated an 8-bit grayscale image and was

used in the linear region. All experimental data were collected under the conditions of a dark room to avoid noise generated by background light.

To evaluate the effect of speckle reduction due to the individual vibrating lens, the SCR was measured for each laser source when either LVM_1 or LVM_2 was turned on. **Figure 4-8** shows the measured SCR versus vibrational frequency over a range from 0 to 130 Hz.

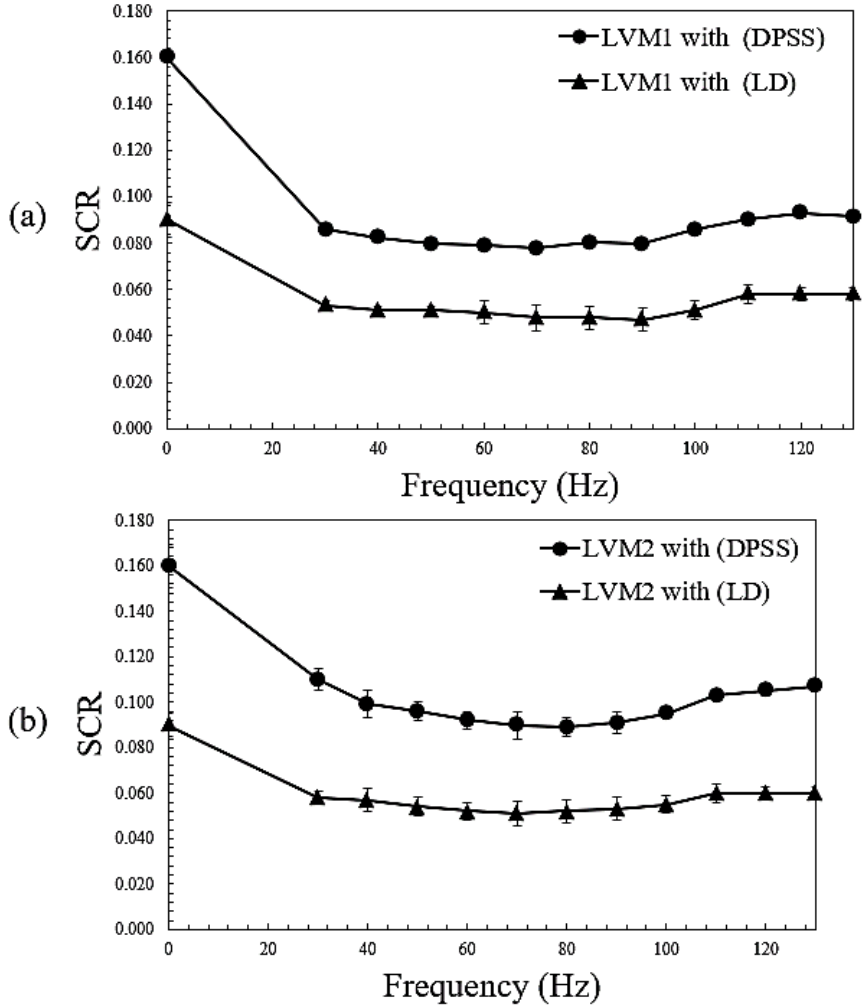

Figure 4-8: The measured SCR for DPSS and LD source in separate as a function of the frequency of vibration of (a) LVM_1 and (b) LVM_2. The error bars -at each

frequency- are given by calculating the standard deviations of the SCRs for the individual sub-images.

From **Figure 4-8** and **Table 4-1**, the SCR values were 0.093 and 0.160 for the LD and DPSS laser, respectively when neither LVM_1 or LVM_2 were vibrating. Once the modules began to vibrate, the SCR began to decrease with increasing vibration amplitude. It can be seen from **Figure 4-8** that the minimum SCR was achieved within the range of 50 Hz to 80 Hz. With only the DPSS laser as a source, and LVM_1(or LVM_2) vibrating, the minimum SCR was 0.078 (or 0.90). With only the LD laser as a source, and LVM_1(or LVM_2) vibrating, the minimum SCR was close to 0.051 (or 0.052). This can be attributed to the linewidth of the LD being much broader than the linewidth of the DPSS laser (2 nm versus 0.1 nm). This also shows that the vibration along the x- and y- direction alone cannot achieve an SCR below the human-perception limit of 5% for both the green LD and DPSS laser. Therefore, wavelength diversity is required in combination with angular diversity to further reduce the SCR.

Table 4-1: The speckle reduction efficiency of the LD and DPSS laser sources for each LVM module.

LVM	**LVM_1**		**LVM_2**	
Laser Source	DPSS	LD	DPSS	LD
SCR when both LVMs are OFF	0.160	0.093	0.160	0.093
Minimum SCR (Frequency of LVM_1 or LVM_2 are "70 Hz")	0.078	0.051	0.090	0.052
Reduction Efficiency: $(1 - \frac{\text{Minimum SCR}}{\text{Original SCR}}) \times 100$	51.25	43.33	43.75	42.22

OPTIMIZATION OF A GREEN LASER SOURCE

Figure 4-9 shows the relation between the SCR and the power ratio. That is, the ratio between the power of the LD to the total power of the two laser sources when both LVMs are OFF. According to Goodman's theory [13], when blending two lasers of equal linewidths, the optimum speckle-noise reduction occurs at a power ratio of 1:1. However, when blending lasers of two separate linewidths the optimal power ratio will not be at a ratio of 1:1 [13]. From **Figure 4-9**, the minimum SCR was achieved when the power of the LD was four times larger than that of the DPSS laser ($P_{LD}: P_{DPSS} = 4: 1$). At this power ratio, the green point in the color gamut wheel would be shifted closer to 520 nm. This is not preferred in terms of color gamut coverage as it is far from the ideal wavelength of 532 nm as

recommended by Rec.2020 [25]. Therefore, a trade-off exists between color quality and minimum SCR however it must be noted that solving this problem is not the main target of our study. Although the combination of the green LD and DPSS laser can achieve much better color gamut coverage and even lower SCR, the power ratio which yields these benefits is not the same for both. That is, the power ratio which offers increased color gamut coverage is not the same the ratio which yields the lowest SCR. Once again, optimization must be performed to obtain the best result taking into consideration the results from both effects.

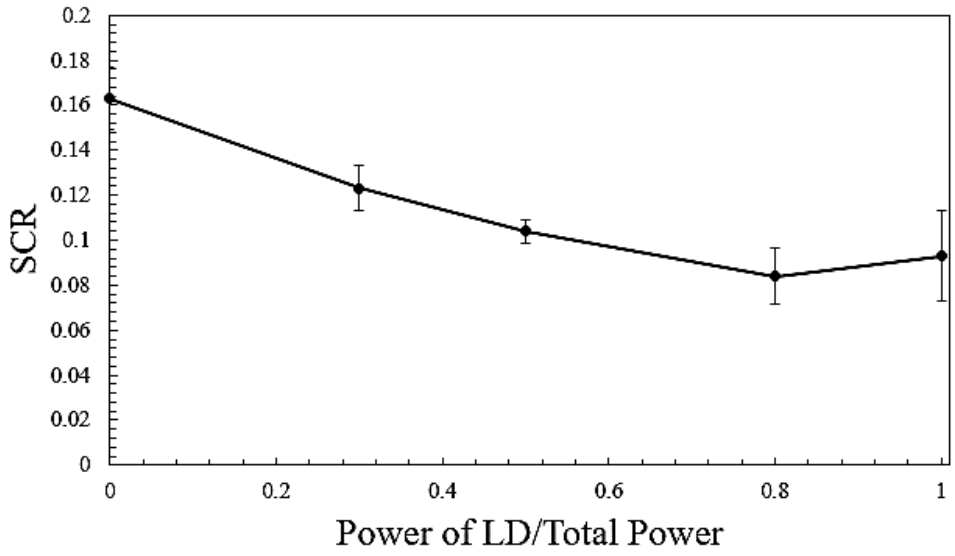

Figure 4-9: Measured SCR using wavelength blending of a green LD and a green DPSS laser versus the power of the LD divided by total power, where from a power ratio of 0 to 1 both LVMs are in the "off" state. The error bars -at each frequency- are given by calculating the standard deviations of the SCRs when different areas similar are selected.

OPTIMIZATION OF OPERATING FREQUENCIES

After optimizing the power ration between the LD to the power of the DPSS laser to be 4:1, the operating frequencies must be optimized. **Figure 4-10** shows the relation between the SCR versus the frequencies of LVM_1 and LVM_2. From **Figure 4-10**, it can also be seen that the lowest SCR was achieved between a frequency of 40 and 60 Hz for vertical vibration and between a frequency of 60 and 100 Hz for horizontal vibration. It can, therefore, be shown that a minimum SCR ranging from 0.035 to 0.04 can be achieved by employing two green lasers and two-dimensional vibration of lenses. The SCR can be further reduced to be under 4% by using optical diffusers or even a combination of them [18], but this will be on the expense of the optical efficiency of the illumination system [30]. For example, in ref. [23], the SCR was < 5% with optical efficiency from 34 to 43% by using pairs of diffusers under vibration. In any pico-projector, the brightness (optical efficiency) must be considered when creating these laser projection systems. Therefore, it is very beneficial that an SCR of less than 5% was achieved without using any diffuser. Obviously, the value of SCR can be further decreased by inserting a low divergence angle optical diffuser (e.g. < 15°). Such a low divergence angle diffusers are preferred as it has no significant optical loss [31].

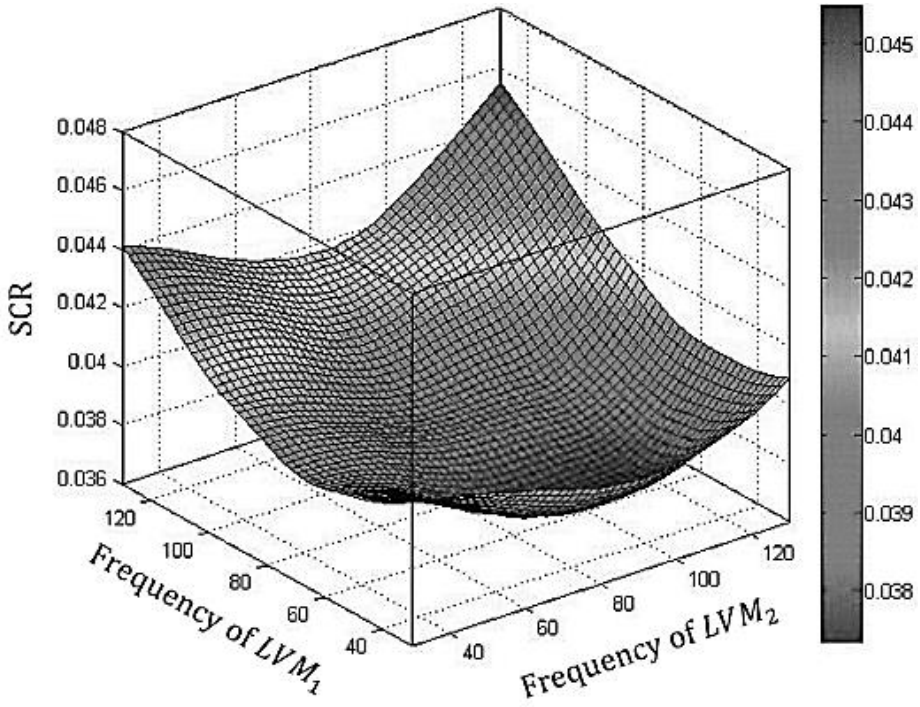

Figure 4-10: A 3D curve for measured SCR in the 2D scanning of vibration frequencies.

Figure 4-11 shows the measured speckle image when the frequency of LVM_1 and LVM_2 is 50 Hz and 90 Hz (dynamic state), respectively by the setup is shown in **Figure 4-7**. The SCR was 0.084 in a static state (no vibration for both modules and the power ratio between LD and DPSS laser is 4:1) and 0.035+0.003 in a dynamic state. This is implying that the efficiency of speckle-noise reduction is 56.25% for wavelength diversity and angular diversity ($\left[1-\frac{0.035}{0.08}\right]\times 100\%$).

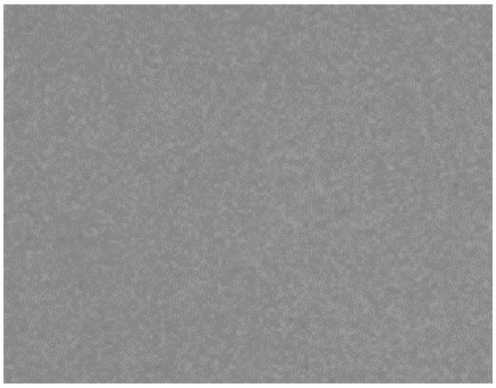

Figure 4-11: Measured speckle image at the frequency of LVM_1/ LVM_2 is 50 Hz/ 90 Hz.

In the above discussion, the focus was on achieving the minimum SCR value. To fully encompass all the necessities of practical laser display applications, another important parameter must be considered which is the output image flickering. The flickering in the output light field on the output screen was noticed at some vibration frequencies. According to [32], the output Lissajous shape parameters, such as line density and repetition rate for each shape from both LVMs as well as the scanning area on the 1st lens array are related to the frequency applied to each LVM. First, the repetition rate is the main cause of the flickering which will result in decreasing the output image quality. From [33], the repetition frequency of the output can be calculated by finding the greatest common divisor (GCD (f_1, f_2), where f_1 and f_2 are the frequency of LVM_1 and LVM_2, respectively) for the frequency of LVM_1 and LVM_2. The expected highest repetition frequency can be achieved at $f_1 = f_2$ or $f_1 = 2f_2$. For instance, the GCD (50 Hz, 50 Hz) = 50 Hz, and GCD (50 Hz, 100 Hz) = 50 Hz. This means that the repetition frequency of the

output light field will be 50 Hz. As a result, the output light field will appear fixed without any flickering with respect to the human eye, as the repetition rate is sufficiently greater than the perception threshold of 25 Hz.

Secondly, as the scanned area increases, the time needed to complete one scanning cycle will increase as well [32,33]. The dimensions of the scanned area corresponding to the 1st lens array depend on the amplitude of the two vibrating lenses and the distance between the second vibrating lens and the first lens array. Figure **4-12** shows the measured speckle images from the experimental setup in **Figure 4-7**. In **Figure 4-12a**, the green laser source was a DPSS laser with $f_1=f_2=$ 70 Hz. The SCR was 0.068. In **Figure 4-12b**, the green laser source was an LD with $f_1=f_2=$ 70 Hz. The SCR was 0.05. In **Figure 4-12c**, the LD and DPSS green laser power were blended with a power ratio of 4:1 (as mentioned in section 5.2) with $f_1=f_2=$ 50 Hz. The SCR was 0.04. In **Figure 4-12** the output images are free of flickering under the proposed frequencies, with 10 mm distance between the 2nd vibrating lens and the 1st vibrating lens.

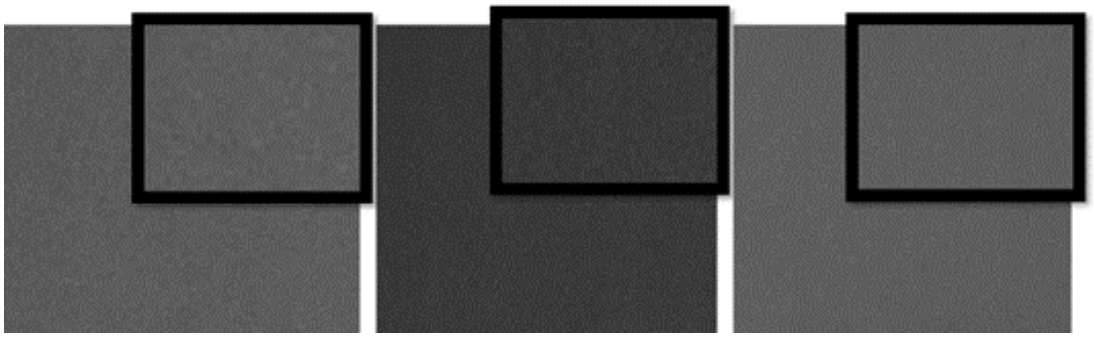

Figure 4-12: Speckle images for (a) DPSS laser source with $f_1=f_2=$ 70 Hz, (b) LD laser source with $f_1=f_2=$70 Hz, and (c) CGL source with $f_1=f_2=$50 Hz.

4.7. CONCLUSIONS

In conclusion, it has been demonstrated that a SCR below the human-eye perception limit (5%) can be achieved by employing novel two-dimensional vibrating lenses coupled with the wavelength diversity techniques. Our proposed optimized method can achieve excellent output image quality with an SCR of 4% and no image flickering.

The proposed method is compact because it does not require any modification of the optical path. In our proposed method, the optical power efficiency (for green laser) was 69.62%. The optical efficiency can be further increased by at least 15.38% via the application of an anti-reflection coating to the two vibrational lenses.

The proposed projection system has the potential to significantly improve the brightness, optical-to-optical efficiency, and colour gamut coverage of laser

projection systems. Therefore, reduced cost and size alongside increased efficiency makes this laser projection system ideal for practical mini-/pico-projection systems.

In the future, the proposed method will be optimized as follows: First, the use of anti-reflection coated lenses to increase the transmissivity. Second, design and manufacturing of a 2D scanning device with single aspheric lens and with high resonance frequencies. Third, using a low divergence angle diffuser (<15degree) to reduce the SCR. Fourth and finally, using a DPSS laser with wide linewidth in order to further optimize the blending ratio. Fifth, as known that the luminance of the output projected images from the laser projector would influence the human perception of the speckle noise. Therefore, a study of the best power ratio between the RGB lasers used has to be performed to achieve the optimum luminance.

4.8. ACKNOWLEDGEMENT

The authors would like to thank Liam Flannigan for his careful proofreading of the manuscript, and the NSERC Discovery grant for the support of the project.

4.9. NOTATIONS

b:	Fracture aperture
M_1:	1st permanent magnet,
M_2:	2nd permanent magnet.
LVM_1:	1st Lens vibrating module
LVM_2:	2nd Lens vibrating module
SG_1:	signal generator of LVM_1
SG_2:	signal generator of LVM_2
L_1:	relay lens
L_2	comprise the 1st telescopic lens system.
L_3:	comprise the 2nd telescopic lens system
P_{LD}:	The power of LD
P_{DPSS}	The power of DPSS

Greek Letters:

σ:	standard deviation
$\bar{I}$:	mean light intensity

4.10.ACRONYMS

SCR:	Speckle contrast ratio
LD:	laser diode
DPSS:	diode-pumped solid-state
LEDs	light-emitting diodes
HUD:	heads-up display
MEMS:	micro-electro-mechanical systems ()

RGB: the red, green blue

LVM: lens vibrating module

FC: focusing coil

TC: tracking coil

TTL: transistor-transistor logic

CCD: Charged-coupled device

PBS: polarizing beam splitter

LCoS: liquid-crystal on silicon

CGL: compound green laser

LBH: laser beam homogenizer

RL: relay lens

FL: field lens

PL: projection lens

4.11. REFERENCES

[1] Lee J-H, Mun Y-K, Do S-W, Ko Y-C, Kong D-H, Choi B-S, Kim J-M, Hong C-W and Jeon D-Y 2003 Laser TV for home theater *Projection Displays VIII* **4657** 138–45

[2] Verschaffelt G, Roelandt S, Meuret Y, Van Den Broeck W, Kilpi K, Lievens B, Jacobs A, Janssens P and Thienpont H 2015 Speckle disturbance limit in laser-based cinema projection systems *Scientific Reports* **5** 14105

[3] Lyubin V, Arsh A, Klebanov M, Sroumin N, Kantarovich K, Bar I, Dror R and Sfez B 2008 Nonlinear photoresist films fabricated by coevaporation of As 2S3 glass and silver *Journal of Optoelectronics and Advanced Materials* **10** 3182–7

[4] Perkins M and Koebel A 2017 Lasers, lamps, or phosphors - choices for the future of digital cinema *Digest of Technical Papers - SID International Symposium* **48** 513–6

[5] Basu C, Meinhardt-Wollweber M and Roth B 2013 Lighting with laser diodes *Advanced Optical Technologies* **2** 313–21

[6] Chellappan K V, Erden E and Urey H 2010 Laser-based displays : a review *Applied optics* **49** 79–98

[7] Trisnadi J I, Carlisle C B and Monteverde R 2004 Overview and applications of Grating-Light-Valve-based optical write engines for high-speed digital imaging *MOEMS Display and Imaging Systems II* **5348** 52--64

[8] Ryf R, Chen G, Basavanhally N, Dinu M, Duque A, Low YL, Wiesenfeld JM, Shapiro Y G R 2009 The Alcatel-Lucent microprojector: what every cell phone needs *Bell Labs Technical Journal* **14** 99--112

[9] Freeman M O 2011 MEMS scanned laser head-up display *MOEMS and Miniaturized Systems X* **7930** 79300G

[10] Akram M N and Chen X 2016 Speckle reduction methods in laser-based picture projectors *Optical Review* **23** 108–20

[11] Yamada H, Moriyasu K, Sato H and Hatanaka H 2017 Effect of incidence/observation angles and angular diversity on speckle reduction by wavelength diversity in laser projection systems *Optics Express* **25** 32132

[12] Akram M N, Tong Z, Ouyang G, Chen X and Kartashov V 2010 Laser speckle reduction due to spatial and angular diversity introduced by fast scanning micromirror *Applied Optics* **49** 3297

[13] Goodman J W 2007 *Speckle Phenomena in Optics: Theory and Applications* (Roberts and Company Publishers)

[14] Akram M N, Tong Z, Ouyang G, Chen X and Kartashov V 2010 Laser speckle reduction due to spatial and angular diversity introduced by fast scanning micromirror *Applied Optics* **49** 3297–304

[15] Furukawa A, Ohse N, Sato Y, Imanishi D, Wakabayashi K, Ito S, Tamamura K and Hirata S 2008 Effective speckle reduction in laser projection displays *Emerging Liquid Crystal Technologies III* vol 6911 p 69110T

[16] Lee J Y, Kim T H, Bu J U and Kim Y J 2015 Speckle reduction using twin green laser diodes and oscillation of MEMS scanning mirror for pico-projector *MOC 2015 - Technical Digest of 20th Microoptics Conference* (The Japan Society of Applied Physics) pp 1-2 IEEE
[17] Abelé N, Le Gros C, Masson J and Kilcher L 2014 Speckle reduction technique for embeddable MEMS-laser pico-projector *MOEMS and Miniaturized Systems XIII* **8977** 89770P
[18] Chen H-A, Pan J-W and Yang Z-P 2017 Speckle reduction using deformable mirrors with diffusers in a laser pico-projector *Optics Express* **25** 18140
[19] Lapchuk A, Gorbov I, Le Z, Xiong Q, Lu Z, Prygun O and Pankratova A 2018 Experimental demonstration of a flexible DOE loop with wideband speckle suppression for laser pico-projectors *Optics Express* **26** 26188
[20] Pan J W and Shih C H 2017 Speckle noise reduction in the laser mini-projector by vibrating diffuser *Journal of Optics (United Kingdom)* **19** 045606
[21] Mohamed M, Qianli M A, Flannigan L and Xu C-Q 2019 Laser speckle reduction utilized by lens vibration for laser projection applications *Engineering Research Express* **1** 015036
[22] Hwu E E Te and Boisen A 2018 Hacking CD/DVD/Blu-ray for Biosensing *ACS Sensors* **3** 1222–32
[23] Pan J-W and Shih C-H 2014 Speckle reduction and maintaining contrast in a LASER pico-projector using a vibrating symmetric diffuser *Optics Express* **22** 6464
[24] Shevlin F P 2012 Speckle reduction in laser-illuminated picoprojectors *MOEMS and Miniaturized Systems XI* vol 8252 (International Society for Optics and Photonics) p 825206
[25] Ma Q and Xu C Q 2017 Wavelength blending with reduced speckle and improved color for laser projection *Optics and Lasers in Engineering* **97** 27–33
[26] Mullen B Y K T 1985 The contrast sensitivity of human colour vision to red-green and blue-yellow chromatic gratings. *The Journal of Physiology* **359** 381–400
[27] Pan J-W and Shih C-H 2014 Speckle reduction and maintaining contrast in a LASER pico-projector using a vibrating symmetric diffuser *Optics Express* **22** 6464
[28] Tsao C-W, Chen H-A, Pan J-W and Yang Z-P 2018 63-1: Speckle Reduction for Laser Pico-projector with Dynamic Deformable Mirrors *SID Symposium Digest of Technical Papers* **49** 823–6
[29] Pan J W and Shih C H 2017 Speckle noise reduction in the laser mini-projector by vibrating diffuser *Journal of Optics (United Kingdom)* **19** 045606
[30] Pan J W and Shih C H 2017 Speckle noise reduction in the laser mini-projector by vibrating diffuser *Journal of Optics (United Kingdom)* **19** 045606
[31] Kamynin VL B T 2015 Estimates for the highest derivative solutions of non-divertive parabolic equations with unlimited coefficients. *Herald of the National Nuclear Research University MEPhI* **4** 35–40

[32] Seo Y-H, Hwang K, Kim H and Jeong K-H 2019 Scanning MEMS Mirror for High Definition and High Frame Rate Lissajous Patterns *Micromachines* **10** 67

[33] Kim K, Hwang J and Ji C H 2018 Intensity-based laser distance measurement system using 2D electromagnetic scanning micromirror *Micro and Nano Systems Letters* **6** 4–10

Chapter 5

SUMMARY, CONCLUSIONS, AND RECOMMENDATIONS

5.1. SUMMARY

Pico-projectors are strongly demanded because it can be embedded into many devices to enable many applications such as automotive, defence & aerospace, healthcare, media & entertainment, and other end-user industries [1].

The presented research in this thesis aims to find a suitable and practical solution for the problem of laser speckles in the handheld projectors such as pico-/micro-projectors.

In this research, three approaches are presented for speckle suppression. The first approach is to modify the design of the laser source to emit dual wavelengths at the same time. The output laser with dual wavelengths has high optical efficiency, high power stability, compact size, and with minimum laser speckle noise.

The second approach is to use a new method which is performed outside the laser source to reduce the laser speckle noise. The proposed method reduced the speckle contrast ratio to shallow level closes to 5%. The method shows a capability for introducing speckle reduction with low cost, low vibrational noise, low power consumption, and compact size. Such features are beneficial for handheld projectors.

The third approach is to optimise the proposed method by adding compound green laser sources after optimising their power ratios to achieve low speckle noise and enhancing the colour quality.

5.2. CONCLUSIONS AND CONTRIBUTIONS

The research in the present study introduces efficient solutions for solving the speckle noise in handheld projectors. In Chapter 2, the proposed design for the laser source can generate two lasers (at 1062.4 nm and 1063.9 nm) at the same time form a resonator with just 10 mm length. The output power ratio is fixed, and the optical to optical efficiency was 48.9 %. The output power instability is 0.4%. The speckle contrast ratio (SCR) is reduced from 70% to 53.9%.

In Chapter 3, the proposed method at this study was able to reduce the SCR to 11% and 6% for both diode-pumped-solid-state (DPSS) laser and laser diode (LD), respectively. The reduction efficiency for DPSS and LD laser sources is 42.1% and 50%, respectively. The wavelength of the DPSS/LD laser is 532 nm/520 nm at linewidth 0.1 nm/1.2 nm.

In Chapter 4, the optimisation of the proposed method in Chapter 3 is introduced into to steps. Firstly, by blending the two laser sources (532 nm from DPSS laser and 520 nm from LD laser), the optimised power ratio between LD to DPSS laser is 4 to 1 to achieve the lowest SCR. Secondly, adding a second dimension to increase the angular diversity in two dimensions instead of one dimension in chapter 3. A pair of lens arrays with shaping optics were used to

homogenising the output light field. Eventually, the output image was projected by using a real pico-projector projection lens.

5.3. RECOMMENDATIONS FOR FUTURE RESEARCH

The research presented in this dissertation is beneficial for handheld laser projection applications. Many future steps can be initiated to increase the usefulness from this research as follows:

- First, convert the output emission from the presented laser source to its second harmonic by using a specially designed second nonlinear crystals. This will transfer the output emission from infra-red (invisible) to a green colour (visible). Many optimisations and specially designed features must be considered to increase the efficiency of the output green emission.
- Second, using the three-dimensional (3D) printing in manufacturing a 3D laser scanning device equipped with an anti-reflection coated lens and increasing the resonance frequencies of operation for each degree of freedom
- Third, using the new 3D printed module with the new optimised green laser source to construct a free focus pico-projector for automotive applications.

5.4. NOTATIONS

-- --

Greek Letters:

-- --

5.5. ACRONYMS

SCR:	speckle contrast ratio
DPSS:	diode-pumped-solid-state
LD:	laser diode
3D:	three-dimensional

5.6. REFERENCES

[1] Mordor Intelligence, “PICO PROJECTOR MARKET - GROWTH, TRENDS, AND FORECAST (2019 - 2024),” mordorintelligence.com, 2019. [Online]. Available: https://www.mordorintelligence.com/industry-reports/pico-projector-market.